**UNIVERSITY OF KASDI MERBAH-OUARGLA**

**Faculty of New Technologies of Information and Communication**

**Department of Electronics and Communications**

# Dissertation

Thesis Submitted to the Department of Electronics and telecommunications in Candidacy for the Degree of "Doctor" 3rd Cycle LMD in automation and Industrial computing

**Presented by:**

***TAMISSA Younes***

*Theme*

## Fault-Tolerant Voltage Source Inverter for Induction Motor Drive Using Intelligent Techniques

Publically defended:

On:.... /2023

**Before the jury:**

| | | | |
|---|---|---|---|
| SAMAI Djamel | Professor | President | UKM Ouargla |
| CHARIF Fella | Professor | Thesis Director | UKM Ouargla |
| BENCHABANE Abderrazak | MCA | Thesis Co-director | UKM Ouargla |
| Bensid Khaled | MCA | Examiner | UKM Ouargla |
| AJGOU Riyad | Professor | Examiner | UHL EL-OUED |
| HETTIRI Messaoud | MCA | Examiner | UHL EL-OUED |

**Academic Year 2023/2024**

# *Dedication*

*I dedicate to my mother and father, who has been a source of encouragement and inspiration to me throughout my life, Listening to my ideas and offered encouragement when it was most needed. Throughout my life, you have actively supported me in my determination to find and realize my potential, and to make this contribution to our country. I am also very grateful to all my friends and family. I don't forget to thanks all Teachers and workers in department of electronic*

# ***الملخص***

*يمكن أن تتعرض الأنظمة الكهربائية للأعطال لأسباب مختلفة. قد تحدث هذه الأخطاء نتيجة لتقادم المكونات أو ظروف الاستخدام أو عيوب التصنيع التي لم يكن من الممكن اكتشافها أثناء التشغيل. يمكن تصنيف الأخطاء بشكل عام إلى فئتين: تلك التي تحدث داخل الآلة الكهربائية مثل أعطال اللف وميل المحور، وتلك التي تحدث خارج الآلة الكهربائية في سلسلة القيادة، مثل الأعطال في علبة التروس الميكانيكية.*

*يركز أحد مجالات البحث الرئيسية على مراقبة حالة المحول الذي يزود الطاقة لجهاز غير متزامن. قد يكون للمحول، مثل عاكس تعديل عرض النبض (PWM)، عيوب هيكلية مثل المفاتيح المعطلة (أشباه الموصلات) التي قد تؤدي إلى تلف النظام بأكمله. من الضروري الاستثمار في اكتشاف الأعطال لمنع مثل هذه العيوب من التسبب في ضرر لا يمكن إصلاحه للنظام.*

*توفر تقنيات مراقبة وتشخيص الحالة القائمة على الذكاء الاصطناعي (AI) مزايا مختلفة مقارنة بالطرق التقليدية. تلغي هذه التقنيات الحاجة إلى نماذج رياضية، مما يقلل من وقت الهندسة والتطوير بشكل كبير. تعتمد التقنيات القائمة على الذكاء الاصطناعي على مجموعات بيانات النظام أو معرفة الخبراء لإجراء تنبؤات دقيقة. في حالة التحكم في محرك حثي يعمل بواسطة عاكس جهد PWM، يمكن للطرق المعتمدة على الذكاء الاصطناعي اكتشاف أخطاء الدائرة المفتوحة و/أو الدائرة القصيرة واتخاذ التدابير التصحيحية لضمان عمل النظام بكفاءة مع الحفاظ على المستوى المطلوب من الأمان.*

*في هذه الأطروحة، قمنا بتحليل جدوى استخدام تقنيات الذكاء الاصطناعي في اكتشاف وتشخيص وإعادة تشكيل الأخطاء في العاكس ثلاثي الطور الذي يعمل على تشغيل المحرك التعريفي. لقد قدمنا وصفًا تفصيليًا لأخطاء تبديل العاكس وقمنا بتطوير طريقة بسيطة لاستخلاص الخصائص لدراسة إمكانية اكتشاف وتشخيص هذه العيوب. لقد حاولنا أيضًا إعادة تكوين نظام العاكس لمنع حدوث الأخطاء.*

***كلمات مفتاحية:*** *تصنيف الأخطاء، العاكس المتسامح مع الأخطاء، المحرك غير المتزامن، تشخيص الأخطاء، إعادة تكوين العاكس.*

# *Abstract*

Electrical systems can experience faults due to various reasons. These faults may occur as a result of aging components, conditions of use, or manufacturing defects that were undetectable during commissioning. The faults can be broadly classified into two categories: those that occur within the electrical machine such as winding faults and axis tilt, and those that occur outside the electrical machine in the drive chain, such as faults in the mechanical gearbox.

One major area of research is focused on monitoring the state of the converter that supplies power to an asynchronous machine. A converter, such as a Pulse Width Modulation (PWM) inverter, may have structural defects like malfunctioning switches (semiconductors) that could damage the entire system. It's crucial to invest in malfunction detection to prevent such defects from causing irreparable harm to the system.

Artificial intelligence (AI) based condition monitoring and diagnosis techniques offer various advantages over traditional methods. These techniques eliminate the need for mathematical models, which reduces engineering and development time significantly. AI-based techniques rely on system datasets or expert knowledge to make accurate predictions. In the case of controlling an induction motor powered by a PWM voltage inverter, AI-based methods can detect open circuit and/or short circuit faults and take corrective measures to ensure the system operates efficiently while maintaining the required level of security.

In this thesis, we analyzed the feasibility of using artificial intelligence techniques in detecting, diagnosing, and reconfiguring faults in a three-phase inverter that powers an induction motor. We provided a detailed description of inverter switching faults and developed a simple method to extract characteristics for studying the possibility of detecting and diagnosing these defects. We also attempted to reconfigure the inverter system to prevent faults from occurring.

**Keywords:** *Fault Classification, Fault Tolerant Inverter, Asynchronous Motor, Fault Diagnosis, Inverter Reconfiguration.*

# *Résume*

Les systèmes électriques peuvent rencontrer des pannes pour diverses raisons. Ces défauts peuvent survenir suite au vieillissement des composants, aux conditions d'utilisation ou à des défauts de fabrication indétectables lors de la mise en service. Les défauts peuvent être globalement classés en deux catégories : ceux qui surviennent au sein de la machine électrique comme les défauts de bobinage et d'inclinaison des axes, et ceux qui surviennent à l'extérieur de la machine électrique dans la chaîne d'entraînement, comme les défauts de la boîte de vitesses mécanique.

Un domaine de recherche majeur porte sur la surveillance de l'état du convertisseur qui alimente une machine asynchrone. Un convertisseur, tel qu'un onduleur à modulation de largeur d'impulsion (PWM), peut présenter des défauts structurels tels que des commutateurs (semiconducteurs) défectueux qui pourraient endommager l'ensemble du système. Il est crucial d'investir dans la détection des dysfonctionnements pour éviter que ces défauts ne causent des dommages irréparables au système.

Les techniques de surveillance conditionnelle et de diagnostic basées sur l'intelligence artificielle (IA) offrent divers avantages par rapport aux méthodes traditionnelles. Ces techniques éliminent le besoin de modèles mathématiques, ce qui réduit considérablement le temps d'ingénierie et de développement. Les techniques basées sur l'IA s'appuient sur des ensembles de données système ou des connaissances d'experts pour effectuer des prédictions précises. Dans le cas du contrôle d'un moteur à induction alimenté par un onduleur de tension PWM, les méthodes basées sur l'IA peuvent détecter les défauts de circuit ouvert et/ou de court-circuit et prendre des mesures correctives pour garantir le fonctionnement efficace du système tout en maintenant le niveau de sécurité requis.

Dans cette thèse, nous avons analysé la faisabilité d'utiliser des techniques d'intelligence artificielle pour détecter, diagnostiquer et reconfigurer les défauts d'un onduleur triphasé qui alimente un moteur à induction. Nous avons fourni une description détaillée des défauts de commutation de l'onduleur et développé une méthode simple pour extraire les caractéristiques afin d'étudier la possibilité de détecter et de diagnostiquer ces défauts. Nous avons également tenté de reconfigurer le système d'onduleur pour éviter que des pannes ne se produisent.

**Mots-clés:** *Classification de défauts, Onduleur Tolérant aux Défauts, Moteur asynchrone, Diagnostic de Défauts, Reconfiguration d'onduleur.*

# Contents

# List of Figures

# List of Tables

# ABBREVIATIONS

ANN : Artificial Neural Network

ANFI : Adaptive Neuro - Fuzzy Interference System

ASM: Asynchronous machine

BNN : Biological Neural Network

CNN : Convolutional Neural Network

DTC : Direct Torque Control.

DTC-SVM : Direct Torque Control- Space Vector Modulation

DSC : Direct Self-Control

ELM : Extreme learning machine

FFT : Fast Fourier transformation

FLC : Fuzzy Logic Control

FOC : Field Oriented Control

MSE : Mean Squared Error

MOM : Mean-max membership

MLP : Multiple Layer Perceptron

OCF : Open-Circuit Fault

PWM : Pulse With Modulation

RNN : Recurrent Neural Network

SLP : Single Layer Perceptron

SVM : Space-Vector Modulation

SCF: Short-Circuit Fault

t-SNE : t-Distributed Stochastic Neighbor Embedding

VSI : Voltage-Source Inverter

WRFA : Weighted Random Forests Algorithm

$S_a, S_b, S_c$ : Inverter switches

$\phi_s$ :Stator flux

$T_e$ :Electromagnetic stator Torque

$\theta_s$ : Stator flux position

$U_s$ : Voltage stator vector

$\omega_r$ : Motor Speed

$K_\phi$ : Amplitude of hysteresis flux comparator

$K_T$ : Amplitude of hysteresis torque comparator

$I_s$ : Stator currant vector

$p$ : Number of Pole Pair of Induction Motor

$(\phi_{s\alpha}, \phi_{s\beta})$ : Estimated Flux Magnitudes

($I_a$,$I_b$ ,$I_c$) : Currant in three dimension vector

($I_{s\alpha}$,$I_{s\beta}$) : Currant in two dimension vector

($V_{s\alpha}$,$V_{s\beta}$) : Voltage in two dimension vector

($S_\alpha$,$S_\beta$) : Surface Currant Calculation In Two Dimension From Feature Extraction

($V_\alpha$,$V_\beta$) : Voltage In Two Dimension From Fast Fourier Transformation

# GENERAL INTRODUCTION

In the mid-1980s,a new technique for the torque control of induction motors well-known as Direct Torque Control (DTC) [1]. Shortly after, M. Depenbrock introduced Direct Self Control (DSC) [2]. These two techniques are referred to conventional DTC. Since their inception, they have undergone continuous development and improvement by numerous researchers. DTC is known for its simple structure and excellent dynamic behavior. However, it has several drawbacks, the most significant of which is variable switching frequency.

Recently, a new control technique called Direct Torque Control - Space Vector Modulated (DTC-SVM) has been developed from the classical DTC methods. This new method eliminates the disadvantages of classical DTC and operates with a constant switching frequency. The DTC-SVM strategies are based on the same fundamentals and drive analysis as classical DTC, and they are the main subject of this thesis.

AC drives may face various issues with different components such as stator winding, inverter arm cut, switching device, DC bus, rotor and stator, drive chain, faults, and power supply [3]. Switching devices are susceptible to faults due to their frailty [4]. Many electrical power system defaults have already been invented and published to address these issues [5].

To manage induction motors, intelligent algorithms have been advanced, such as Artificial Neural Networks (ANN) [6], Fuzzy Logic Control (FLC) [7], and Adaptive Neuro-Fuzzy Interference System (ANFIS).

Artificial Neural Networks (ANN) are based on the human brain's functioning and modeled as a network of connected neurons. It can be used to address various computer-based application problems in different industries. However, before a neural network can solve problems, it needs to be trained [8]. Fuzzy logic control is gaining attention from many scientists worldwide

as it can control a system without knowing its mathematical model. It uses the experience of people's knowledge to form its control rule base [9].

To achieve accurate fault diagnosis with neural networks, it is essential to have appropriate features. Researchers have now started using deep neural networks to automatically extract features from raw data. However, when dealing with signals using Convolutional Neural Networks (CNN), it is necessary to convert the raw data into an image using various techniques [10].

A study will be conducted on the assembly of the induction motor and voltage inverter. Control structures will be implemented for the induction motor powered by an inverter that can tolerate various types of faults. Solutions based on detection techniques and self-adaptation to failure using artificial intelligence such as fuzzy and neural will be employed to ensure the safety and dependability of the motor-inverter system. These solutions will involve the development of estimators, comparison and decision-making algorithms, as well as substitution commands to control the system in the presence of failure.

The thesis is comprised of six chapters. Chapter one provides an overview of control strategies employed for induction motors and the current condition of inverter fault diagnosis. Chapter Two covers artificial intelligence. In Chapter Three, we analyze the diagnosis system using artificial intelligence. Here, we select two types of control strategies, DTC and DTC-SVM, and perform diagnosis using both fuzzy logic and neural network. Chapter Four presents a diagnosis of multiple Open Circuit faults in neural direct torque control of induction motor drive using neural networks. In this chapter, we implant an artificial neural network in DTC command after diagnosis using a neural network. Chapter Five discusses the use of a type of deep learning convolution neural network, CNN AlexNet, for Open Switch fault detection in a phase inverter feeding induction motor. In the last chapter, we explain the present three-phase inverter reconfiguration, which solves the problem when a fault is detected and located in the inverter. Finally, we conclude.

# Chapter 1

# State of the art for induction motor control strategies and inverter fault diagnosis

## 1.1 Introduction

Induction motors (IMs) have developed since their creation and gradually replaced DC motors to become the most widely used electric machine in the sector [11]. In the beginning, IMs were chosen for constant speed applications due to their robustness, compactness, low production cost, and ease of maintenance. Accurate speed control applications have been added to the scope of IMs in recent years due to the rapid growth of power electronics [12].

Scalar control and vector control are two important groupings of approaches in the field of speed control. The voltage/frequency ratio is often controlled as a constant in the scalar method. Scalars have the benefits of being inexpensive, having an easy control algorithm, and not requiring sensors. Scalar control techniques are so frequently employed in low-performance applications. However, because of its inability to properly manage the moment, it is unsuitable for applications requiring rapid dynamics or exact speed and torque control [13].

Although the vector control approach has limitations, such as challenging control algorithms and complex hardware design, it is dependable and suitable for applications with high precision requirements [14, 15]. Field Oriented Control (FOC) and direct self-control (DSC) are the two primary methods used in the vector control technology. The stator flux space vector is the key control technique of the DSC method, whereas the rotor flux angle is the primary control technique of the FOC method for controlling the current's components [12]. The controller

needs the feedback signal from the current, rotor speed, and voltage sensors to carry out the control orders in the FOC approach.

We call these techniques conventional DTC. Numerous researchers have been working to continuously enhance and improve them since 1985. DTC's key characteristics are its excellent dynamic behavior and straightforward structure. Nevertheless, there are a number of drawbacks to traditional DTC, the most significant of which being its changeable switching frequency. Direct Torque Control – Space Vector Modulated (DTC-SVM) is a novel control approach that was created recently to replace the traditional DTC methods. The strategies of this methods is operates with constant switching frequency. The foundations and driving analysis of structures are the same as those of classical DTC. The DTC-SVM approach that is being presented has a straightforward structure and offers dynamic behavior that is similar to traditional DTC. However, in steady state operation, the DTC-SVM approach is distinguished by significantly improved parameters [16]

## 1.2 Modulation Techniques

### Carrier-Based Pulse-Width Modulation (PWM)

Carrier-Based Pulse-Width Modulation (PWM) is a technique used in electronic systems to control the amount of power delivered to a load by varying the pulse width of a constant-frequency carrier signal. PWM offers simplicity in implementation and flexibility in control parameters. This modulation technique is widely used in power electronics, motor control, and communication systems [17]. In this technique, the reference signals $(U_{AC}, U_{BC}, U_{CC})$ are compared with a triangular carrier signal $(U_t)$ to generate three logical signals $(S_a, S_b, S_c)$ that define the switching instants of the power transistors. This method is often referred to as "comparator-based PWM."

As is shown in Fig. 1.1, the triangular carrier signal is a waveform that linearly increases from a minimum value to a maximum value and then resets to the minimum value. This signal provides the timing reference for generating the PWM signals. The reference signals $(U_{AC}, U_{BC}, U_{CC})$ represent the desired output voltages or currents that need to be controlled. They are typically sinusoidal waveforms in applications such as motor control or can be any other desired waveform based on the specific application requirements. The reference signals $(U_{AC}, U_{BC}, U_{CC})$ are individually compared with the triangular carrier signal $(U_t)$ using comparators. When the reference signal amplitude is higher than the carrier signal, the corresponding comparator

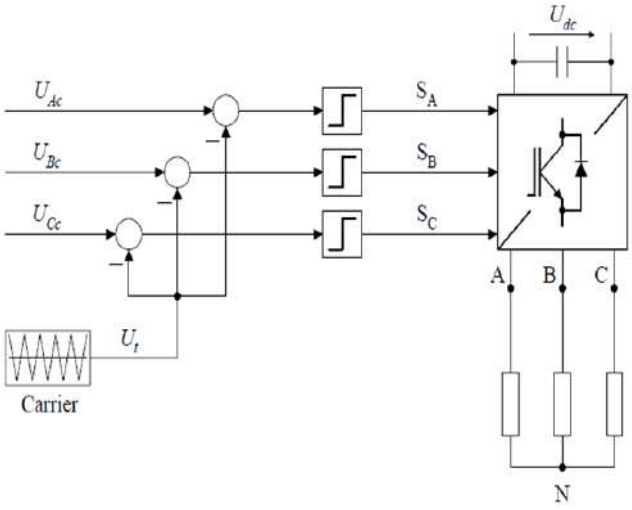


Figure 1.1: Block scheme of carrier based sinusoidal PWM [18]

outputs a logical high signal; otherwise, it outputs a logical low signal. The outputs of the comparators form the logical signals $S_a, S_b$ and $S_c$. These signals indicate the switching states of the power transistors [18].

## Space-Vector Modulation (SVM)

Space-Vector Modulation (SVM) is a popular technique used in power electronics to control the output voltage of three-phase inverters. It is commonly employed in applications such as motor drives, renewable energy systems, and power converters. SVM offers several advantages over other modulation techniques, including better output voltage quality, reduced harmonics, and improved efficiency. Figure 1.2 illustrates the process of SVM implementation, which generally involves three stages: first, identifying the sector; second, determining the region; and third, selecting a suitable switching sequence. [19]

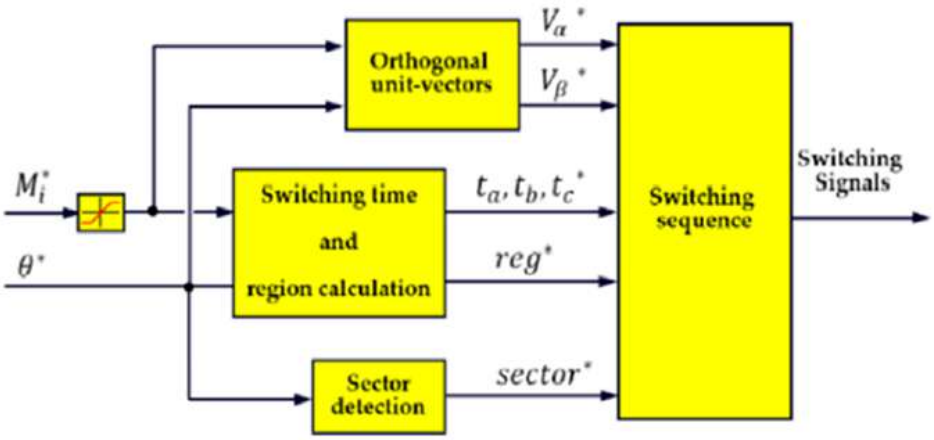


Figure 1.2: Space Vector Modulation (SVM) model [19]

## 1.3 Overview of Control Methods for Three-Phase Induction Machines

The methods used for controlling Induction Motors (IM) can be categorized into scalar and vector control techniques. Figure 1.3 illustrates the overall classification of IM control strategies based on variable frequency control [18,20]. The following section provides a brief overview of both types of methods.

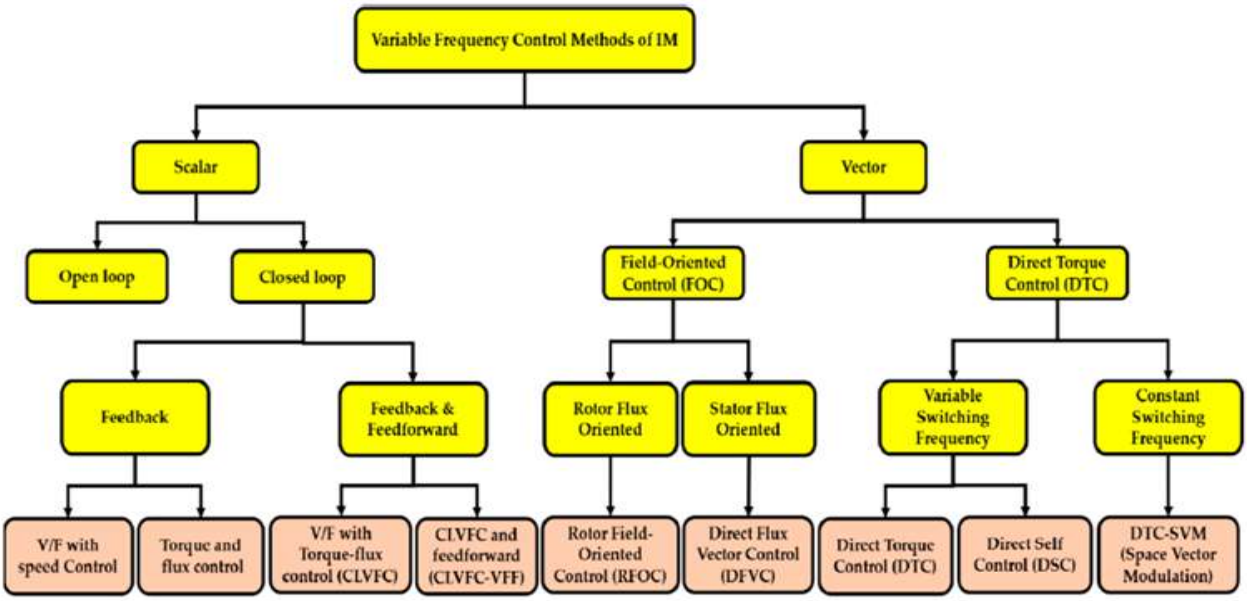


Figure 1.3: Control methods for IMs [19]

### Scalar based controllers

Scalar control methods, also known as V/f control or Volts per Hertz control, are simple and widely utilized in pumps, fans, and other simple industrial applications where precise control is not a primary requirement. Scalar control methods are suitable for many applications that do not require high-performance control. Here are the key scalar control methods used in induction motors:

1. **Open-Loop V/f Control**

   In open-loop V/f control, the V/f ratio is kept constant for the entire speed range of the motor. The voltage and frequency are varied together. It is widely used in industry. A shown in figure 1.4, feedback signal are not required. This type of motor control is advantaged due to its low cost and simplicity. However, this method lacks torque control, limiting access to the desired torque only at the nominal operating point. If the load

torque varies, it leads to corresponding changes in the motor's speed [21-25].

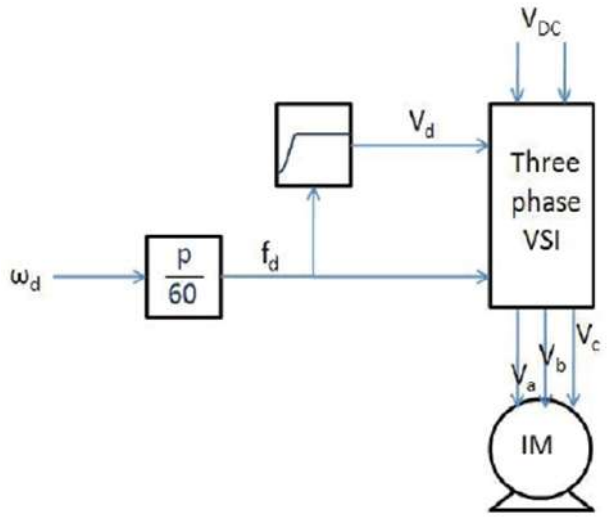


Figure 1.4: Open-Loop V/Hz constant Control [25]

2. **Closed Loop V/f Control**

The closed-loop approach outperforms the open-loop method in speed control. Additionally, it also regulates the torque. Within the closed-loop system, a slip control loop is incorporated since slip is directly related to torque. The system compares the actual speed with the target speed, and the disparity is minimized to zero through the PI controller, ensuring the motor achieves the desired speed efficiently. This technique does not allow the control of the magnetic flux [21, 24].

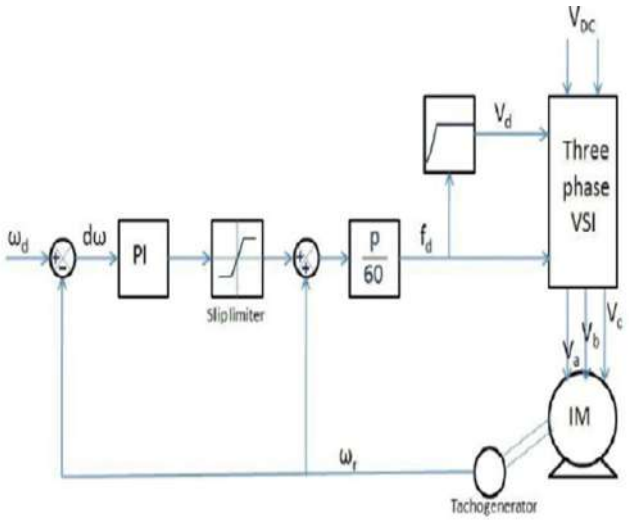


Figure 1.5: Closed-Loop V/Hz constant Control [25]

## Vector-based controllers

Vector control methods, also known as Field-Oriented Control (FOC) or Direct Torque Control (DTC), offer more precise and sophisticated control of induction motors. Vector control decouples the control variables, such as torque and flux, allowing independent control of these quantities. Vector control methods are more complex and require additional sensors and control algorithms compared to scalar control. However, they offer superior control precision, faster dynamic response, and improved efficiency over a wide range of operating conditions. Scalar control, on the other hand, is simpler and more cost-effective, suitable for applications where precise control is not critical.

1. **Field Oriented Control (FOC)**

   FOC is one of the vector control strategies that has the ability to control the torque and flux separately [26- 28]. The reference torque and flux are generated by the voltage, current, and speed parameters from the induction motor [29].

2. **Direct Torque Control (DTC)**

   Direct Torque Control (DTC) is a popular vector control technique that directly regulates torque and flux in an induction motor. It involves estimating the stator flux and torque components based on the motor model and measured or estimated quantities. DTC provides excellent control performance and fast torque response, making it suitable for high-performance applications. DTC with a constant switching frequency calculates the required stator voltage vector over a sampling period to achieve the desired torque and stator flux. This section is more detailed in Chapter 3.

3. **Direct Torque Control- Space Vector Modulation (DTC-SVM)**

   A good and quick response can be achieved in an induction motor with DTC control by directly controlling the torque and stator flux without regulating the current. In order to minimize high flux and torque ripples and achieve a fixed switching frequency, space vector modulation has been used. This section is more detailed in Chapter 3.

4. **Direct-Self Control (DSC)**

   Direct-Self Control (DSC) is an advanced control technique that enables precise control of motor speed and torque with reduced complexity and improved performance. DSC is based on the principle of directly controlling the stator flux and torque of the motor. It eliminates the need for complex mathematical calculations and uses a simpler algorithm

to achieve control. Similar to Direct Flux and Torque Control (DTC), DSC also does not require a speed sensor for feedback.

## 1.4 Inverter fault diagnosis

### Structure of the voltage source inverter

The basic structure of the voltage source inverter is shown in figure (1.6). It contains six Insulated-Gate Bipolar Transistors (IGBT)$T_i i = 1, ..., 6$ which work complimentary and six freewheel diodes$D_i i = 1, ..., 6$. The inverter provides entirely balanced 3-phase sinusoidal currents and voltages [30-31].

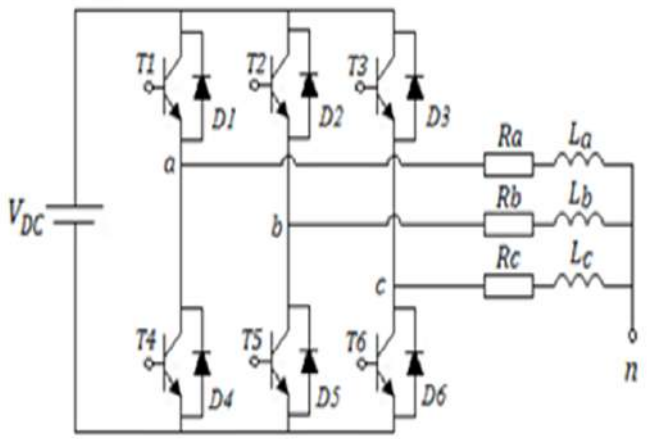


Figure 1.6: Drawing of a VSI feeding three-phase induction motor

The voltage source inverter faults are subdivided into short and open circuits. In the open switch fault, the IGBT remains off state. Open-circuit faults do not cause system shutdown, the system continue functioning in degradation mode. In the short circuit case, an overcurrent is detected by the standard protection system, and shutdown is carried out.

### Open circuit faults

Open circuit faults can be classified into three categories: single switch faults, double switch faults in the same bridge arm, and double switch faults in different bridge arms. All possible faults are shown in table 1.1 [32].

1. **Single open switch fault**

Consider the scenario of an open switch fault, specifically when switch $T_1$ is open. In this situation, during the positive half-cycle of the input AC voltage, current cannot flow through phase A via the upper bridge arm, resulting in zero output current for phase A. This absence of current in phase A disrupts the balance of the three-phase system, leading to distorted currents in the remaining phases during this half-period. However, during the negative half-cycle, when the current is in the negative range, phase A current can circulate through the lower bridge arm using the freewheel diode $D_4$. In this configuration, the currents in all three phases remain undistorted during this half-period.This analysis applies similarly to other switches in the system, as described in reference [32].

2. **Double-switch faults in the same bridge arm**

   In the scenario of a double switch fault occurring within the same bridge arm, the current in the considered phase is zero. As a result, the currents in the remaining phases become distorted; they are out of phase.

   For example if T2 and T5 are open,[32]. $i_a(t) = -i_c(t)$

3. **Double-switch faults in different bridge arms**

   In this scenario, where both switches T1 and T2 are open, specific conditions arise.Within the interval $[2k\pi, 2k\pi + 2\pi/3]$, the current in phase A becomes zero due to the open switch fault in T1 . Concurrently, the current in phase B becomes negative and flows through diode D5. Phase C experiences a slightly distorted but generally normal current flow. Notably, the currents in phases B and C are in opposition, meaning they flow in opposite directions during this interval. In the intervals $[2k\pi + 2\pi/3, 2k\pi + \pi]$, the current in phase A remains at zero due to a fault in switch T2 . Consequently, phase B , which should be positive, also remains inactive. Since both phases A and B have zero current, phase C is forced to be at zero as well. In the interval $[2k\pi + \pi, 2k\pi + 5\pi/3]$, phase A 's current flows through freewheel diode D4 , while phase B 's current stays at zero. This situation causes a distortion in phase C 's current. Finally, in the last interval $[2k\pi + 5\pi/3, 2k\pi + 2\pi]$, all three currents flow normally through D4 and D5 in the upper bridge arm [32].

## Short circuit faults

When a short circuit occurs in an electrical system, the stator currents can increase significantly, potentially leading to catastrophic failure of the inverter and other connected components. Due to the rapid and intense increase in current during a short circuit, relying solely on stator

currents to detect such faults may not be practical or effective. It is essential to employ other protective measures, such as circuit breakers, fuses, or more sophisticated fault detection techniques like impedance-based methods or digital protective relays, to quickly and accurately identify short-circuit faults and prevent further damage to the system. These protective devices can respond much faster and are designed to handle such high-current situations, ensuring the safety and reliability of the electrical system [32].

Table 1.1: Faults types and location

| Fault types | Fault location |
|---|---|
| Healthy mode | - |
| Single open switch fault | T1, T2, T3, T4 T5, T6 |
| Double open-switch fault in the same bridge arm | T1-T4, T2-T5, T3-T6 |
| Double open-switch fault in different bridge arms | T1-T2, T1-T3, T1-T5, T1-T6 , T2-T3, T2-T4,T2-T6, T3-T4, T3-T6 T4-T5, T4-T6, T5-T6 |
| Single short-circuit fault | S1, S2, S3, S4 ,S5, S6 |

## Detection methods for open circuit faults in IGBTs

IGBTs (Insulated Gate Bipolar Transistors) are widely used in power electronics and are essential components in a variety of applications, including electric vehicles, renewable energy systems, and industrial automation. However, IGBTs are prone to faults, including open-circuit faults, which can cause system failures and damage to other components. Therefore, detecting open-circuit faults in IGBTs is crucial to ensure the reliability and safety of these systems.

There are several detection methods for open-circuit faults in IGBTs, including:

1. Voltage measurement method: This method involves measuring the voltage across the IGBT and comparing it to a threshold value. If the voltage is below the threshold value, it indicates that there is an open-circuit fault.

2. Current measurement method: This method involves measuring the current flowing through the IGBT and comparing it to a threshold value. If the current is below the threshold value, it indicates that there is an open-circuit fault.

3. Gate voltage measurement method: This method involves measuring the gate voltage of the IGBT and comparing it to a threshold value. If the gate voltage is below the threshold value, it indicates that there is an open-circuit fault.

4. Gate pulse width measurement method: This method involves measuring the width of the gate pulse and comparing it to a threshold value. If the pulse width is below the threshold value, it indicates that there is an open-circuit fault.

5. Emitter current measurement method: This method involves measuring the emitter current of the IGBT and comparing it to a threshold value. If the emitter current is below the threshold value, it indicates that there is an open-circuit fault.

These methods can be implemented using hardware-based or software-based solutions, depending on the application requirements. Additionally, advanced techniques such as machine learning and artificial intelligence can be used to improve the accuracy and speed of fault detection in IGBTs. Overall, detecting open-circuit faults in IGBTs is essential to ensure the safe and reliable operation of power electronics systems.

## Research in open-circuit fault in 3-phase inverter-fed induction motors

Open-circuit faults (OCF) and short-circuits faults (SCF) are common types of faults that can occur in electrical power systems. Research in these areas typically focuses on developing methods for detecting, diagnosing, and mitigating these faults to improve the reliability and safety of power systems.

There has been significant research conducted on open-circuit fault (OCF) detection and diagnosis in 3-phase inverter fed induction motors. The technique proposed by Bo Wang et al. [33] for open-circuit fault diagnosis is based on voltage residual analysis and eliminates the need for extra voltage sensors. In this method, the characteristics of the reference voltage and the actual output voltage are analyzed under both normal (healthy) and faulty conditions. The paper likely discusses the theoretical framework, methodology, experimental setup, and evaluation of the proposed method for open-circuit fault diagnosis in modular multilevel converters. Another technique for diagnosing open-circuit faults based on feature extraction with JADE–ICA algorithm and neural network has been proposed by Hailin Hu et Al. in [34]. The finite element analysis is also conducted for open-circuit fault of multiple IGBTs switches in a PWM. In [35], the authors aim to investigate the effects of these faults on the performance of the induction motor using FEA modeling. The method described in reference [14] involves extracting a fuzzy basis by analyzing current vector patterns under various fault conditions. The goal is to use fuzzy logic to locate the faulty switch in the system. In the frequency domain analysis, the

Fourier transform [36] and wavelet-based multi-resolution analysis [37-38] are widely utilized techniques for detecting open-circuit faults in power-converter drives. For instance, in reference [36], the fault-signature spectrum derived from three-phase currents is utilized as a distinguishing feature. Additionally, a dimensionally reduced Fast Fourier Transform (FFT) employing principal component analysis is proposed in this context. Meanwhile, in another approach described in [38], wavelet coefficients serve as the feature vector. Principal component analysis is applied to reduce the dimensionality of this feature vector [39,40]. The resulting feature vector is then employed in classification tasks using various machine learning algorithms, including linear classifiers such as k-nearest neighbors (kNN), decision trees, support vector machines (SVM), and neural networks (NN) [4,41]. Open-circuit fault diagnosis with neural networks is treated as a pattern recognition challenge [5,42-45], involving two essential stages: feature extraction and fault classification.

In the time domain, features are directly derived from the three stator currents or the Clark currents transform [6,46]. For instance, features like current angle and diameter were considered in reference [7]. These features are effective for classifying single faults. To address the detection of multiple faults, mean, surface, and angle parameters extracted from Clark currents are taken into account [47-48].

Nevertheless, the effectiveness of neural networks in fault diagnosis significantly relies on the choice of features used. These features act as the foundation for fault diagnosis. As a result, researchers have increasingly turned to deep neural networks to automatically extract relevant features from raw data. In the context of working with signals, utilizing Convolutional Neural Networks (CNN) necessitates the transformation of raw data into images. Various techniques are employed to accomplish this conversion, enabling CNNs to process and analyze the data effectively. [37-39].

## 1.5 Conclusion

In this chapter, a detailed comparative analysis of scalar and vector control strategies for railway traction applications has been discussed, with a special focus on their operation at high speeds. This study has reviewed several faults types in 3-phase inverter fed induction motors which are a common problem in industrial applications, and there has been significant research in this area in monitoring and fault diagnostic. Different failure detection and diagnosis-based methodologies in 3-phase inverter such as open or short circuit were explored from the prior literature, highlighted their advantages and disadvantages.

# Chapter 2

# Diagnosis system for DTC and DTC-SVM using Artificial Intelligence

## 2.1 Introduction

Direct Torque Control (DTC) is widely used in permanent magnet synchronous motor control with its simple control mode, fast torque response, and strong perturbation of internal parameters and external disturbance [47]. It has been examined during the last decade in the area of AC drives. This control strategy was confirmed by Takahashi in 1986 [1].

From the conventional DTC techniques, a new control strategy called as Direct Torque Control-Space Vector Modulated (DTC-SVM) has recently been developed. This innovative strategy gets rid of the drawbacks of the conventional DTC. Basically, DTC-SVM strategies are methods that employ a constant switching frequency [18]. The described DTC-SVM technique has a simple structure, exhibits dynamic behavior, and dramatically improves parameters during steady-state operation [47]. The modeling of inverters and induction motors has been covered extensively in numerous articles [48–54].

Inverters feeding induction motors are key element in driving process at variable speeds. Most common inverter faults are mainly caused by damaged power semiconductor switches. Power semiconductor switch faults can be divided into short- circuit faults and open circuit faults. The detection of open or short-circuit switches fault in power converters have been extensively studied [43,55-56].

By applying the Fast Fourier Transform and sum surface algebraic feature extraction techniques, we will investigate the potential for fault detection and diagnosis for short and open circuit faults in the inverter. The chapter makes use of fuzzy logic control and artificial neural

networks to accomplish this purpose. However, the features that are employed are crucial for problem identification and have a significant impact on the neural network's performance. Because of this, researchers are now using deep neural networks to automatically extract features from unprocessed data. It is well known that working with signals on convolutional neural networks (CNNs) necessitates employing several strategies to transform the raw input into an image [57–59].

The chapter summaries the Direct Torque Control (DTC) principle in the second section. The third section is dedicated to introducing the DTC-SVM. Section four describes the concept of feature extraction for diagnosing. The fifth section involves the application of Artificial Neural Networks (ANN) and Fuzzy logic control to diagnose issues in both DTC and DTC-SVM-IM settings. Finally, conclusion.

## 2.2 DTC Basic

### Basic Principle of DTC

Two control loops corresponding to the stator flux and torque magnitudes. The reference values for torque and flux $(\phi_s^*, T_e^*)$ are compared with actual values $(\phi_s, T_e)$, inducing errors that feed into two hysteresis blocks. The outputs from these hysteresis blocks, as well as the stator flux position $(\theta_s)$, serve as inputs to the switching table. Using these errors and the position of the stator flux, the inverter is switched on via six-region control. As a result, the inverter operates in six-step operation with six active vectors and two zero vectors, as shown in Figure 1. The inverter output voltage vector is adjusted to minimize flux and torque errors and define the direction of the flux rotation, as demonstrated by previous works cited from sources numbered [43,60-61].

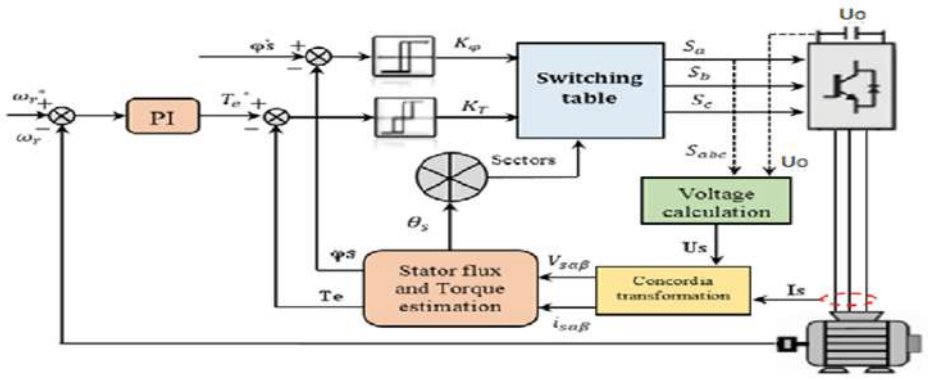


Figure 2.1: Basic DTC block diagram.[62]

1. Voltage calculation

   The inverter output Us is obtained via the switching status (Sa,Sb and Sc) and the DC voltage source that fed the inverter $U_0$. It is formed as follows [125-128]:

$$U_s = \sqrt{\frac{2}{3}} U_0 \left[ S_a + S_b \exp\left(i\frac{2\pi}{3}\right) + S_c \exp\left(i\frac{4\pi}{3}\right) \right] \tag{2.1}$$

2. Clarke-Concordia transformation

   The line currents of the three phases with respect to the neutral are represented in the $\alpha\beta$ -reference frame by a simple vector addition of these three-phase variables. These two new vectors are obtained by applying the Clarke-Concordia transformation. Therefore, the measured currents ($I_{sa}$,$I_{sb}$ ,$I_{sc}$) are transformed into two dimensions ($I_{s\alpha}$,$I_{s\beta}$) by [56]:

$$\begin{cases} I_\alpha = \dfrac{2}{3} I_a - \dfrac{1}{3} I_b - \dfrac{1}{3} I_b \\ I_\beta = \dfrac{1}{\sqrt{3}} \left( \dfrac{1}{3} I_b - \dfrac{1}{3} I_b \right) \end{cases} \tag{2.2}$$

   Also the voltage ($V_{s\alpha}$,$V_{s\beta}$) obtained by applying the Clarke-Concordia transformation. The stator voltages in $\alpha\beta$ -reference frame are determined as:

$$\begin{cases} V_{s\alpha} = \sqrt{\dfrac{2}{3}} U_0 (S_a - \dfrac{1}{2}(S_b - S_c)) \\ V_{s\beta} = \dfrac{1}{\sqrt{2}} U_0 (S_b - S_c) \end{cases} \tag{2.3}$$

3. Flux and Torque Estimator

   The estimator calculates the stator flux and the electromagnetic torque. are given by:

$$\overline{\phi_s} = \int_0^t (\overline{V_s} - R_s \overline{I_s})\, dt \tag{2.4}$$

$$\overline{\phi_s} = \phi_{s\alpha} + i\phi_{s\beta} \tag{2.5}$$

$$\begin{cases} \phi_{s\alpha} = \int_0^t (V_{s\alpha} - R_s I_{s\alpha})\, dt \\ \phi_{s\beta} = \int_0^t (V_{s\beta} - R_s I_{s\beta})\, dt \end{cases} \tag{2.6}$$

$$\phi_s = \sqrt{\phi_{s\alpha}^2 + \phi_{s\beta}^2} \tag{2.7}$$

The angle $\theta_s$ is given by equation 8.

$$\theta_s = \arctan \frac{\phi_{s\beta}}{\phi_{s\alpha}} \tag{2.8}$$

The electromagnetic torque can be estimated from the estimated flux magnitudes $\phi_{s\alpha}$,$\phi_{s\beta}$ and the calculated magnitudes of the current $I_{s\alpha}$,$I_{s\beta}$ It is evaluated by equation 9.

$$T_e = \frac{3}{2} p(I_{s\beta}\phi_{s\alpha} - I_{s\alpha}\phi_{s\beta}) \tag{2.9}$$

p: pole number

4. PI Controller

   A common cascaded control method in variable-speed motor drives is PI control. Using this method, PI controllers are applied to the DTC drive's speed as well as the flux, torque, and speed of the DTC-SVM drive. A PID controller is utilized in the speed control mode, and its input is the difference between the motor's real speed and the reference speed. In the event of saturation, anti-windup is employed to accurately modify the regulator's integral action. Achalhi, Jnayah, and other authors' works are quoted in support of these conclusions. [67–71]

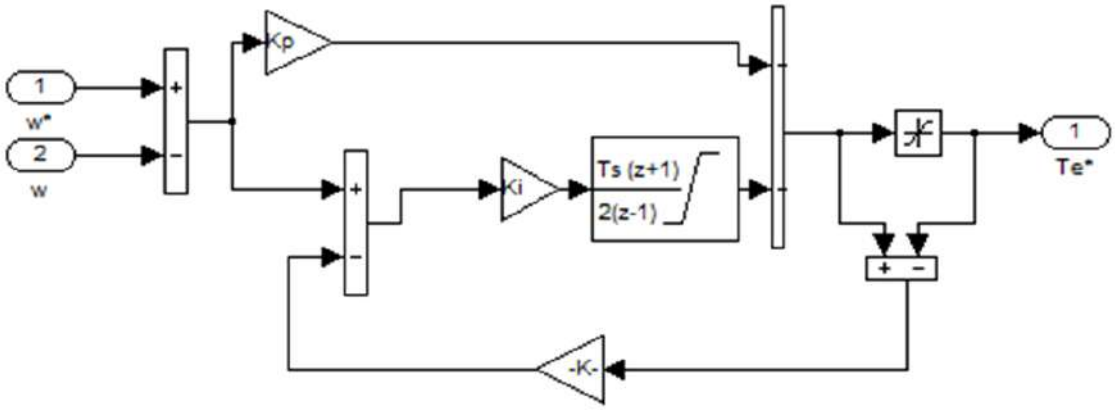


Figure 2.2: Structure of the speed PI controller with anti-windup [67,72].

## 2.3 DTC-SVM Basic

### DTC-SVM Principle

The DTC-SVM operates at constant switching frequency. A scheme presented in Figure.3 has speed, torque and flux loops operating with PI controllers [133,135].The motor speed ($\omega_r$) is sensed using a speed sensor, which converts the mechanical speed into an equivalent voltage value compared with the reference speed($\omega_r^*$ ).The speed error is processed through a PI controller, generating the reference torque ($T_e^*$).The reference torque is compared with the estimated torque ($T_e$), generating the torque error , which is handled through a torque PI controller ($V_q^*$). The estimated flux ($\phi_s$), is compared with the reference flux ($\phi_s^*$), and the flux error is processed through a flux PI controller, generating ($V_d^*$).Ones ($V_d^*, V_q^*$) are obtained, the transformation of variables from the synchronous to stationary frame ($\alpha\beta$) using ($\theta_s$) estimator, then injected into the SVM modulation block which generates the inverter control orders. Equations (2) and (3) describe the calculation to obtain Currents ($I_a$,$I_b$ ,$I_c$) and voltage ($V_a$,$V_b$ ,$V_c$) generated form inverter transformed into the stationary frame (d-q) to generate ($V_{sd}, V_{sq}, I_{sd}, I_{sq}$) that used to estimate torque, flux and sector ($T_e, \phi_s, \theta_s$) [18,49,53,60 ,74].

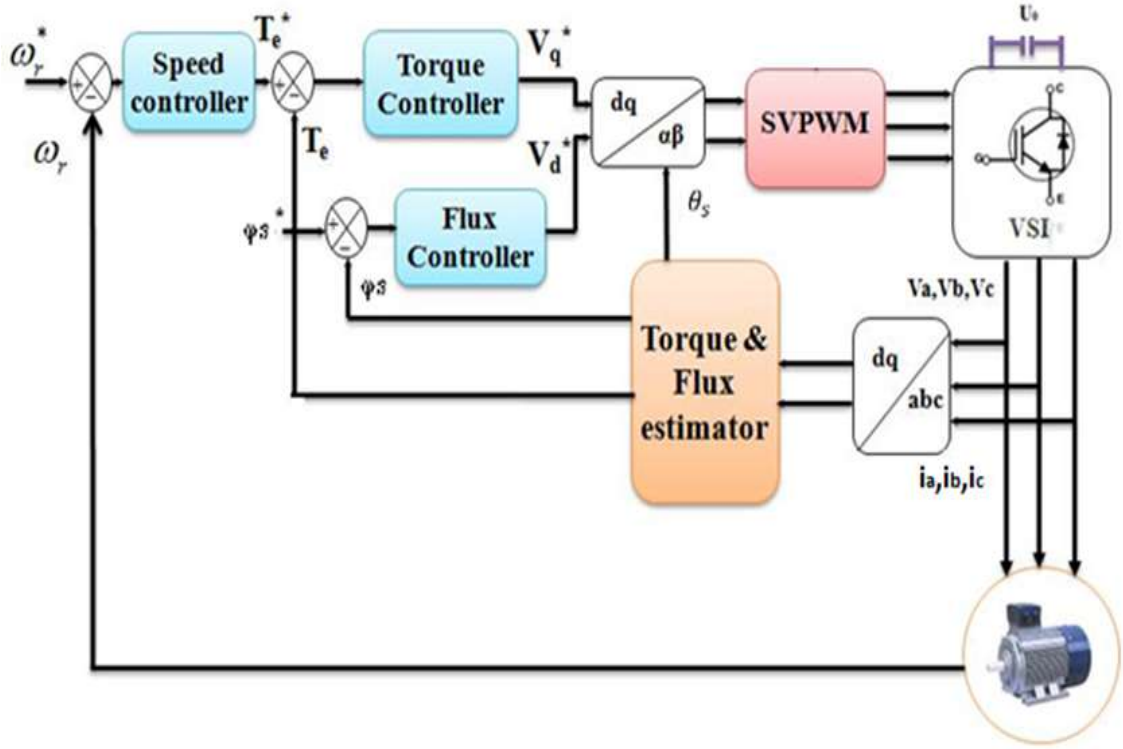


Figure 2.3: Block diagram of DTC-SVM of Induction motor [53].

Output voltages in $(d-q)$ reference of the PI regulators are transferred into $(\alpha-\beta)$ reference.

$$V_\alpha = V_d^* \cos(\theta) - V_q^* \sin(\theta) \tag{2.10}$$

$$V_\beta = V_d^* \cos(\theta) + V_q^* \sin(\theta) \tag{2.11}$$

$$V_s = \sqrt{V_\alpha^2 + V_\beta^2} \tag{2.12}$$

$$V_{sd} = \frac{2}{3}V_a - \frac{1}{3}V_b - \frac{1}{3}V_c \tag{2.13}$$

$$V_{sq} = 0 + \frac{1}{\sqrt{3}}V_b - \frac{1}{\sqrt{3}}V_c \tag{2.14}$$

$$I_{sd} = \frac{2}{3}I_a - \frac{1}{3}I_b - \frac{1}{3}I_c \tag{2.15}$$

$$I_{sq} = 0 + \frac{1}{\sqrt{3}}I_b - \frac{1}{\sqrt{3}}I_c \tag{2.16}$$

$$\begin{cases} \phi_{sd} = \int_0^t (V_{sd} - R_s I_{sd})\, dt \\ \phi_{sq} = \int_0^t (V_{sq} - R_s I_{sq})\, dt \end{cases} \tag{2.17}$$

$$\phi_s = \sqrt{\phi_{sd}^2 + \phi_{sq}^2} \tag{2.18}$$

$$\theta_s = \arctan \frac{\phi_{sq}}{\phi_{sd}} \tag{2.19}$$

$$T_e = \frac{3}{2}p(I_{sq}\phi_{sd} - I_{sd}\phi_{sq}) \tag{2.20}$$

## 2.4 Simulation (DTC and DTC SVM)

- SIMULATION FOR DTC

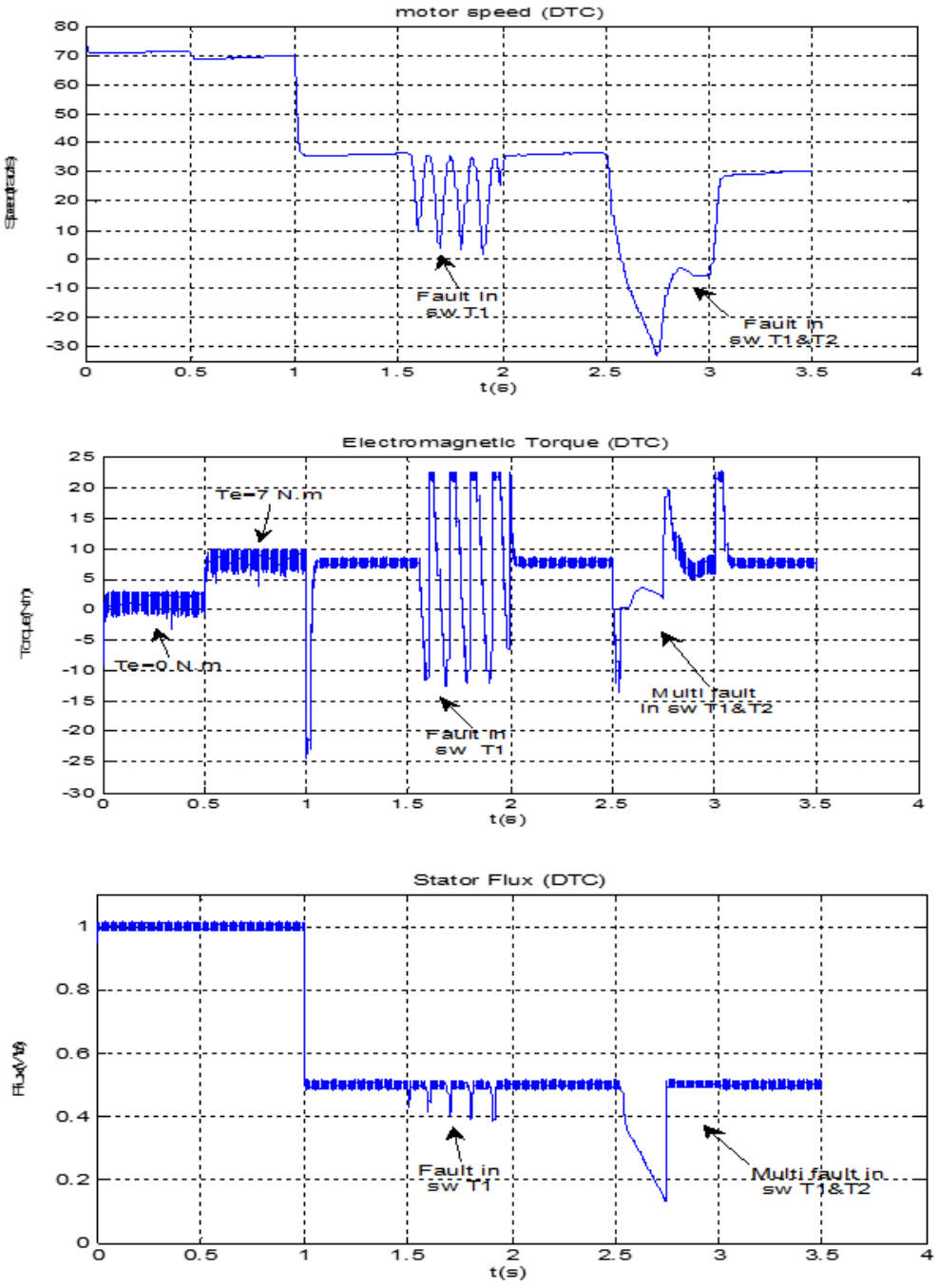


Figure 2.4: Basic DTC Simulation in Permanent State for a Speed, Torque, Flux Variation in healthy and faulty Mode.

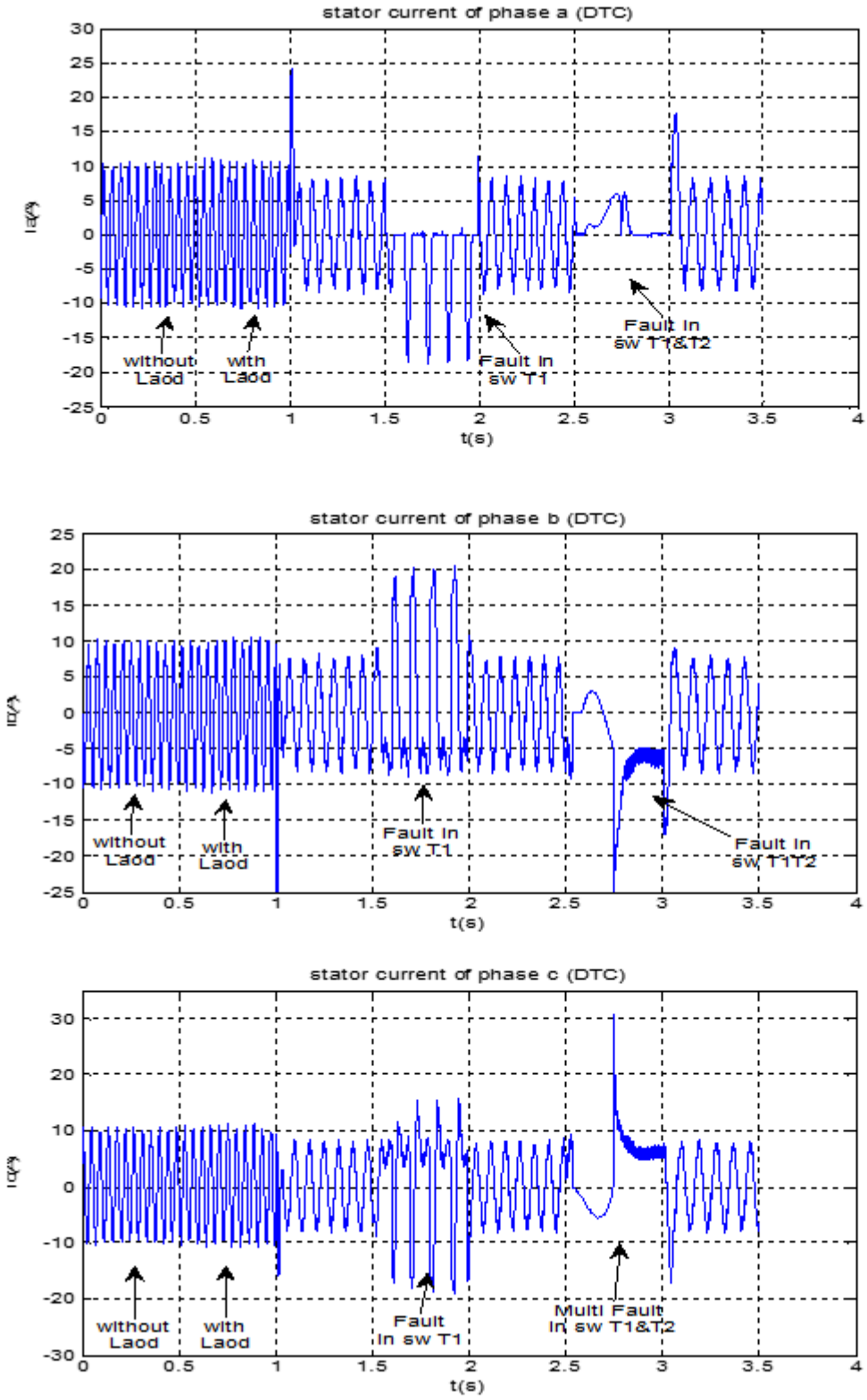


Figure 2.5: Basic DTC Simulation in Permanent State for currents Variation in healthy and faulty Mode.

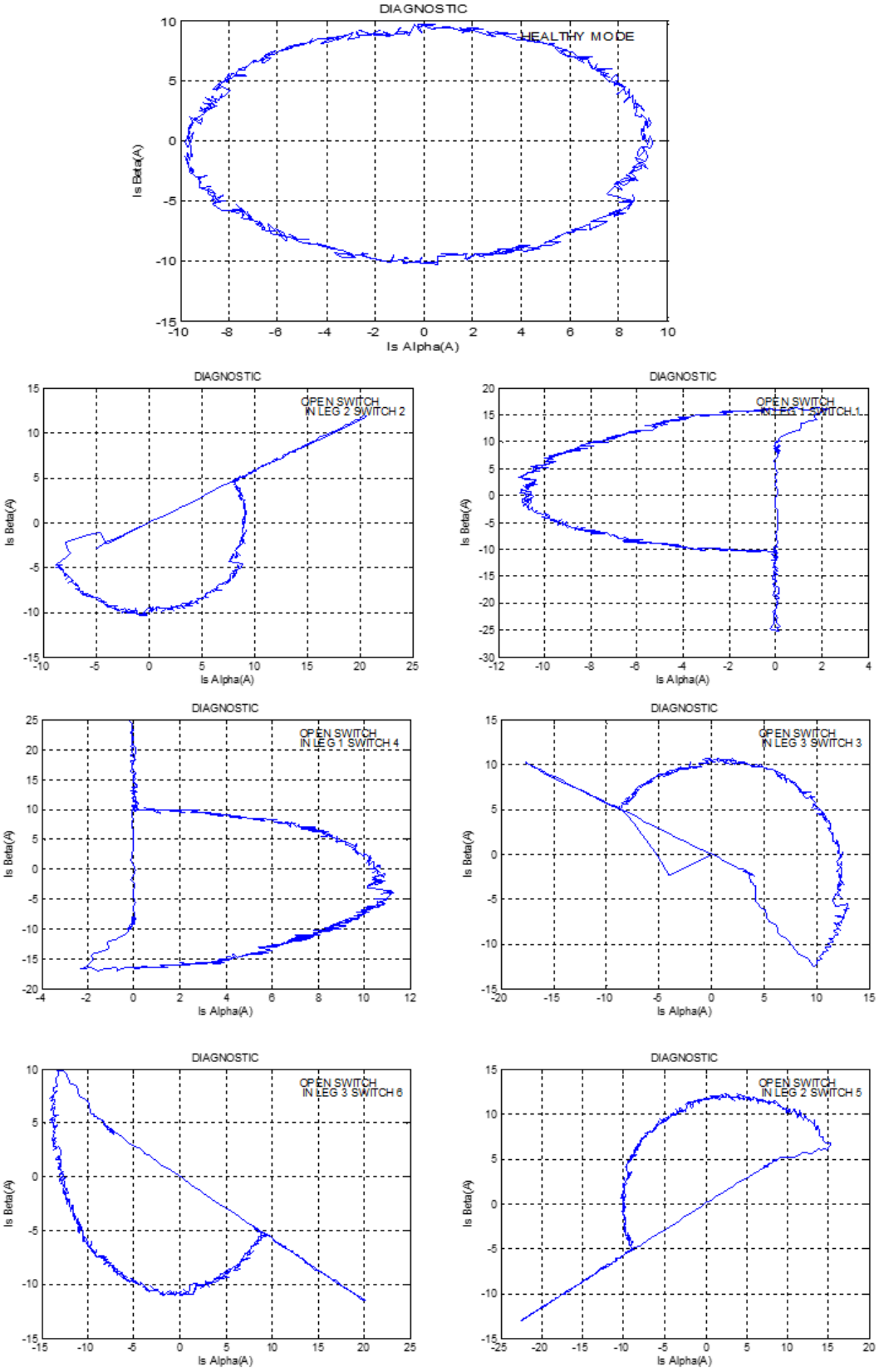


Figure 2.6: Fault current patterns in healthy and faulty Mode in DTC (open switch).

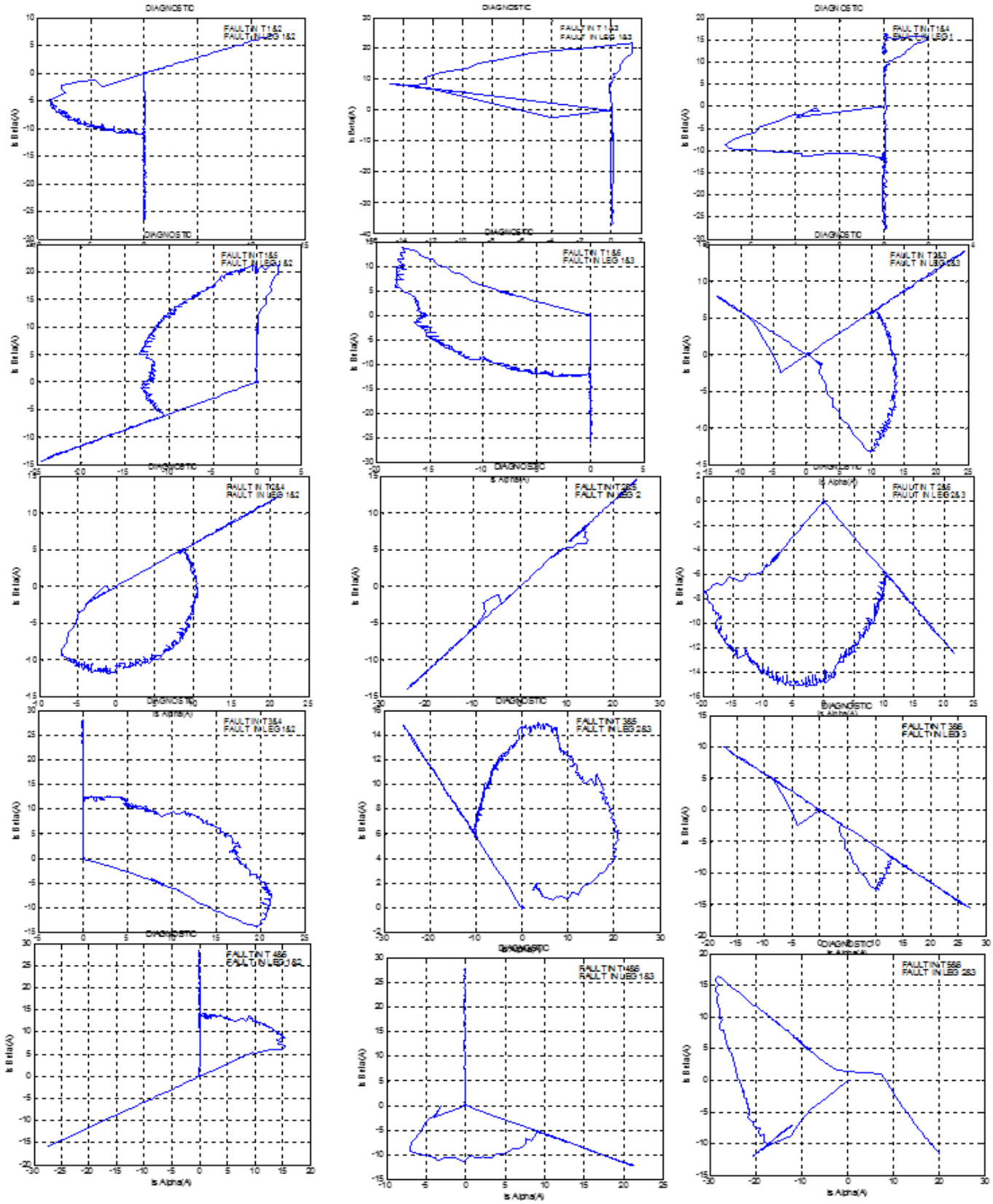


Figure 2.7: Fault current patterns in multiple faults Mode in DTC

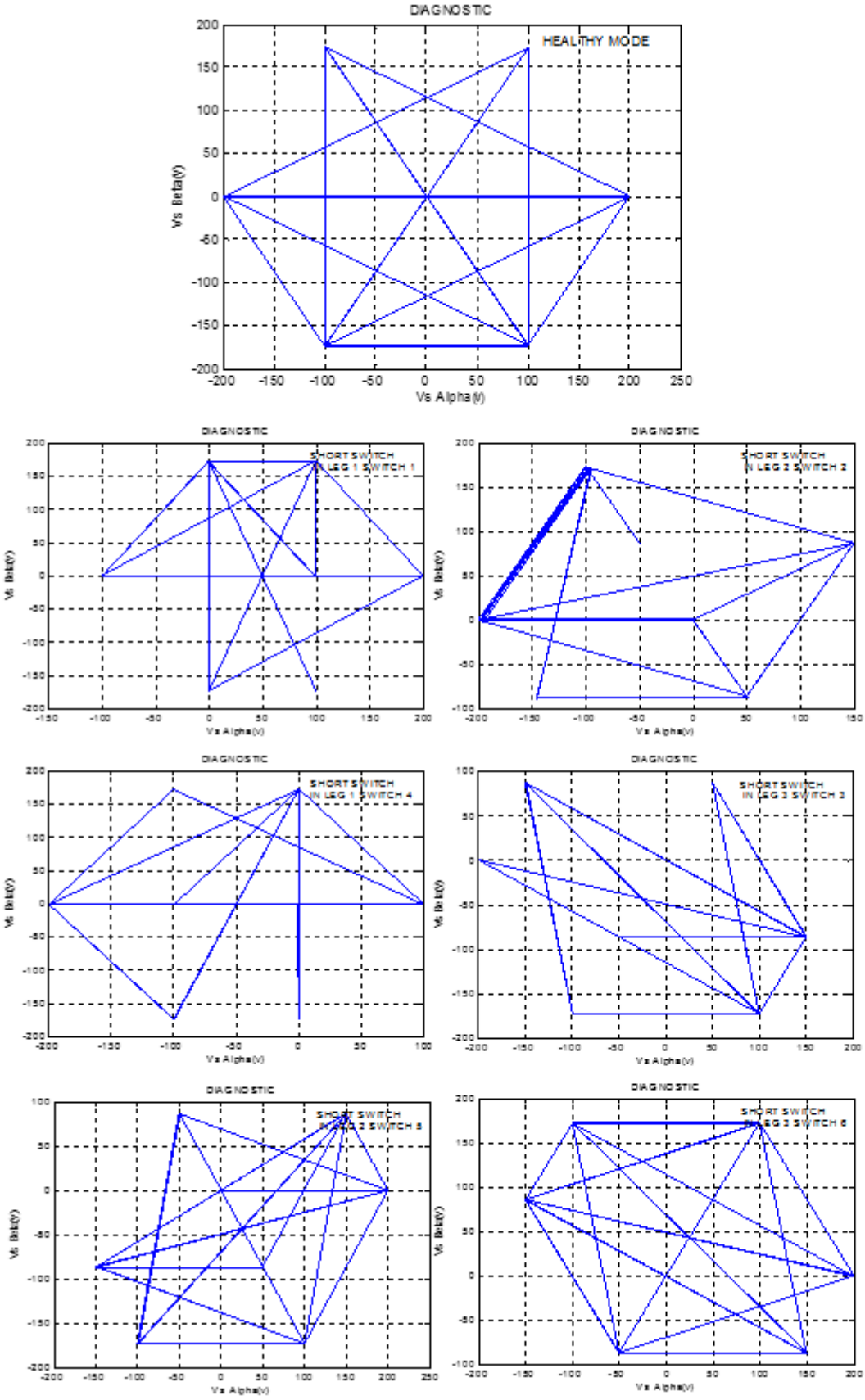


Figure 2.8: Fault voltage patterns in healthy and faulty Mode in DTC (short witch)

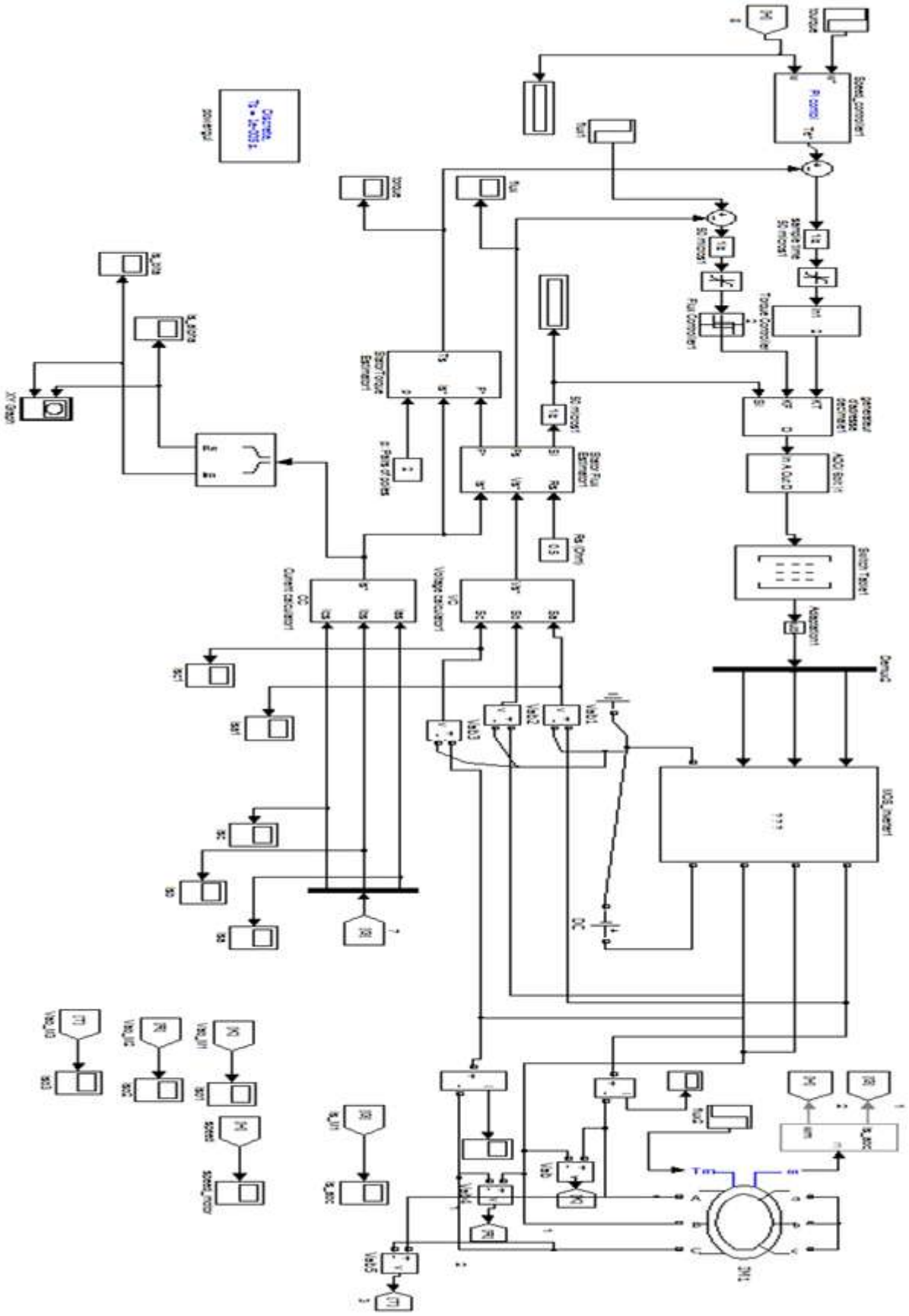

Figure 2.9: Matlab/Simulink block diagram of PWM inverter controlled by DTC

- SIMULATION FOR DTC-SVM

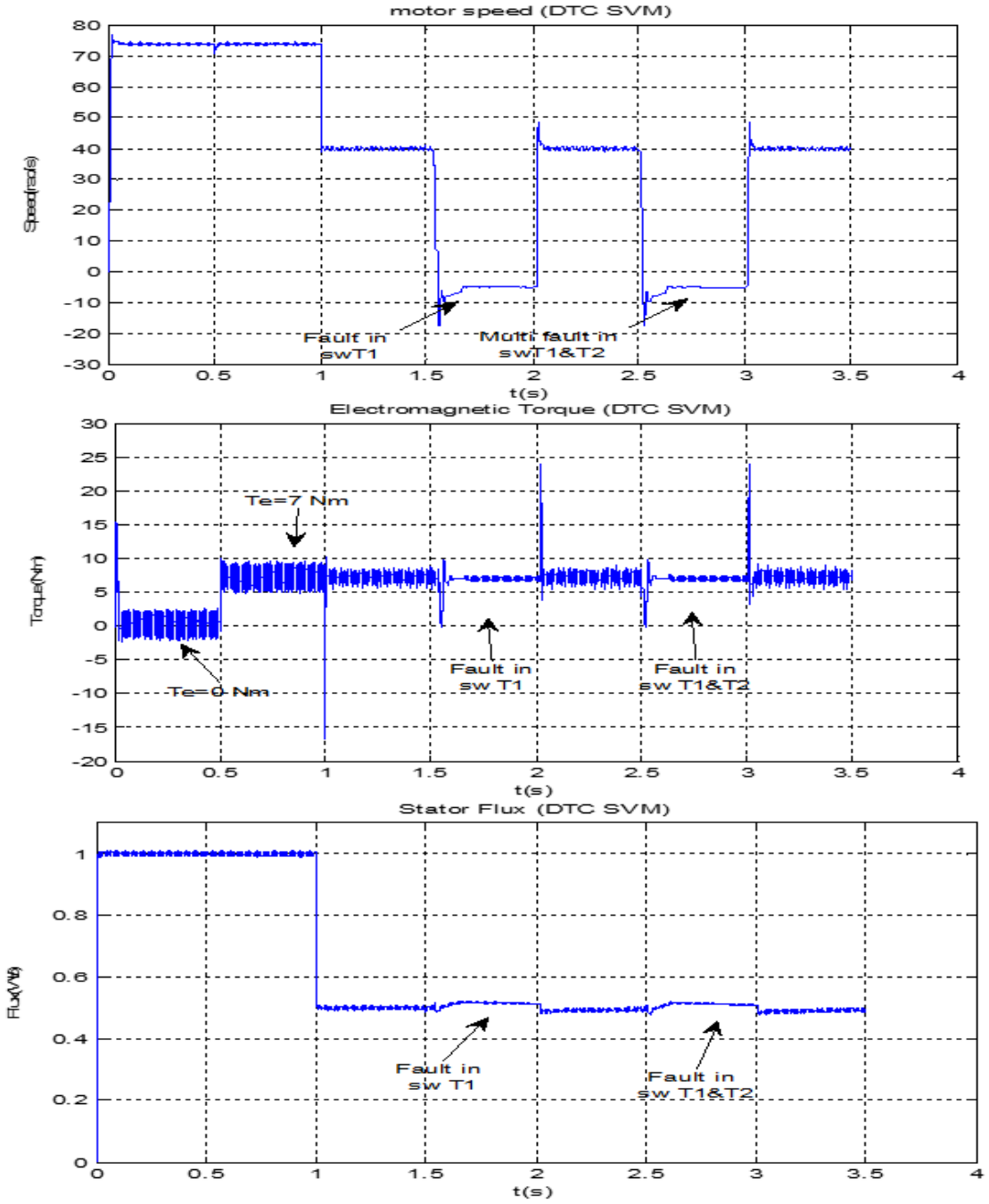


Figure 2.10: Basic DTC-SVM Simulation in Permanent State for a Speed, Torque, Flux Variation in healthy and faulty Mode

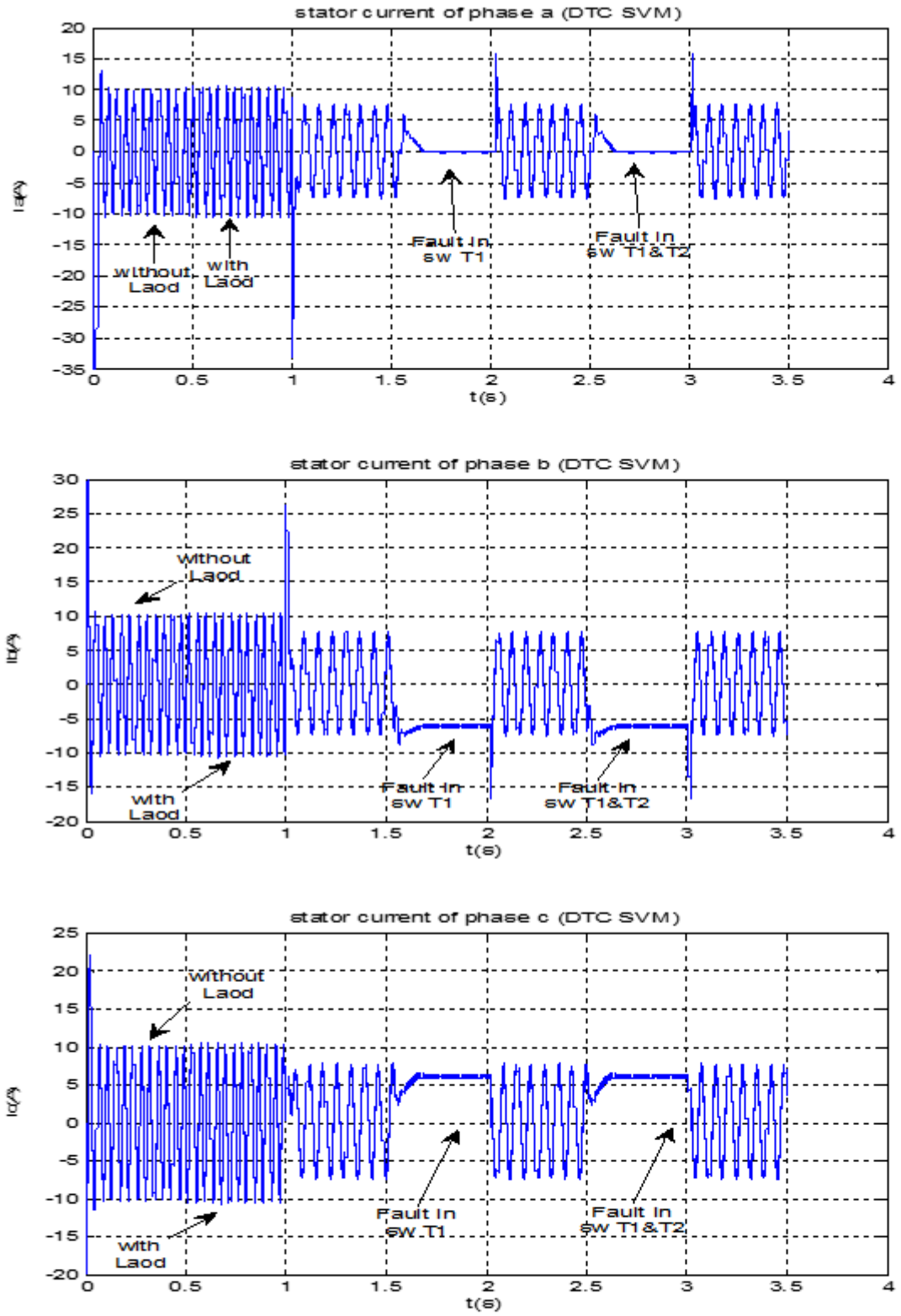


Figure 2.11: Basic DTC-SVM Simulation in Permanent State for currents Variation in healthy and faulty Mode

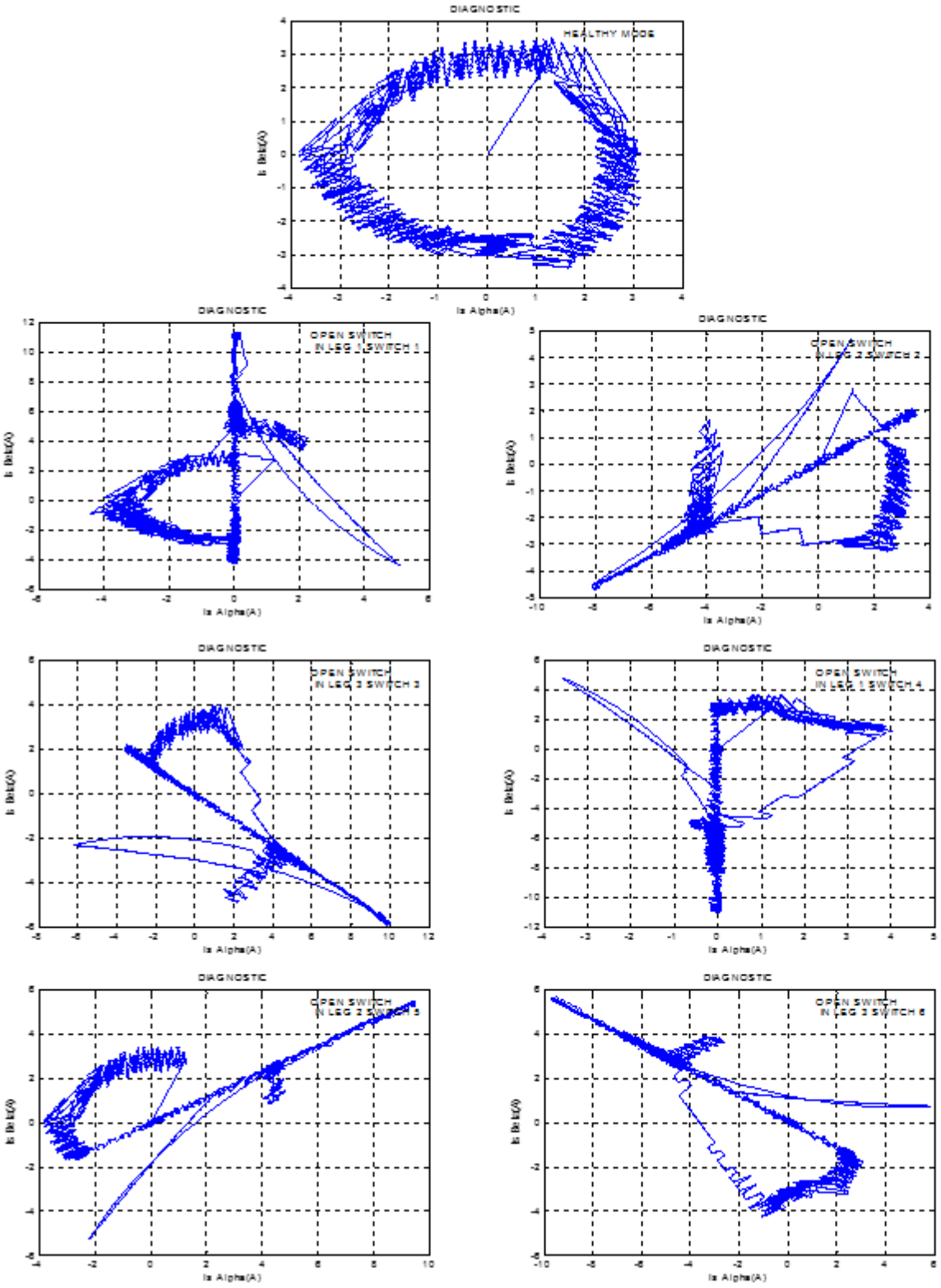


Figure 2.12: Fault currant Patterns in faulty and healthy Mode in DTC-SVM (open witch).

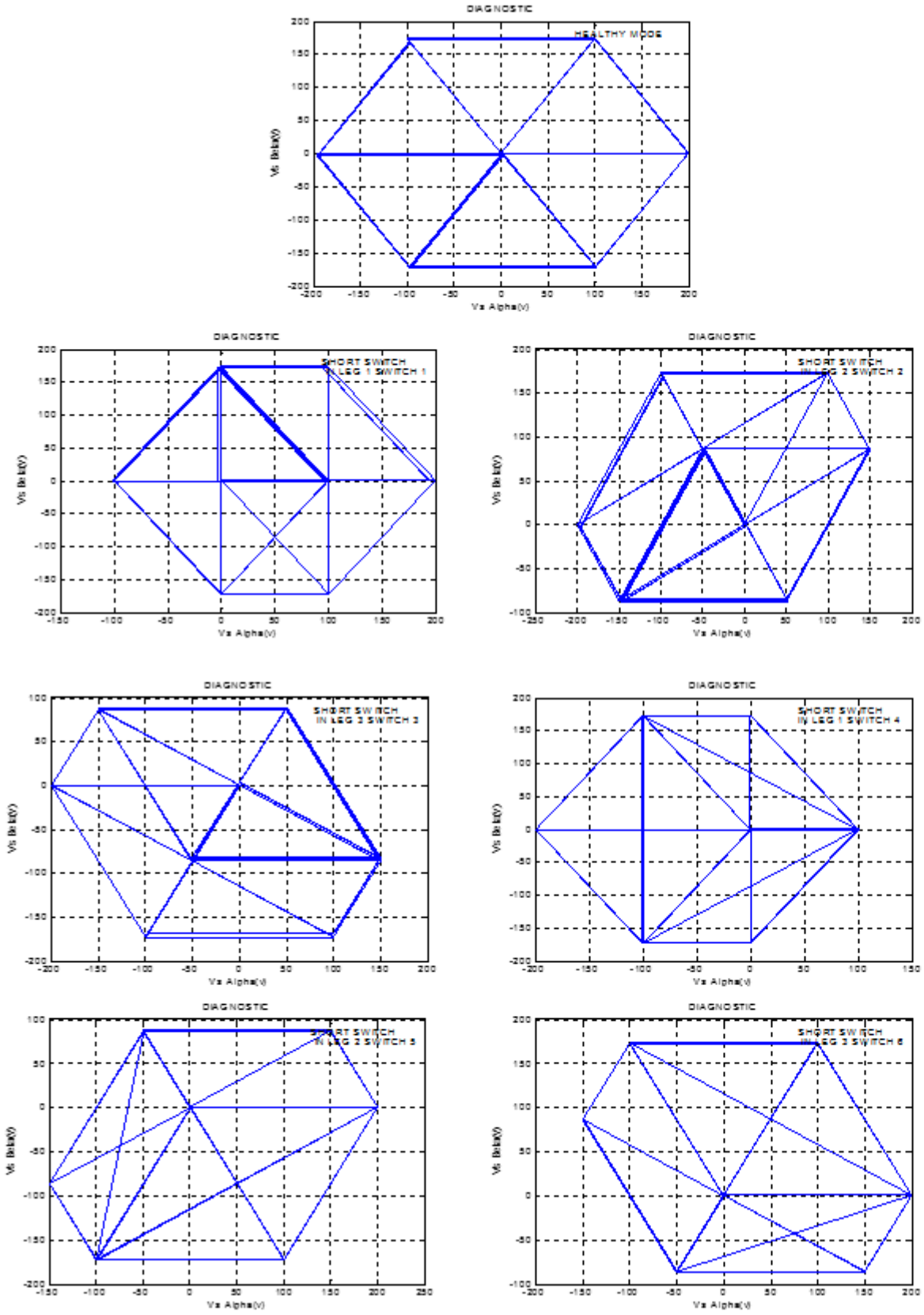


Figure 2.13: Fault voltage patterns in healthy and faulty Mode in DTC-SVM (short witch).

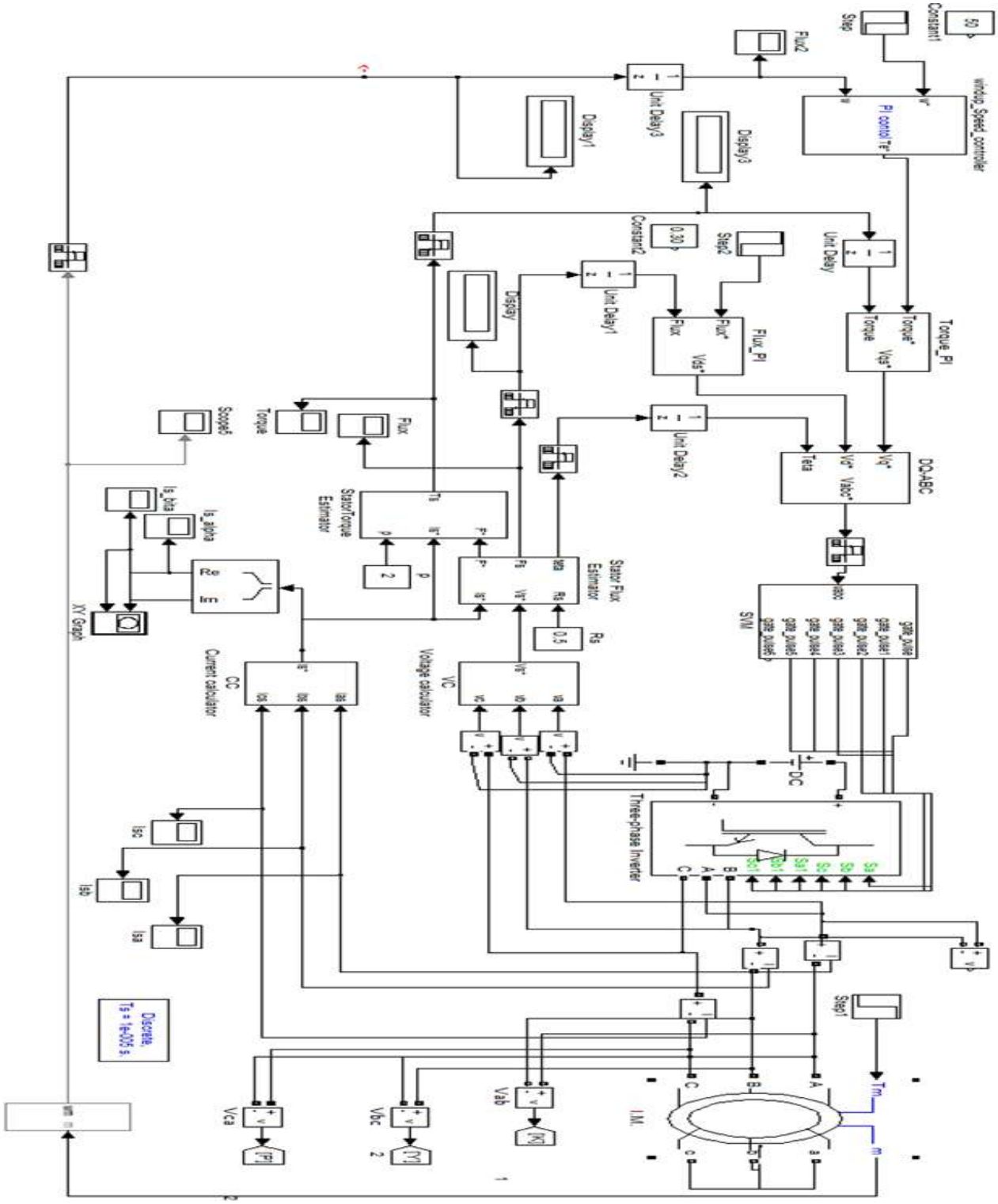


Figure 2.14: Matlab/Simulink block diagram of PWM inverter controlled by DTC-SVM

## 2.5 Discussing the result of simulation

A reference speed of 70 rad/s and a reference flux of 1Wb were fixed between 0 and 1s .Load is integrated to the motor at second 0.5s. After, these desired parameters were changed to 40 rad/s and 0.5Wb respectively. Between 1.5s and (2s), we made an open-switch fault at T1, removed at second 2s. And Between 2.5s and (3s) we made a double faults in T1 and T2, removed at second 3s. As shown in Figure 4&9.

- **Open circuit faults**

  Open circuit faults can be classified into three categories: single switch faults, double switch faults in the same bridge arm, and double switch faults in different bridge arms.

  - *Single open switch fault*

    To see the effect of an open switch fault, consider the case when the switch T1 is open. The current cannot flow in the phase A through the upper bridge arm when this current is positive; the output current of phase A is zero. During this half period, the phase current of the remaining phases are distorted due to the three-phase current balance. When the phase current is in the negative range, the current can flow in the phase A through the lower bridge arm via the freewheel diode D4. The three currents have no distortion in this half-period. The same reasoning remains valid for the other switches [75]. Shape in Figure 5 illustrate single faults in $(\alpha\beta)$ mode.

  - *Double-switch faults in the same bridge arm*

    In the case of a double switch fault in the same bridge arm, the current in the considered phase is zero. Consequently, the currents of the other phases are distorted; they are out of phase. For example if T1 and T4 are open, [75].

  - *Double-switch faults in different bridge arms*

    In this case, consider T1 and T2 are open. The current of phase A is zero following the open switch fault of T1. The current of phase B which is negative in this interval passes through the diode D5. The current of phase C passes normally but with a slight distortion. The currents of phases B and C are in phase opposition [75]. Shape in Figure 6 illustrate multiple faults in $(\alpha\beta)$ mode.

- **Short circuit faults**

  When a short circuit occurs, stator currents increase dramatically leading to catastrophic failure of the inverter [76]. So using stator currents to detect short-circuit fault is not practical. On the other hand, the normalized mean value of stator voltage in the $(\alpha, \beta)$

space for the six short-circuit switches are almost equal to zero, then the short-circuit switches fault cannot be distinguished. To remedy, the stator voltages in the frequency domain are used. Shapes in Figure 10 illustrate single faults in mode ($\alpha\beta$).

## 2.6 Feature extraction

### Feature extraction based on surface calculation

Feature extraction is critical for developing an efficient problem detection and diagnosis system from the output three-phase current signal. It was used to extract data and train a neural network to detect faults. Existing feature extraction approaches have limits in terms of accuracy and time and a lack of sufficient meaningful information in the classification set. Normalized functions should be universal for different reference speeds [64, 31,77].

We employ the extracted feature as an input to artificial neural network and fuzzy logic control, which aids in recognizing and identifying defects. It provides the opportunity to make a system more precise in fault patterns. Feature extraction mathematical model defined in equation (21) [74, 31]:

$$\begin{cases} S_\alpha = \frac{\sum_{i=1}^{N} I_{s\alpha}(i)}{length(I_{s\alpha}) * max(abs(I_{s\alpha}))} \\ \\ S_\beta = \frac{\sum_{i=1}^{N} I_{s\beta}(i)}{length(I_{s\beta}) * max(abs(I_{s\beta}))} \end{cases} \tag{2.21}$$

Where, N defines the number of samples contained in $I_{s\alpha,\beta}$. The choice of N depends on the diagnosis decision time.

Figure 15 shown data acquired under single multiple faults occurrence that will be used to train the neural network.

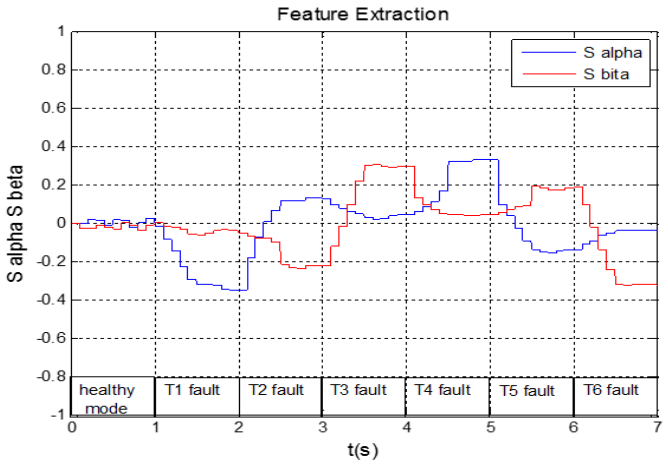


(a)

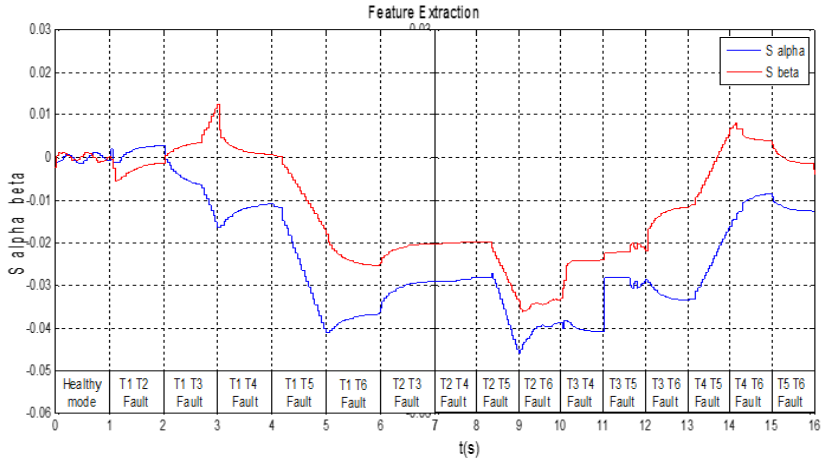


(b)

Figure 2.15: Feature extraction (a) under single fault, (b) under multiple fault occurrence

## Feature extraction based on Fast Fourier transformation (FFT)

The set of detailed signal spectrum values are typically decomposed from one domain to another via a sort of transformation known as the Fast Fourier transform, also referred to as the Fourier Transform (FFT). The signal spectrum that can be processed with a small number of data at each stage of the process is used to estimate the variation in the dataset. Induction motor defects can be found using this FFT algorithm variant. [77] the definition of the FFT.

$$X(k) = \sum_{n=0}^{N=1} x(n) e^{-j2\pi nk/N} \tag{2.22}$$

Where N defines the number of data samples.

K = 0,1,2. . . . . N-1

x(n) = time-domain discrete signal.

Selecting surface computation as the open circuit feature extraction method allows for the presentation of three symmetric levels (negative, zero, and positive) representing the upper switch default, the healthy switch, and the lower switch default. The data are arranged neatly, and classifying the faults will be straightforward. By manually opening the IGBTs gates in the Simulink model that is being used, we are able to create the dataset. The features for single and multiple open switch failures that were found using equation (21) are displayed in Figure 15. Stator currents cannot be used to detect short circuit faults that result in overcurrent, hence this method is not practicable. Additionally, the normalized mean voltage value is nearly zero. Because of this, a suitable substitute for short-circuit defect detection is the power spectrum. We have computed the Discrete Fourier Transform of the two voltage signals, $V_{s\alpha}$,$V_{s\beta}$, using the Fast Fourier Transform (FFT) in order to obtain the power spectrum [77]:

## 2.7 Diagnosis system for DTC and DTC-SVM

The structure bellow (Figure 16) illustrate deferent command techniques and implantation of artificial intelligent for diagnosis system. Figure 17 illustrate matlab Simulink block for

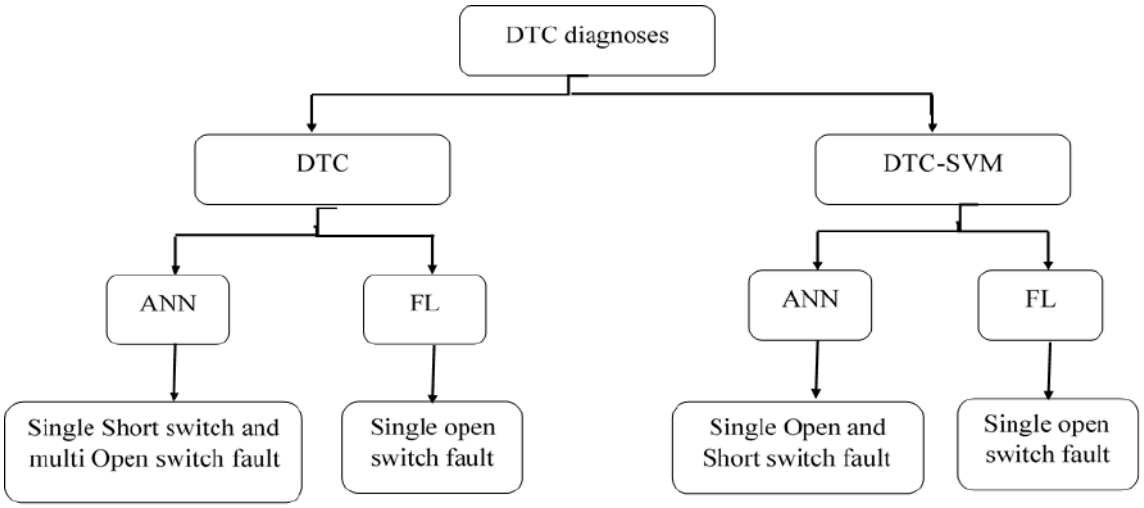


Figure 2.16: Structure of diagnosis system for DTC and DTC-SVM

diagnosis. In (Figure 17a), three stator currents $Is_{abd}$ calculate their surfaces ($Sa, Sb\ and\ Sc$) using feature extraction mathematical model defined in equation (21) diagnosing using fuzzy logic. In (Figure 17b), tow stator currents in mode ($S\alpha\beta$) $I_{s\alpha\beta}$ calculate their surfaces ($S_\alpha, S_\beta$) using the same feature extraction defined in equation (21) diagnosing using neural network.

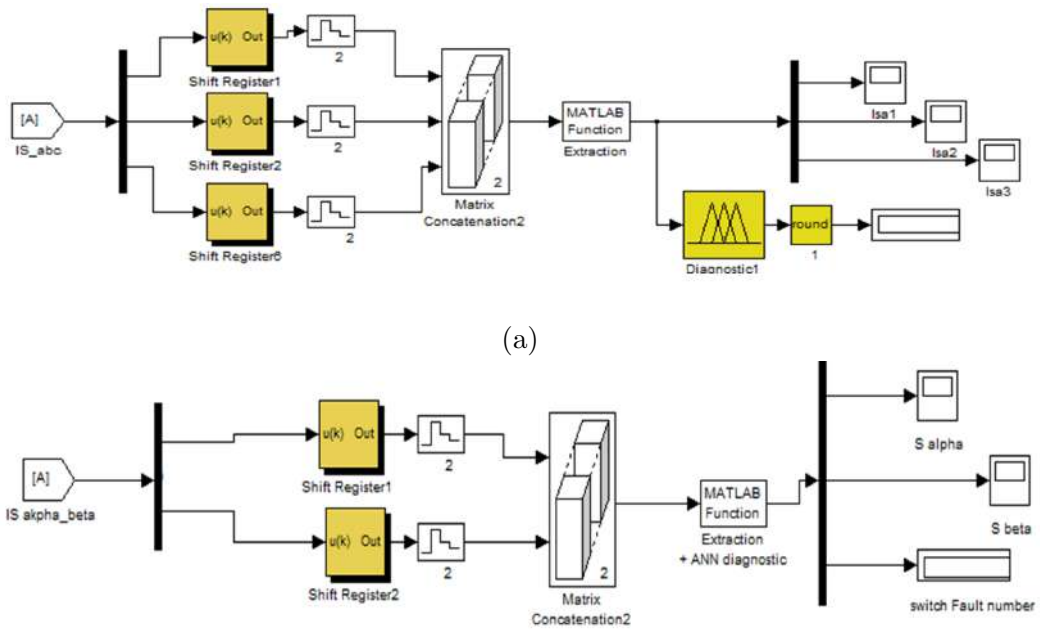


Figure 2.17: Matlab/Simulink block Diagnosis. (a) By using Fuzzy Logic (b) By using ANN

## Diagnosis DTC-ANN for open and short faults

### a) System of Fault Diagnosis

Figure 18 shows the proposed fault diagnosis system in open and short switch. Faulty switch

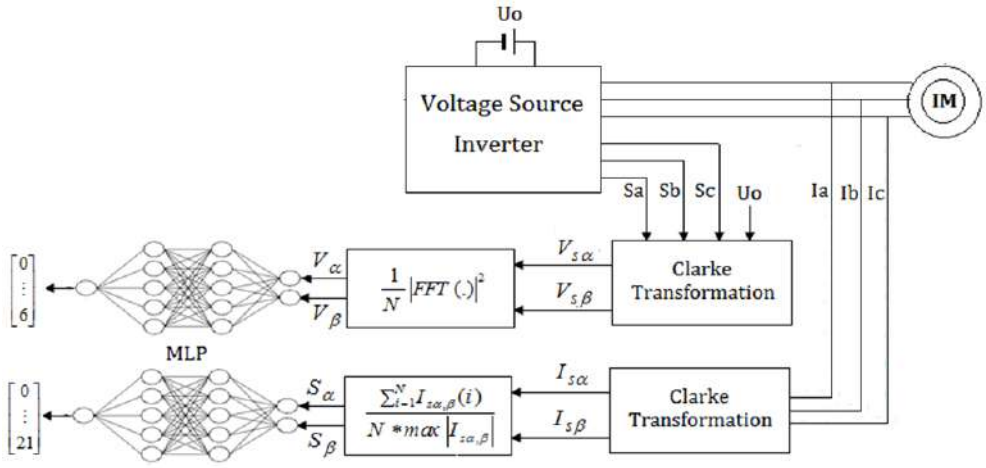


Figure 2.18: Matlab/Simulink block diagram of PWM inverter controlled by DTC-SVM

can be recognized in twenty-nine pattern, twenty-tow pattern for open switch, six-pattern for single fault and fifteen-pattern for multiple faults, a circle shape describes current pattern in healthy mode as illustrate in Figure. 6 and 7, and seven-pattern for single short switch. As illustrate in Figure.8

**b) ANN fault classification**

Neural networks have shown excellent performance in detecting open circuit faults. The main idea is to train a Multi layer Perceptron (MLP) from a data set consisting of input examples and their corresponding desired outputs. As shown in Figure.19, the architecture of the used MLP has two hidden layers $H_1, H_2$ with two input nodes corresponding to the surfaces $S_\alpha$,$S_\beta$in the open switches case and the power spectrums $V_\alpha$,$V_\beta$in the short-circuit case. The output can take values from 0 to 22 for the open switches case and from 0 to 6 in the short-circuit case. This architeture is adopted after multiple training.

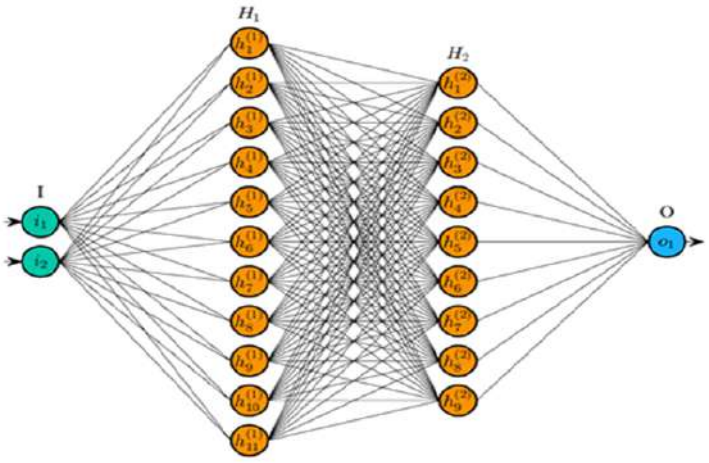


Figure 2.19: Matlab/Simulink block diagram of PWM inverter controlled by DTC-SVM

**c) Simulation Results**

- **Input / Output data**

  In order to create the dataset, we manually flip the switches open or closed, then we run the simulation with the desired torques of 0.5 and 1 N.m. and motor speeds of 40 and 70 round/s. The segmentation of the signal using a sliding window is how the suggested method detects and classifies faults. Every segment that makes up a signal period consists of 450 samples.

  The various fault modes will be used to teach the network. For every pattern input, there are 2000 features in the input data. This yields a healthy pattern of 2000 and a fault occurrence of 2000*21. This results in 44000 vectors. There are 560 features used for the short-circuit instance, with 80 input features for each defect. 50% of these examples of the two cases are used for training, 25% for the validation and 25% for the test.

- **Neural Network training**

  After numerous simulations, we have determined that the optimal design for the two cases is 11 neurons in the first hidden layer and 9 neurons in the second layer. Because of its regular characteristic qualities and quick training time, the Levenberg Marquardt training method is widely employed. When the chosen Mean Squared Error (MSE) is met, the training procedure will come to an end. Equation (23) provides the MSE. [43].

$$MSE = \frac{1}{N}\sum_{i=1}^{N}(y_i - d_i)^2 \tag{2.23}$$

  Where yi the output value of target, di is out of training data, N is training data number.

  Figure.20 shows the convergence curves for training process for 21 open switches faults.

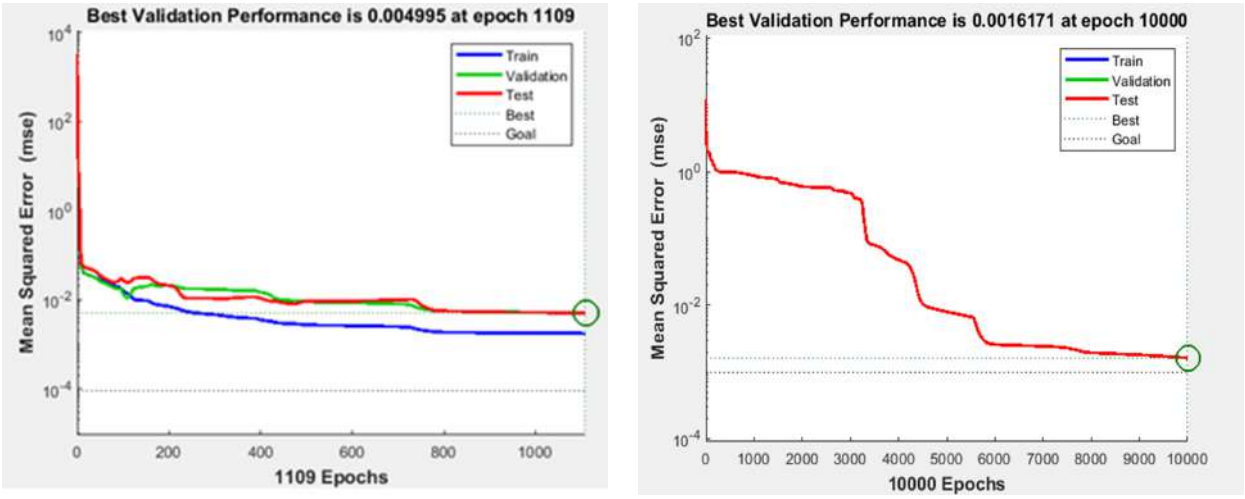


(a) (b)

Figure 2.20: Training process for (a) open-switches and (b) short-circuit cases.

The best validation performance is obtained after 1109 epochs with a MSE of 0.0094. In the short-circuit case, a best performance of 0.0016 is obtained for the all single faults S1,. . . ,S6 after 10000 epochs (see Figure.3. 7b).

Figure.19 shows the performance of the neural network during the training phase. The prediction ration is almost 99.99% for training, validation and testing process in the open and short-circuits cases.

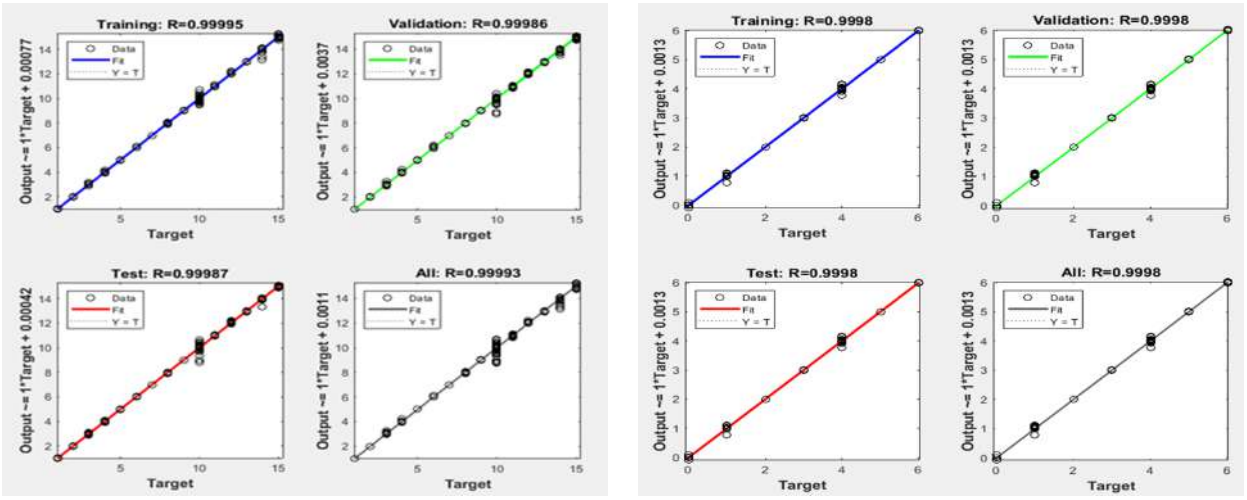


(a) (b)

Figure 2.21: Behavior of the MLP during training, validation and testing process for (a) open-switches and (b) short-circuit cases.

- **Performance Evaluation**

  To evaluate the performance of the trained MLP, accuracy and the confusion matrix metrics have been used to measure the true or the misclassification of different faults [78]. The accuracy is an essential metric for the evaluation of the result. testing data and is the ratio of accurately anticipated defects to total faults. In the event of open switches, the accuracy is 99.84%, whereas 100% accuracy is attained in the case of a short circuit problem. We can see the MLP's performance for the two fault types by defining the confusion matrix in the table. The genuine labels are shown in each row and the predicted labels are shown in each column of the matrix. The accuracy by class is displayed in the confusion matrix. Figure 22 confusion matrix illustrates that for single open switches and short circuit failures, accuracy is 100%. Out of 7500 problems, 12 misclassified faults related to numerous open switches are noticed.

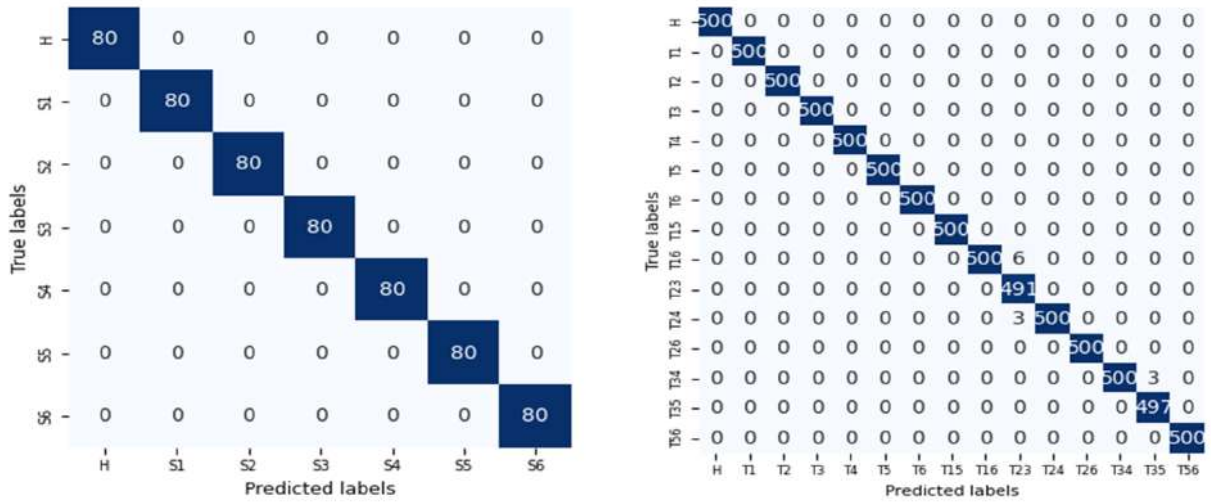


(a) (b)

Figure 2.22: Confusion matrix for test data (a) open switches and (b) short circuit cases.

## Diagnosis DTC-FYZZY for open single switch faults

### a) Structure of Fault Diagnosis System

Figure 23 shows the proposed fault diagnosis system in single open switch faults. Diagnosis System consist feature extraction surfaces sum algebraic and Fuzzy System.

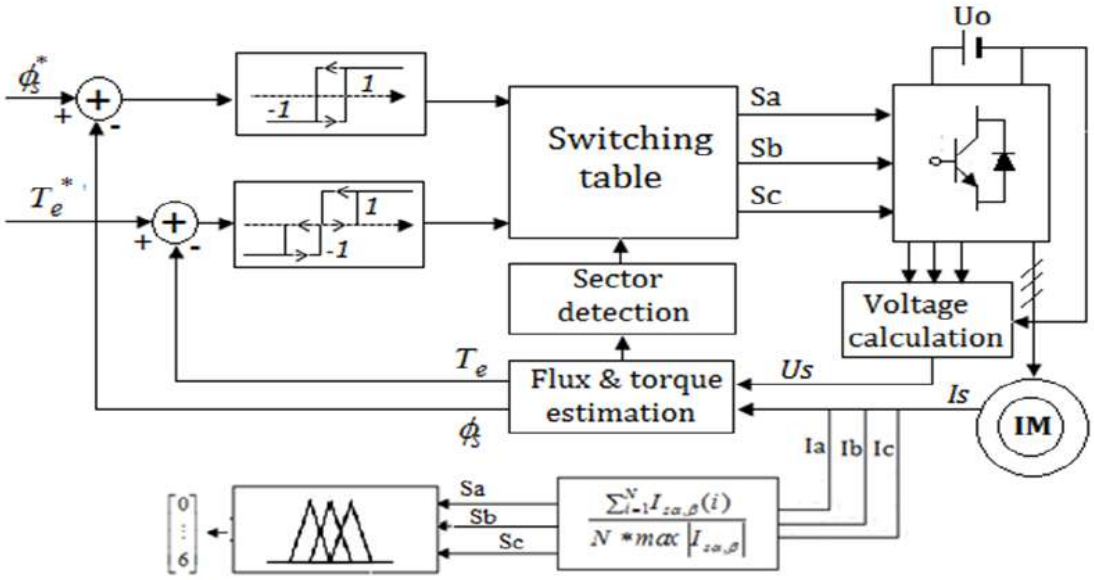


Figure 2.23: DTC-FYZZY proposed fault diagnosis system

### b) Structure of Fuzzy Diagnosis System

– **Fuzzification**

Allows the passage from the digital domain to the symbolic domain in order to determine the membership function of a variable of the fuzzy system [67].

The fuzzification is the process of a mapping from measured or estimated input to the corresponding fuzzy set in the input universe of discourse. In this system there are three inputs. Sa,Sb,Sc are surfaces sum algebraic given by equation (21), The

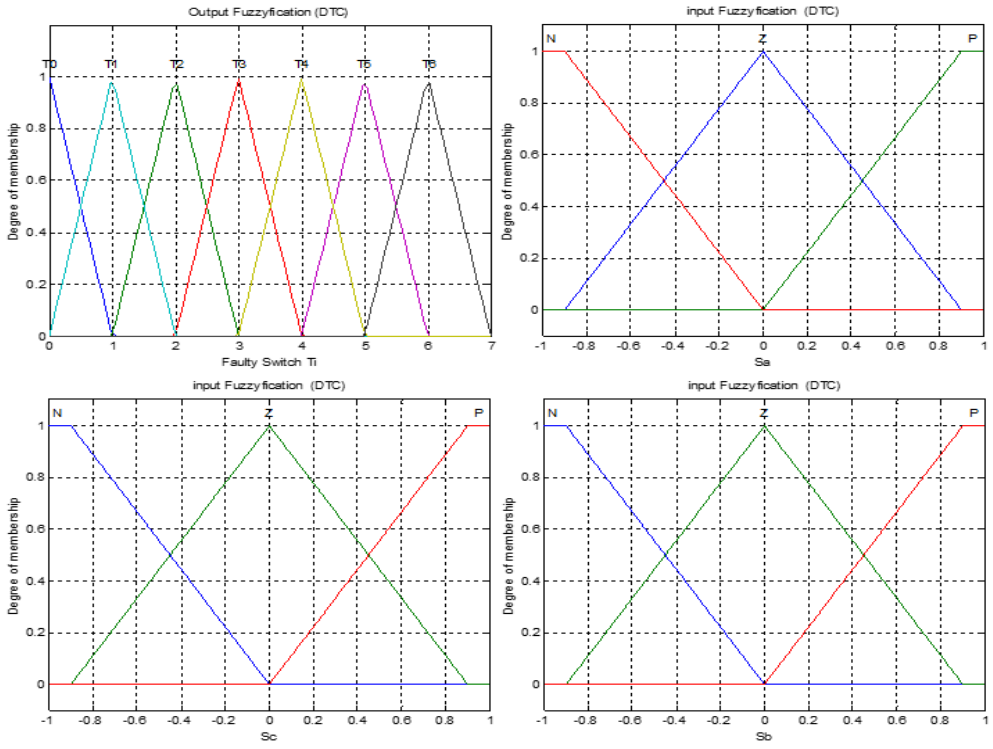


Figure 2.24: Membership function of three inputs and output variables (DTC-FYZZY).

membership functions of the 3 inputs and the output are represented in Figure.24.

Sa,Sb,Sc memberships function is decomposed in three fuzzy sets: N (negative), Z (zero), P (positive)

The Faulty switch membership function is decomposed in seven fuzzy sets: T0 toT6

– **Inference rules**

Forms the basis of the applied inference systems (rules). This block allows one to use the laws of inference to replicate human decision-making and infer the fuzzy regulator's control actions. A fuzzy rule explains how input and output variables relate to one another. [67].

Control rules are often expressed in the IF-THEN format. Rules Ri can be written as:

*R1. If Sa is Z, and If Sb is Z, and If Sc is Z, Than Ti=0: Healthy mode*

*R2. If Sa is N, and If Sb is Z, and If Sc is Z, Than Ti=1: T1 switch is defect*

*R3. If Sa is Z, and If Sb is N, and If Sc is Z, Than Ti=2: T2 switch is defect*

*R4. If Sa is Z, and If Sb is Z, and If Sc is N, Than Ti=3: T3 switch is defect*

*R5. If Sa is P, and If Sb is Z, and If Sc is Z, Than Ti=4: T4 switch is defect*

*R6. If Sa is Z, and If Sb is P, and If Sc is Z, Than Ti=5: T5 switch is defect*

*R7. If Sa is Z, and If Sb is Z, and If Sc is P, Than Ti=6: T6 switch is defect*

These roles obtained after stators currents in phase of feature extraction as illustrated in Figure.25

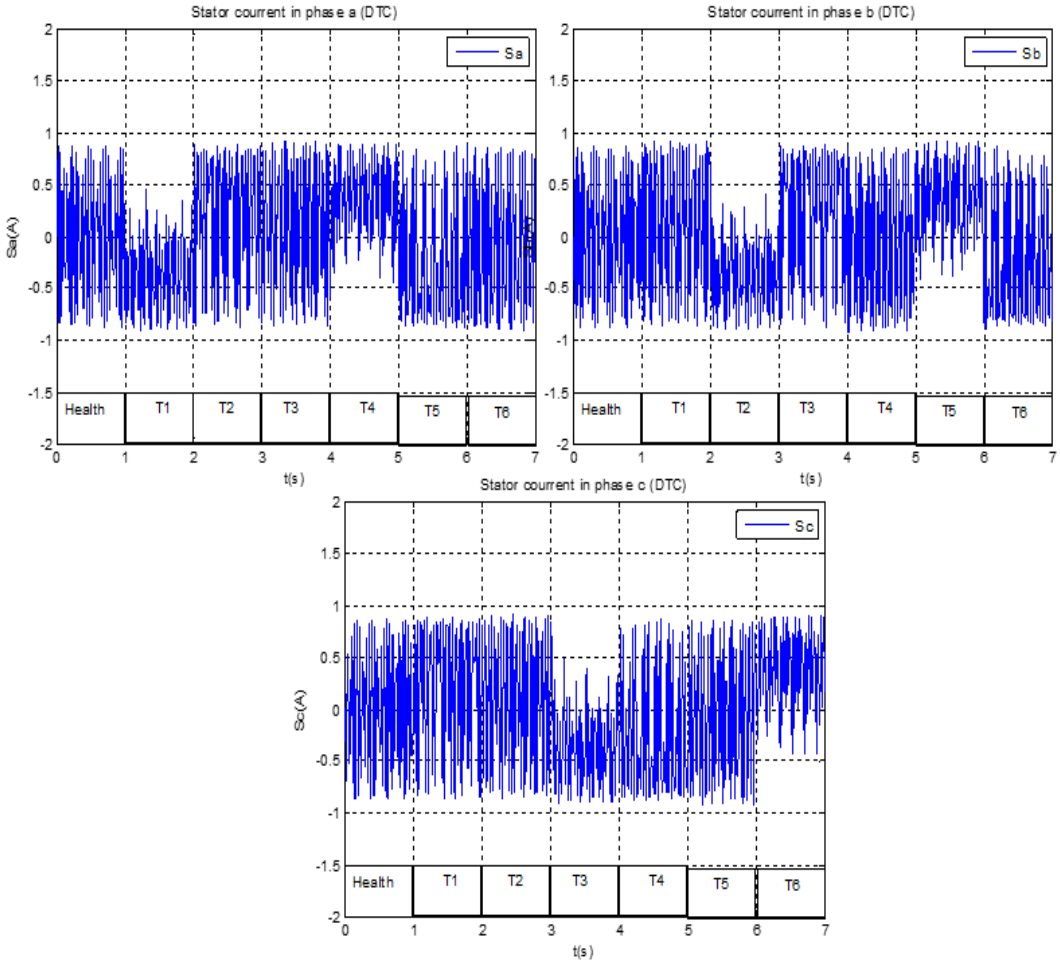


Figure 2.25: Sa,Sb,Sc surfaces currents calculations from feature extraction sum algebraic

– **Défuzzification**

Sets the value ranges of the membership functions from the output variables and performs defuzzification to provide a digital signal [129].

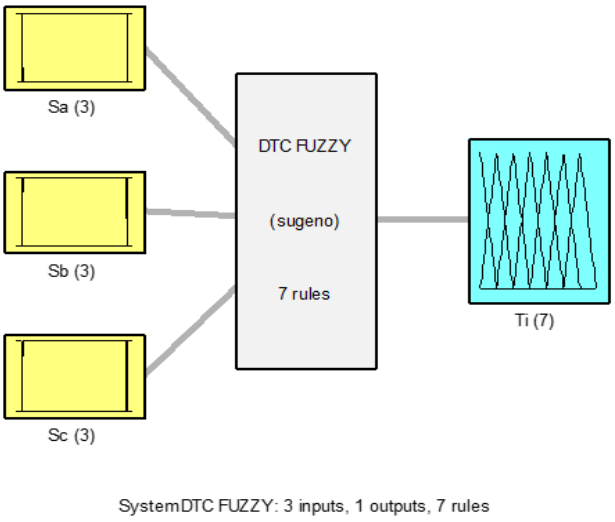


Figure 2.26: The structure of FUZZY DTC controller

## Diagnosis DTC-SVM-ANN for open and short switch single faults

### a) System of Fault Diagnosis

As illustrated in Figure.27. The proposed fault open and short switch in the diagnosis system.

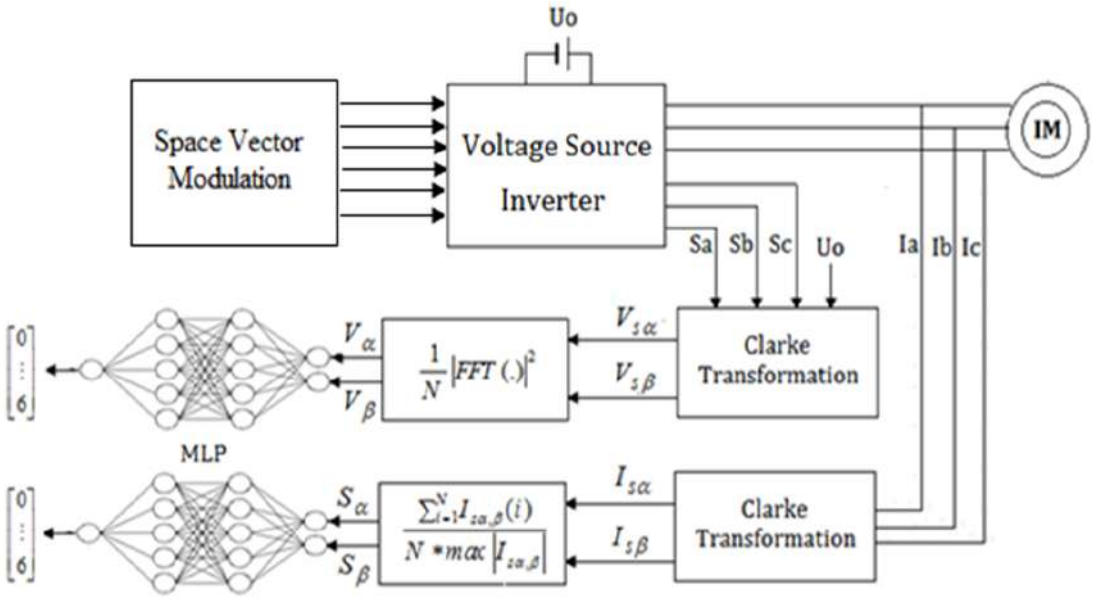


Figure 2.27: The structure of the DTC-SVM-ANN controller

### b) ANN Fault classification

1. **Design of neural network architecture**

   The same architecture illustrated in Figure.19.

2. **Neural Network Training**

   - **Open switch**

     A network will be trained with different faulty modes. The input matrix data is two rows length. ($S_\alpha$,$S_\beta$) Each pattern input has a total of 40000 columns. This gives a healthy pattern a score of 40000. And 40000*6=24000 for fault occurrence. That gives a 280000 data base for neural network training. The output target categorization is represented for various speed references.

   - **Short switch**

     A network train with faulty and healthy modes (T0, T1, T2, T3, T4, T5, T6). The input matrix data is two rows length. ($V_\alpha$,$V_\beta$). 5000 columns for every single pattern inputs. That gives a 35000 data base for neural network training. The output corresponding target is represented for various speed references.

3. **Neural Network Testing**

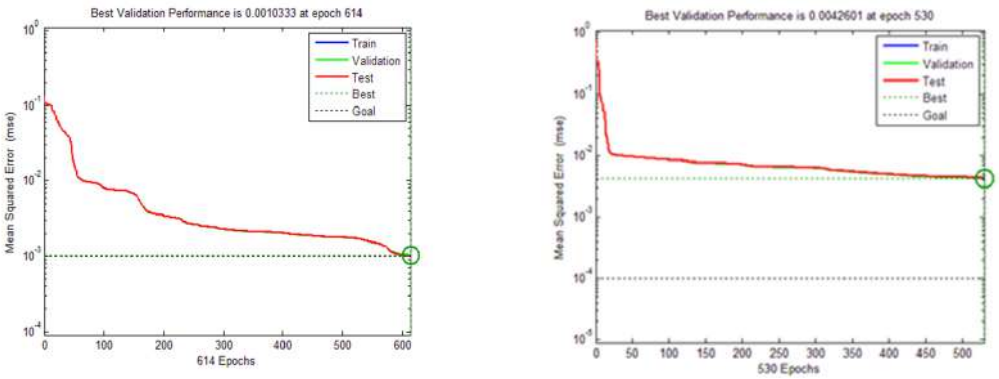


(a) (b)

Figure 2.28: Training, validation, and test errors of the diagnosis ann. (a) Open switch, (b) short switch

***For open switch:*** as shown in is shown in Figure.28a, the number of the off-line training to get 0.001 error is 614 epochs.

***For short switch:*** as shown in is shown in Figure.28b, the number of the off-line training to get 0.042 error is 530 epochs.

## Diagnosis DTC-SVM-FUZZY for open switch single fault

### a) Structure of Fault Diagnosis System

Figure.29 shows the proposed fault diagnosis system in single open switch faults. Diagnosis System consist feature extraction surfaces sum algebraic and Fuzzy System.

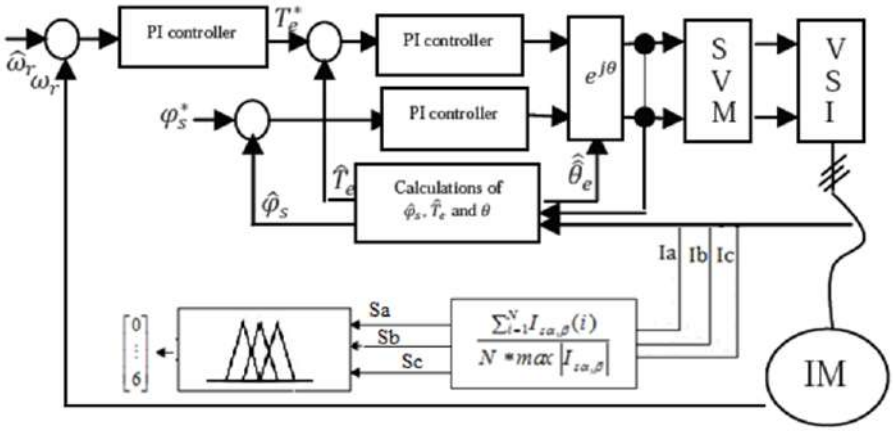


Figure 2.29: DTC-SVM-FUZZY proposed fault diagnosis system

### b) Structure of Fuzzy Diagnosis System

- **Fuzzification**

  Sa,Sb,Sc are surfaces sum algebraic given by equation (21), The membership functions of the 3 inputs and the output are represented in Figure.30.

  The Faulty switch membership function is decomposed in seven fuzzy sets: T0 toT6

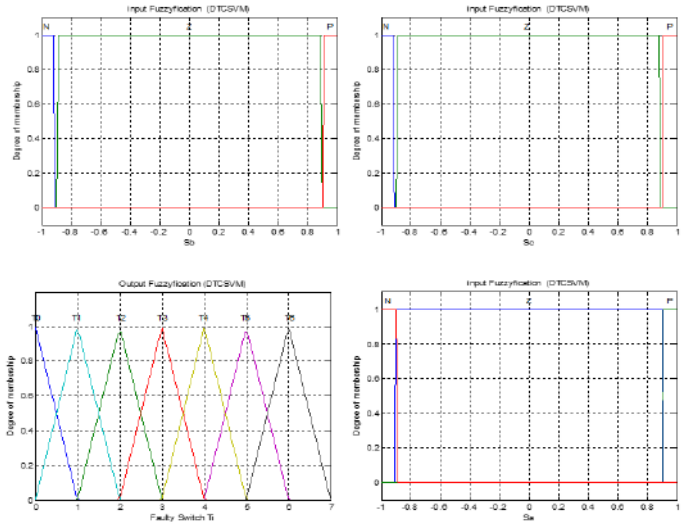

Figure 2.30: Membership function of three inputs and output variables (DTC-SVM-FUZZY)

- **Inference rules**

  Control rules are often expressed in the IF-THEN format. Rules Ri can be written as:

  *R1. If Sa is Z, and If Sb is Z, and If Sc is Z, Than Ti=0: Healthy mode*

  *R2. If Sa is Z, and If Sb is N, and If Sc is P, Than Ti=1: T1 switch is defect*

  *R3. If Sa is P, and If Sb is Z, and If Sc is N, Than Ti=2: T2 switch is defect*

  *R4. If Sa is N, and If Sb is P, and If Sc is Z, Than Ti=3: T3 switch is defect*

  *R5. If Sa is Z, and If Sb is P, and If Sc is P, Than Ti=4: T4 switch is defect*

  *R6. If Sa is Z, and If Sb is Z, and If Sc is P, Than Ti=5: T5 switch is defect*

  *R7. If Sa is P, and If Sb is N, and If Sc is Z, Than Ti=6: T6 switch is defect*

  These roles obtained after stators currents in phase of feature extraction as illustrated in Figure 31

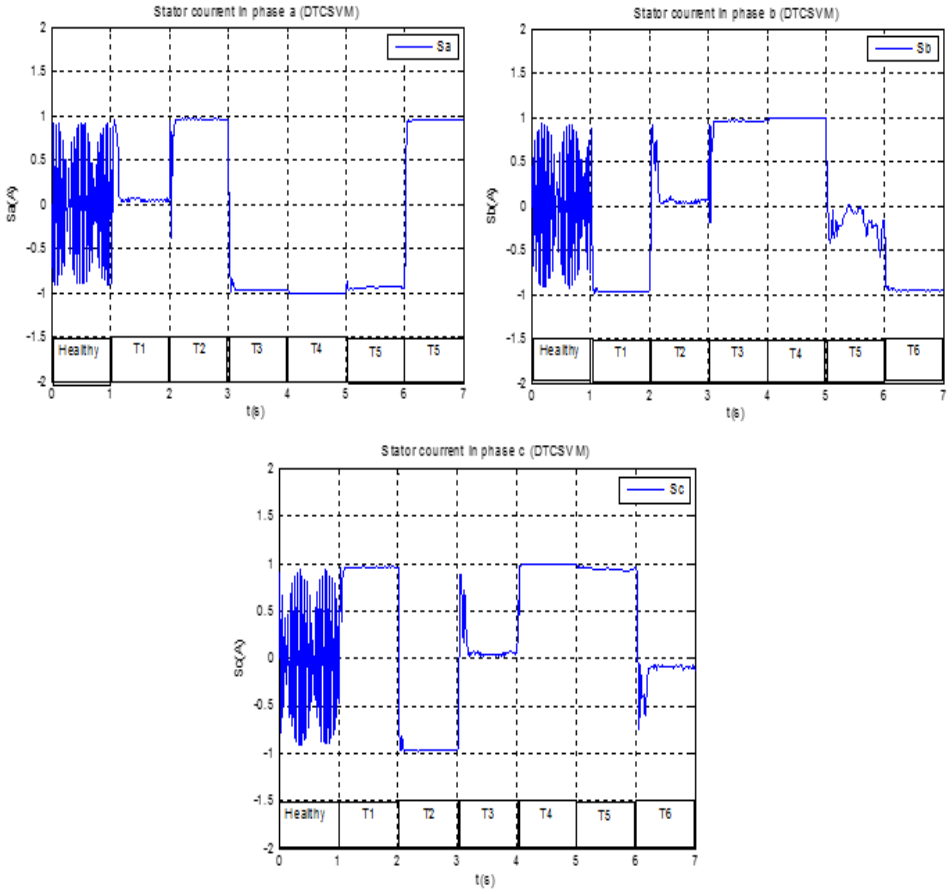


Figure 2.31: Sa,Sb,Sc surfaces currents calculations from feature extraction sum algebraic (DTC-SVM-FUZZY)

- **Défuzzification**

  Sets the value ranges of the membership functions from the output variables and achieves defuzzification to deliver a digital signal [68].

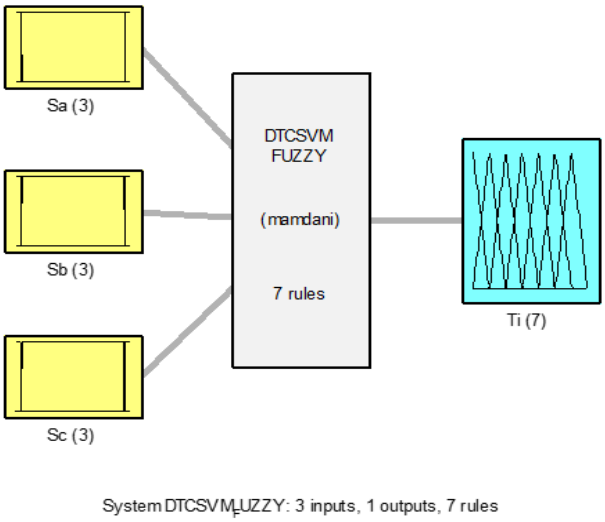


Figure 2.32: The structure of the FUZZY DTCSVM controller,

## 2.8 Conclusion

A Fault Diagnosis System based on DTC and DTC-SVM has been proposed using Fuzzy Logic and Neural Network fault classification methods. The proposed system utilizes a feature extractor based on Normalized Algebraic Sum and Fast Fourier Transform to transform the output stator current and voltage signals, which helps in rating the signal value as an important characteristic for classifying a fault hypothesis. With a good performance, the proposed method has the ability to classify and identify the fault location of both single and multiple open circuits. The models proposed for diagnosis in DTC and DTC-SVM are simple and effective, making it a promising solution to robustness problems and a reliable way to control an induction motor drive.

# Chapter 3

# Diagnosis of Neural Direct Torque Multiple Open Circuit Faults Using neural networks for induction motor drive control

## 3.1 Introduction

Variable Frequency Drives or inverters are widely used in industrial applications for controlling the speed and torque of alternative current (AC) motors. Direct Torque Control (DTC) is a powerful control technique for electric motor drives, providing high-performance and efficient control of motor torque and speed. The key principle behind DTC is to directly estimate the stator flux and torque based on the motor voltage and current measurements. By having direct access to these quantities, DTC can quickly and accurately adjust the motor control variables to achieve the desired torque and speed.

Insulated Gate Bipolar Transistors (IGBTs) play an important role in the operation of inverters by converting DC power into variable-frequency AC power, enabling motor control. However, IGBTs are among the components that commonly encounter issues. IGBT faults can have a significant impact on the performance and reliability of the feeding systems [42]. In order to prevent further damage and ensure reliable operation, various fault diagnosis methods based on signal analysis have been developed for electrical machine drives [44,79,64,60,80]. The advantage of these methods is that they only require measurements of line currents or line-to-line voltages [31,75,81-82]. As with other engineering problems, fault detection using neural networks has

not remained immune. In the literature, we can found that open-circuit fault diagnosis using neural networks is considered as a pattern recognition problem [83-85]. Regardless of the used scheme, open-switches fault detection using neural network consist of two key steps; feature extraction and fault classification. Since neural DTC has been proposed to improve the DTC performance, in particular the reduction in the torque and the flux ripples, we investigate in this chapter how neural networks perform in fault detection problems when neural DTC is used. Instead of using several types of features, or several signal cycles as in previous works, we found that the normalized mean Clark currents and the power value of the signal are sufficient to obtain a full accuracy.

This chapter is organized as follows: Section 2 introduces the neural DTC principle. Section 3 analyses the Fault Diagnosis system under single and multiple open switches. Section 4 presents the proposed method. Section 5 presents simulation results. Section 6 conclusion.

## 3.2 Neural DTC

The neural DTC consists of replacing the two hysteresis blocks and the switch table from basic DTC (figure 1) with a neural network controller shown in Figure 1 [81]. The neural networks has an input layer containing three neurons corresponding to the three inputs $\epsilon_T$ , $\epsilon_s$ , $\theta_s$ , and an output layer containing three neurons corresponding to the three switching status $S_a, S_b$ and $S_c$ .

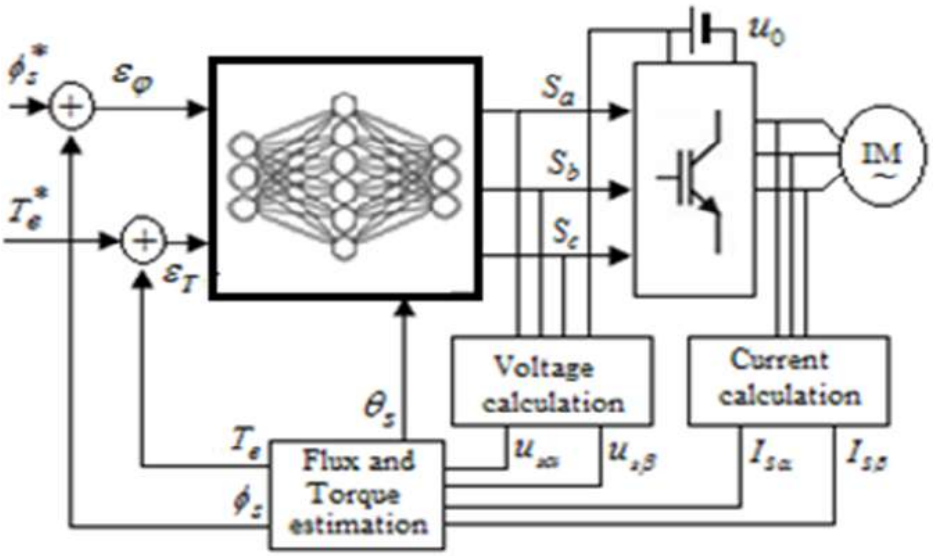


Figure 3.1: Neural DTC block diagram

## 3.3 Open-Switches Fault Diagnosis

Faulty switch can be recognized in twenty-pattern, six-pattern for single fault and fifteen-pattern for multiple faults, current pattern illustrate a fault location. Circle shape describes current pattern in healthy mode. All patterns are illustrated in figure 2.

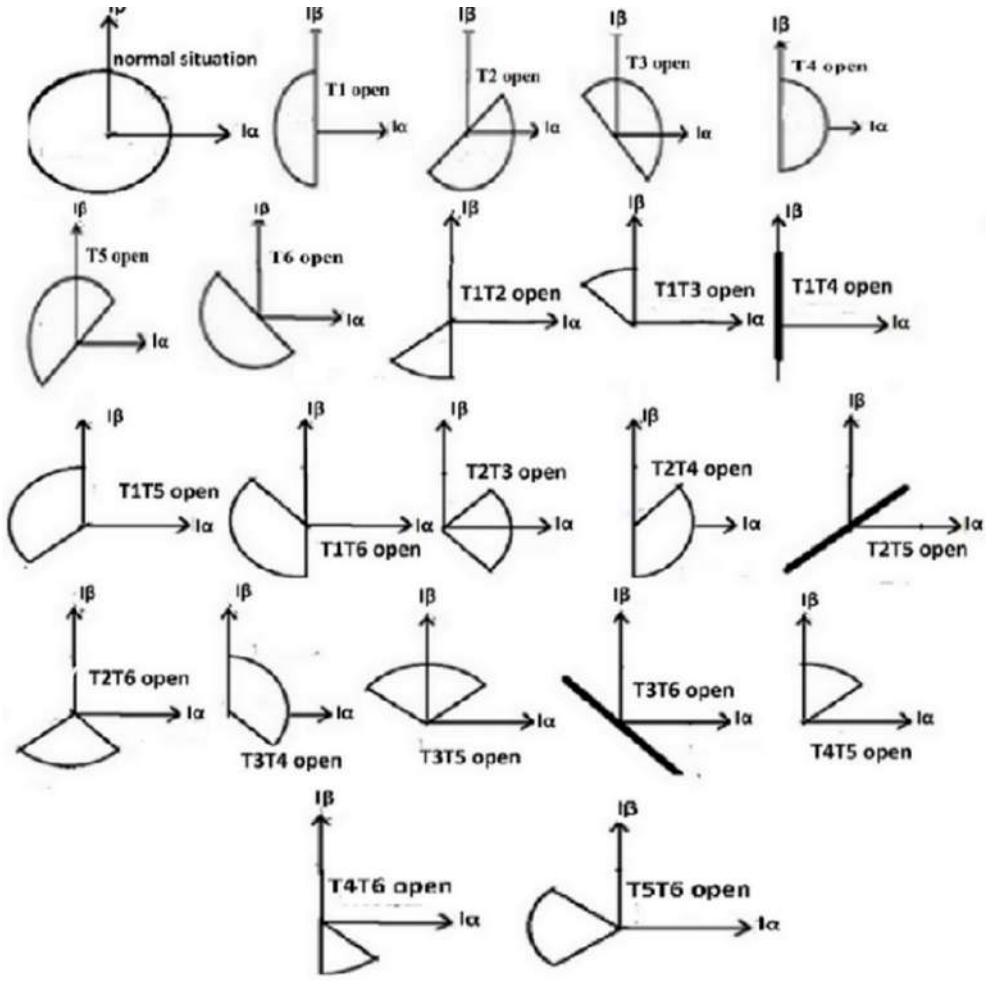


Figure 3.2: Patterns of multiple open-circuit faults

## 3.4 Proposed Method

Effective feature extraction is crucial in the development of a reliable system for detecting and diagnosing open-switches faults from the three-phase current signal output. The purpose of feature extraction is to extract relevant data from the signal and utilize it to train a neural network for fault detection. However, existing approaches have certain limitations in terms of accuracy and processing time. To overcome these challenges, it is recommended to employ normalized and reduced features that can be applied across different reference speeds. By utilizing normalized functions, the feature extraction process can be standardized and optimized, en-

suring consistent and accurate results regardless of the specific operating conditions or speeds. Figure 3 depicts the proposed fault diagnosis system.

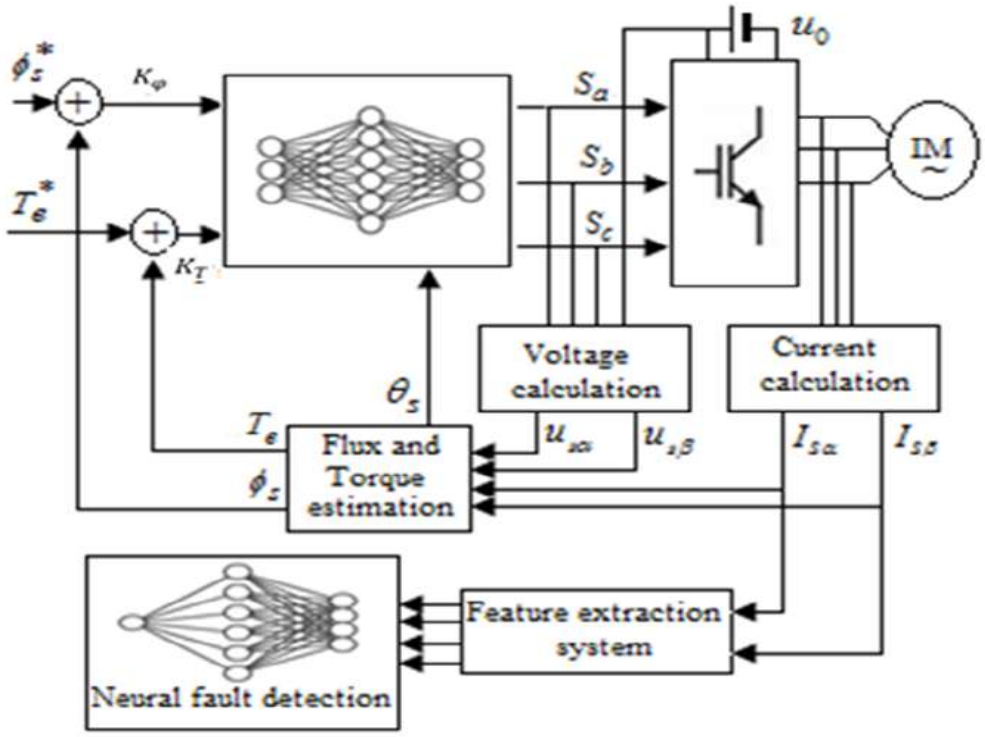


Figure 3.3: Proposed fault diagnosis system

As illustrated in figure (3), to construct the vector of features, the currents measured $I_{sa}$,$I_{sb}$ ,$I_{sc}$ are transformed into two dimensions ($I_{s\alpha}$,$I_{s\beta}$) by equation (3.2) and their surfaces ($S_{s\alpha}$,$S_{s\beta}$) are calculated using feature extraction mathematical model given by the following equations (3.21) [86-87]:

In addition, the autocorrelation function at lag zero of the currents $I_{s\alpha}$,$I_{s\beta}$ are considered to improve the accuracy of the proposed diagnosis fault system [88].

$$r_{s\alpha}(0) = \frac{1}{N}\sum_{i=1}^{N} \mathrm{I}_{s\alpha}^2(i) \tag{3.1}$$

$$r_{s\beta}(0) = \frac{1}{N}\sum_{i=1}^{N} \mathrm{I}_{s\beta}^2(i) \tag{3.2}$$

## 3.5 Simulation Results

### Neural DTC

As mentioned above, the neural DTC has the flux and the torque errors and the sector selection ($K_T$,$K_\phi$,$\phi_s$) as inputs and The switching status (Sa,Sb,Sc) as outputs. After numerous simulations, we have found that two hidden layers with 7 and 3 neurons in each as shown in figure (3.4) provide the best results.

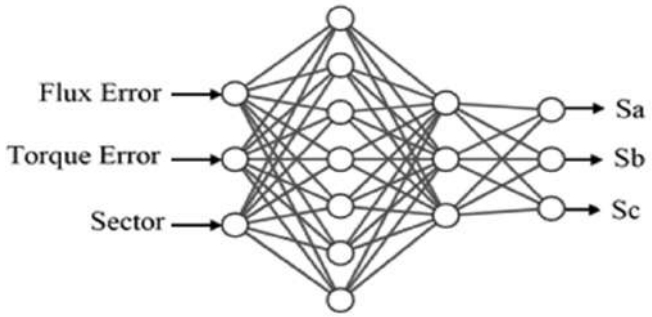


Figure 3.4: Multilayer network architecture for neural DTC

Using this configuration and the Levenberg-Marquardt as training algorithm, a mean squared error (MSE) goal of 0.01 was fixed. To create the test data sets, various simulations with varying speed references were performed. For each input vector and corresponding output vector, 15105 samples were collected where 50% are used for training, 25% for testing and 25% for validation. From figure (5), an MSE of 0.042 was reached in only 465 iterations.

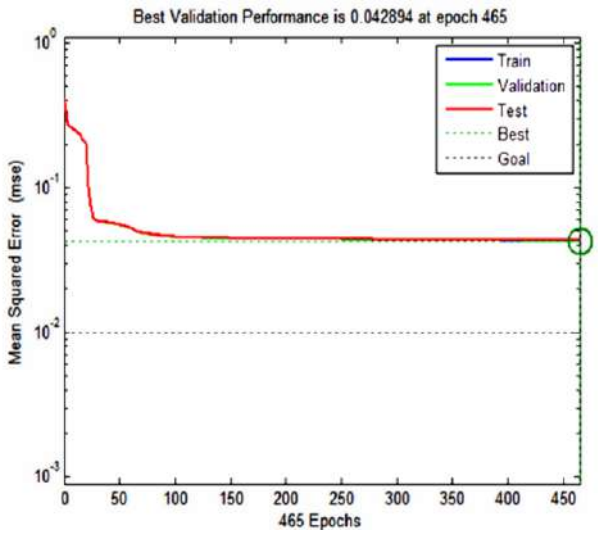


Figure 3.5: The neural DTC in training, validation, test errors

To see the effectiveness of the neural DTC, we construct the data sets for open-swiches faults under basic and neural DTC, a reference speed of 75 rad/s and a reference flux of 1Wb were fixed between 0 and 0.3s. After 0.3s, these desired parameters wre changed to 40 rad/s and 0.5Wb respectively. Between 0.6s and 0.9s, we made an open-swiche fault at T1. At 1.2s, we made a double faults in T1 and T2. As shown in Figure 6, the estimated flux and torque are the same under the basic and neural DTC.

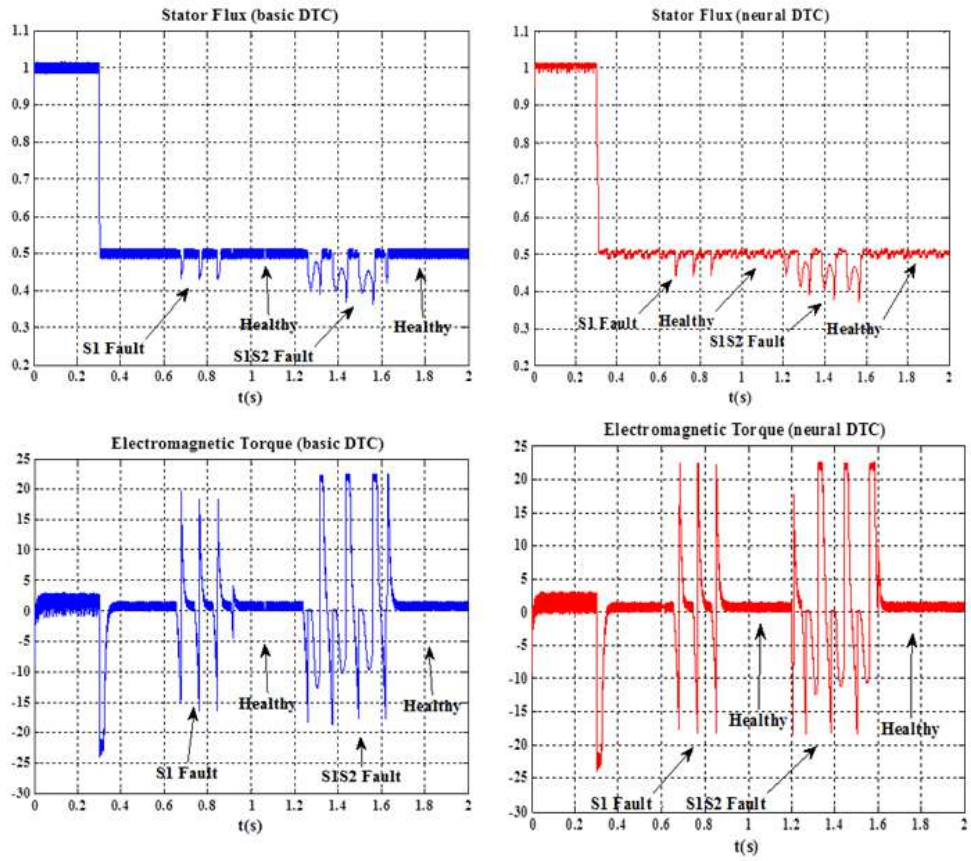


Figure 3.6: Stator flux and torque under basic DTC and neural DTC.

## Fault detection under basic and neural DTC

To create the dataset, we manually produce faults by opening the IGBTs gates in the used Simulink model. Figure 7 shows the obtained features using equations 8 and 9 for healthy and all single and double-open switches. The whole data sets consist of 27500 vectors of 4 components with the correspondent labels as outputs.

The outputs are labeled from 1 to 22 and listed in table 1.

Table 3.1: Fault Labels

| | |
|---|---|
| **Healthy** | T(1) |
| **Single Fault** | T(2),T(3),T(4),T(5),T(6),T(7) |
| **Multiple Fault** | T(8),T(9),T(10),T(11),T(12),T(13),T(14),T(15),T(16), T(17),T(18),T(19),T(20),T(21),T(22) |

Figure (7) shows the evolution of the four components $S_\alpha$,$S_\beta$ ,$r_{s\alpha}(0)$,$r_{s\beta}(0)$ occurring in the same order as in table I.

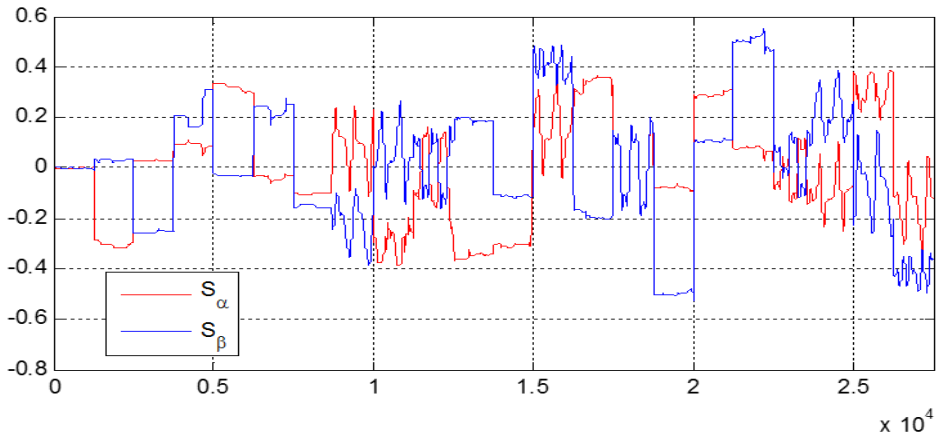


(a) Two features $S_{\alpha,\beta}$

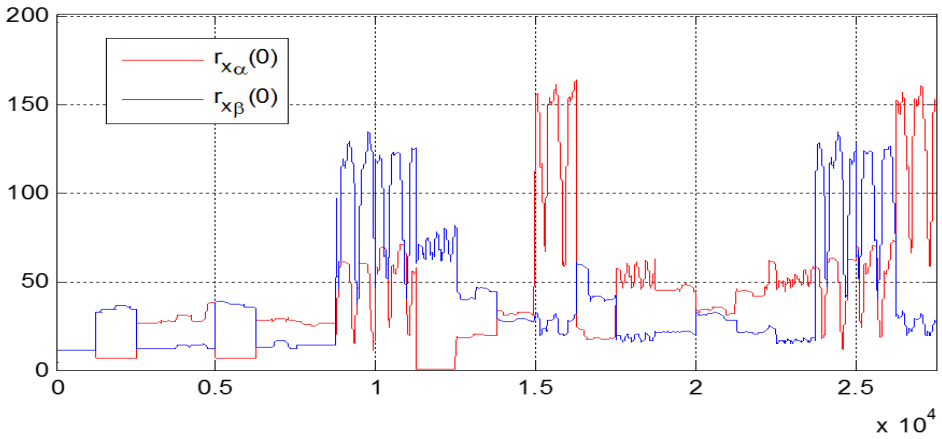


(b) Two features $r_{\alpha,\beta}$

Figure 3.7: Feature extraction under single and multiple fault occurrences

To see how the added feature can improve the fault detection process, we visually explore the datasets using the t-Distributed Stochastic Neighbor Embedding (t-SNE) [89]. As we can see from figure (8), when using the two first components, we can see an overlapping in labels (1,19), (10,19), (2,9) and (8,14). Also the label 21 is divided to two sets.
However, the autocorrelation coefficients added to components make the novel feature more discriminative and will be able to effectively separate different classes in the dataset.

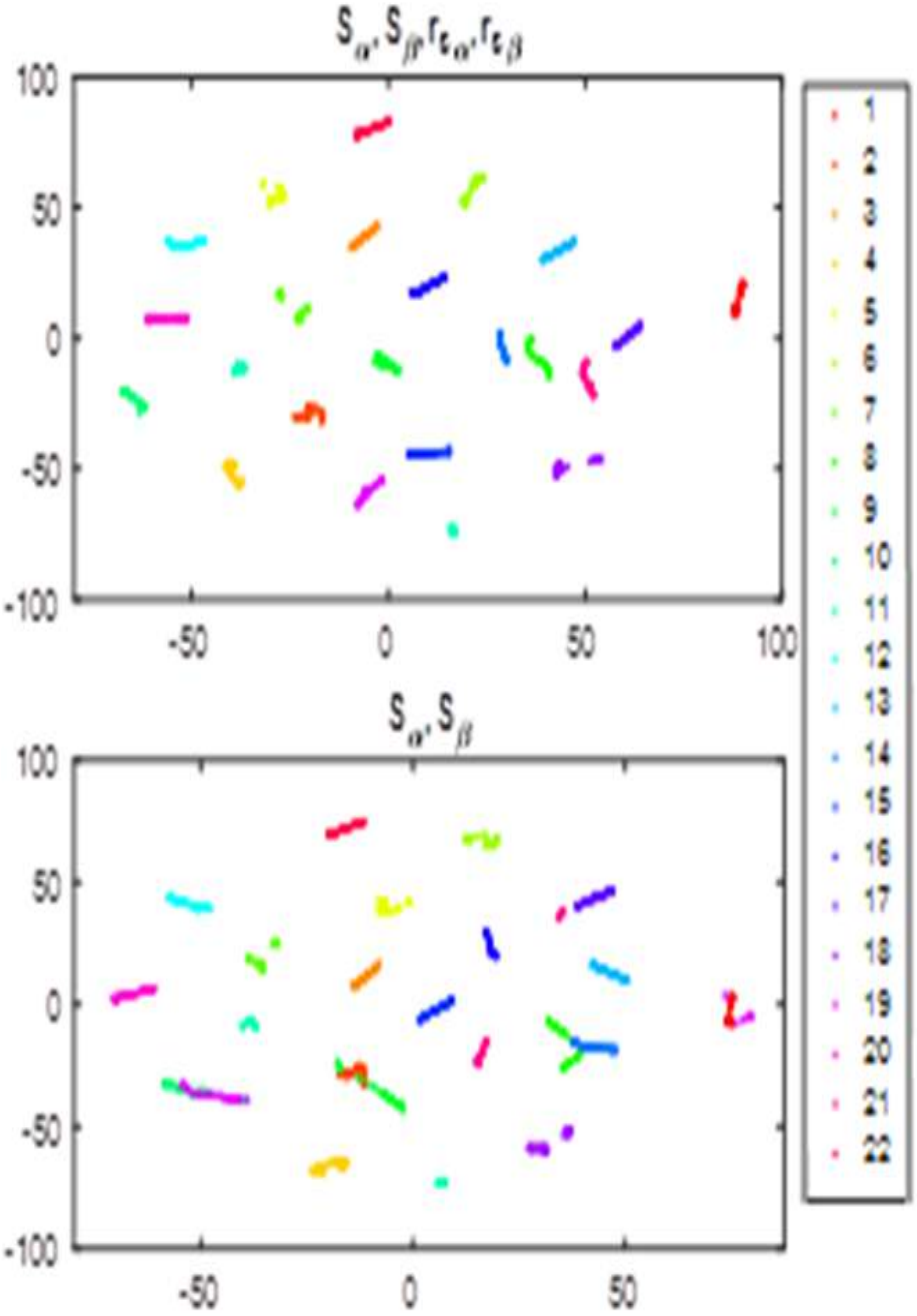


Figure 3.8: t-SNE obtained using two and four features

The simulation model generates a total of 75,000 datasets across 22 different labels. These datasets are then divided into three sections: 50% for training, 25% for testing, and 25% for validation. This means that there are 20625 datasets allocated for both training and validation purposes. For the fault detection problem, we have considered the neural input without and with autocorrelation components. For the two cases, three hidden layers with 20,20,15 neurons were chosen.

Figures 9,10 show the convergence curves and the regression plots respectively. Regression plots

show the relationship between the outputs of the network and the targets. It is evident from regression plots that practically all the data falls directly on the line with the associated slope of 1, expressing the exact match between the neural network output and target data. However in figure (10.a), the scatter plot shows that some of data points like 2,8,9,10,19 and 21 have relatively poor fits which confirm t-SNE discussed above.

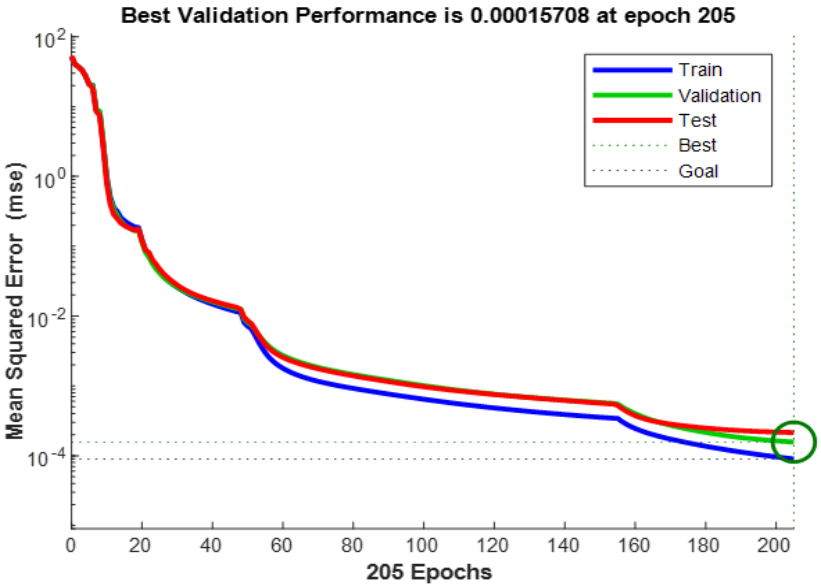


(a) Two features $S_\alpha$,$S_\beta$

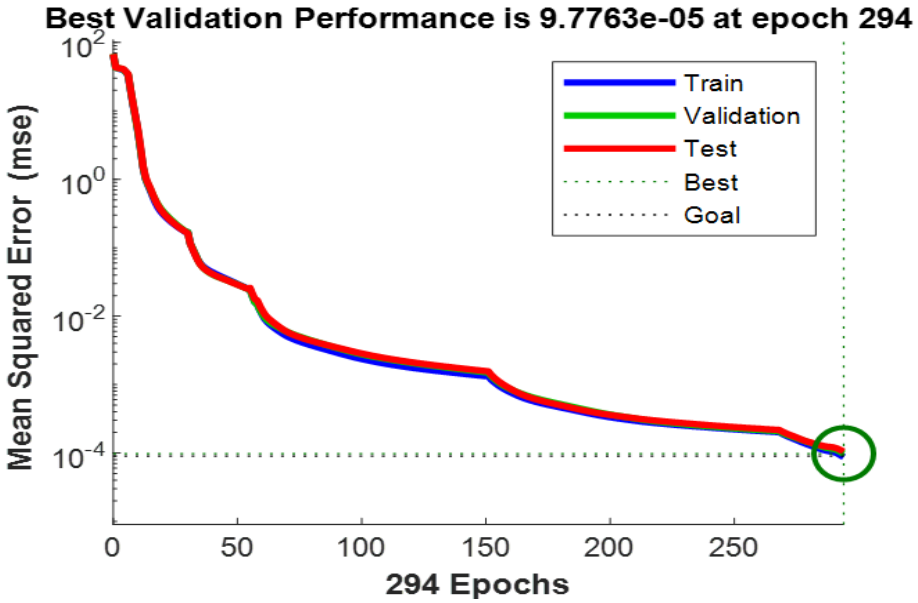


(b) Four features $S_\alpha$,$S_\beta$ ,$r_{s\alpha}$,$r_{s\beta}$

Figure 3.9: Convergence's curves for (a) two inputs and (b) for four inputs.

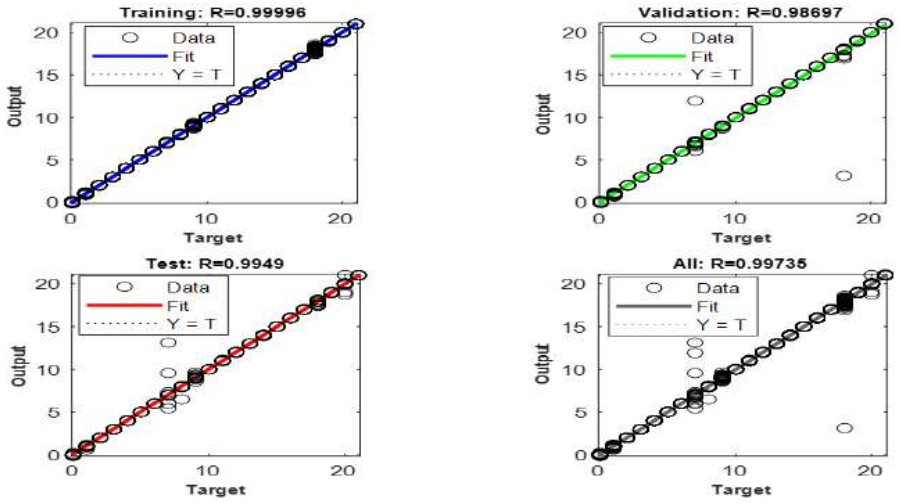


(a) Two features $S_\alpha$,$S_\beta$

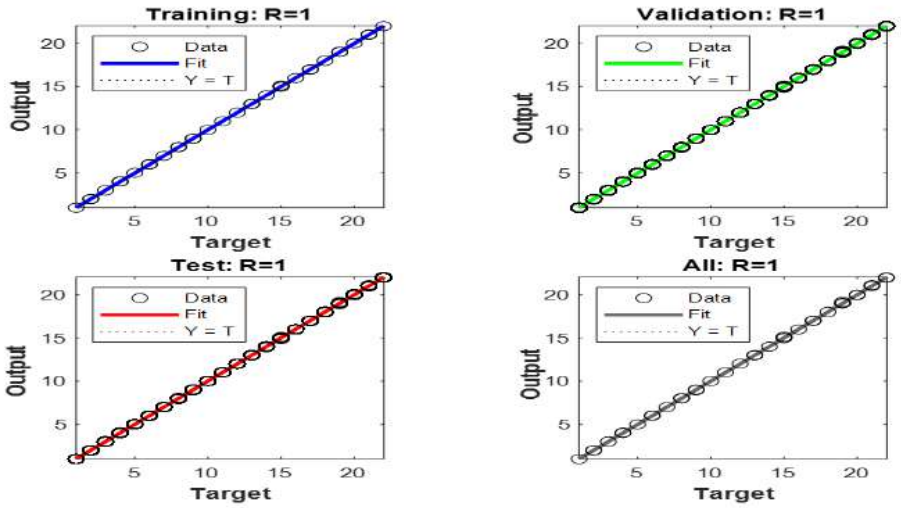


(b) Four features $S_\alpha$,$S_\beta$ ,$r_{s\alpha}$,$r_{s\beta}$

Figure 3.10: Regression plots of the neural network on training, validation, testing and total sets for the (a) two inputs and (b) for four inputs.

After validating and testing the simulation model, it is important to compare its performance with other to evaluate its superiority or effectiveness.

The test accuracy is a performance measure that quantifies the proportion of correctly predicted outcomes by the model on the test dataset. It is calculated by dividing the number of correctly classified instances by the total number of instances in the test set. This metric provides an indication of how well the model can generalize its predictions to unseen data. The test accuracy defined by [87].

$$A = \frac{N - M}{N} * 100\% \tag{3.3}$$

where N is the number of vectors in the test dataset and M the number of misclassified datasets. In the comparative analysis, the proposed method is assessed in comparison with two distinct types of machine learning models: ensemble extreme learning machine (ELM) [72] and the Weighted Random Forests Algorithm [73]. The results presented in Table II show that the proposed algorithm achieves the highest accuracy, reaching 100%. This suggests that the new method successfully identifies all fault types and significantly reduces the occurrence of false negatives (fault miss detection).

Table 3.2: Comparison with other methods

| **Method** | **Test Accuracy** |
|---|---|
| Ensemble ELM [72] | 94.55% |
| WRFA [73] | 96.25% |
| Proposed | 100% |

## 3.6 Conclusion

This chapter proposes a fault recognition and diagnosis in a PWM inverter with an induction motor drive controlled by an artificial neural network direct torque control (NDTC).An effective and simple technique to control an induction motor drive appears in NDTC, providing a promising solution to the robustness problems. The simulations were done on a regular induction motor using a basic and neural direct torque control.

The study focused on identifying open inverter switching faults, both single and multiple, by simulating various defect modes using artificial intelligence methods. The outcomes indicate that the proposed approach successfully detects all types of faults and significantly reduces the likelihood of missed detections.

# Chapter 4

# Deep learning for Open-Switch Faults Detection in Inverter Feeding Induction Motor

## 4.1 Introduction

Nonetheless, the effectiveness of neural networks in fault diagnosis heavily relies on the features utilized, which serve as the fundamental aspects of fault detection. Consequently, researchers have been motivated to employ deep neural networks to automatically extract features from raw data. When dealing with signals, employing Convolutional Neural Networks (CNN) necessitates the conversion of raw data into images through various techniques [44]. In the domain of convolutional neural networks (CNNs), transfer learning is a commonly employed technique for image classification tasks. Its primary advantage lies in leveraging the knowledge acquired from training a model on a large dataset to enhance the performance of a model on a smaller, related dataset. By utilizing a pre-trained model as a starting point, we can retrain only a subset of the network's layers on our specific dataset, instead of initiating the training process from scratch and training the entire network anew. This strategy conserves both time and computational resources, all the while ensuring commendable performance on the intended task. Numerous pre-trained networks, such as AlexNet, VGG16, ResNet, and DenseNet, are readily accessible for various deep learning tasks .

In this chapter, AlexNet is proposed to detect open-circuit faults, taking advantage of its status as a transfer learning model where specific layers are retrained. Initially, the $\alpha\beta$ current signals are converted into images using an appropriate mapping technique. These generated images are

then utilized for training and testing the network. The remainder of this chapter is structured as follows: Section 2 outlines the problem statement and examines the fault diagnosis system concerning both single and multiple open switches. Section 3 introduces the proposed method, while Section 4 presents the simulation results. Finally, Section 5 concludes the study.

## 4.2 Problem statement

### Open-circuit faults

Within the fundamental configuration of the voltage source inverter (figure 5.1), there are six Insulated-Gate Bipolar Transistors (IGBTs) $S_i, i = 1, ..., 6$ that operate complementarily, alongside six freewheel diodes $D_i, i = 1, ..., 6$. This inverter is responsible for supplying perfectly balanced 3-phase sinusoidal currents and voltages. The majority of failures in the rectifier manifests in power electronic switches, primarily in the form of open-circuit faults (OCFs) and short-circuit faults (SCFs). In cases of open switch faults, the IGBT remains in an off state. Unlike short-circuit faults, open-circuit faults do not result in system shutdown; instead, the system continues to function in a degraded mode [87].

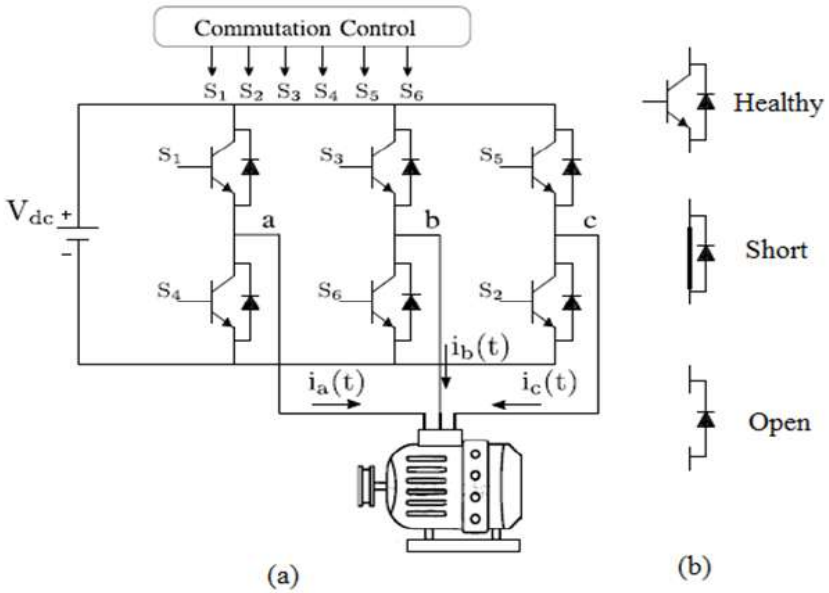


Figure 4.1: Three-phase power converter feeding an electric system (a) and typical faults (b) [149]

Open circuit faults can be categorized into three distinct types: single switch faults, double switch faults occurring within the same bridge arm, and double switch faults emerging in different bridge arms. Table 5.1 [56,87] illustrates all conceivable fault scenarios.

Table 4.1: Summary of different faults

| **Fault type** | **Fault Location** |
|---|---|
| Single open-switch Fault | S1,S2,S3,S4,S5,S6 |
| Double open-switch Fault in the same bridge arms | S1-S4,S2-S5,S3-S6 |
| Double open-switch Fault in different bridge arms | S1-S2,S1-S3,S1-S4,S1-S5,S1-S6,S2-S3,S2-S4, S2-S5,S2-S6,S3-S4,S3-S5,S3-S6,S4-S5,S4-S6,S5-S6, |

## Clarke-Concordia transformation

The measured currents ($I_a$,$I_b$ ,$I_c$) are transformed into two dimensions ($I_\alpha$,$I_\beta$) through the application of the Clarke-Concordia transformation, as outlined in reference [43].

$$\begin{cases} I_\alpha = \frac{2}{3}I_a - \frac{1}{3}I_b - \frac{1}{3}I_b \\ I_\beta = \frac{1}{\sqrt{3}}\left(\frac{1}{3}I_b - \frac{1}{3}I_b\right) \end{cases} \tag{4.1}$$

The Figure 5.2 shows various alpha-beta stator currents forms of defects for different double faulty switches. It can be noted that the path drawn is a portion shape of circle for all cases of defects [39].

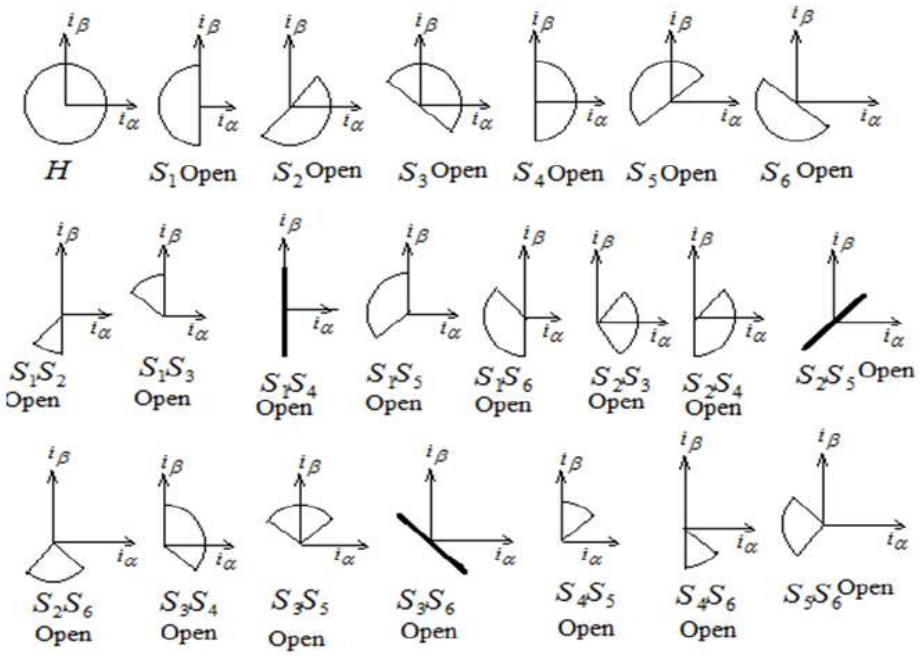


Figure 4.2: Ideal shape of different trajectories of the phase current according to the normal , single , and double faulty modes

Fast detection and isolation of open-circuit faults in IGBT switches are of great importance to prevent damage to other components in the system and to avoid costly downtime. Fault detection and isolation methods are an active area of research in power electronics, and various techniques have been proposed to improve the reliability and fault tolerance of power electronic systems. In this thesis, we propose to use Alexnet to identify and classify multi-open-circuit faults.

## 4.3 Proposed method

The proposed method for open switches fault detection in the induction motor inverter is outlined in Figure 5.3, and comprises three key steps:

- **Raw Currents Data generation:**
  This step is responsible for gathering raw current data from the induction motor inverter. Typically, current sensors installed in the motor drive circuit are utilized for acquiring this data.

- **Data Organization:**
  The purpose of this step is to collect data samples and labels from the raw current data. The data samples correspond to the current signals, whereas the labels denote the associated fault types.

- **Detection and classification:**
  This step employs the AlexNet neural network to extract the most representative features and classify the data into different types of faults.

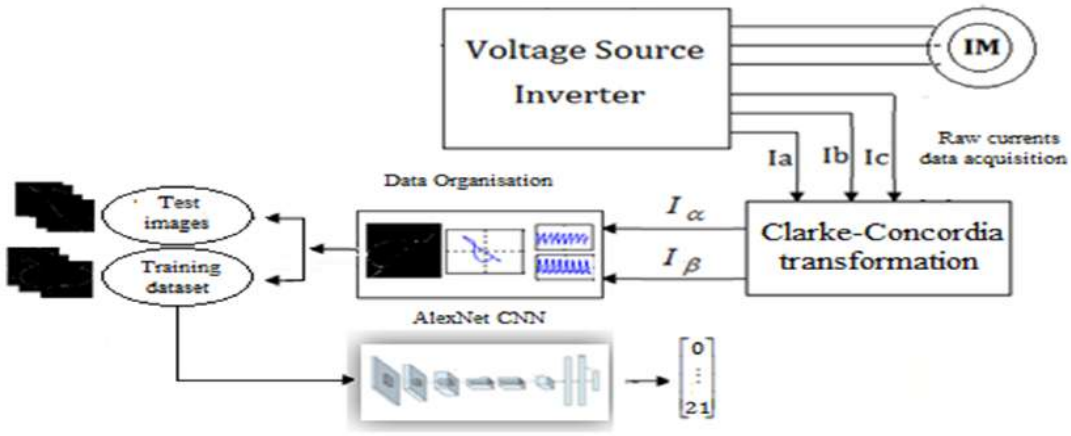


Figure 4.3: Flowchart of the proposed multi-faults diagnosis

## Data organization

To implement deep convolutional neural networks (CNNs) for fault detection, the $\alpha\beta$ current signals are transformed into images through a specific mapping technique. In this process, each sample of $\alpha\beta$ stator currents is represented as a binary pixel belonging to the object's contour. The coordinates for these pixels are determined as follows :

$$x = \frac{[i_\alpha - min(i_\alpha)](L_x - 1)}{max(I_\alpha) - max(I_\alpha)} + 1 \tag{4.2}$$

$$y = \frac{[i_\beta - min(i_\beta)](L_y - 1)}{max(I_\beta) - max(I_\beta)} + 1 \tag{4.3}$$

Where: $i_\alpha$ and $i_\beta$ are the values of each element of the vectors $I_\alpha$ and $I_\beta$ respectively.
Figure 5.4 illustrates the process of reconstructing data from a 1D transform to a 2D format.

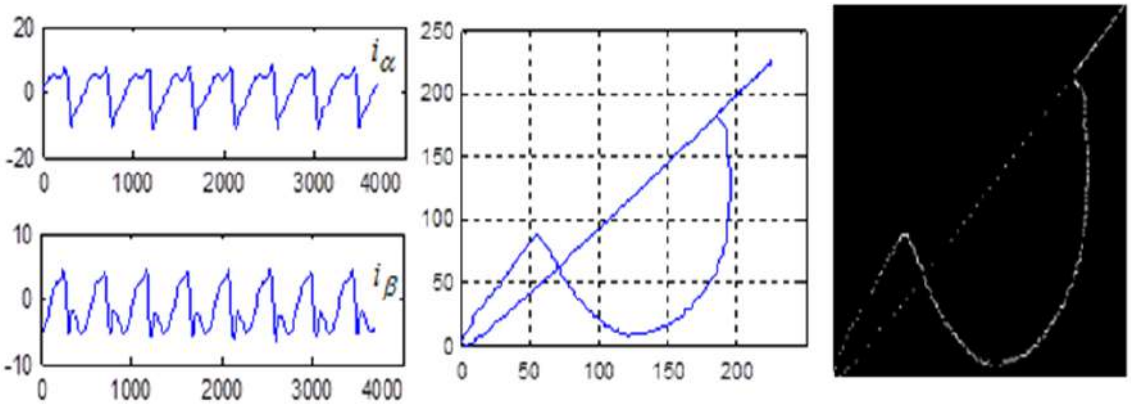


Figure 4.4: Example of the currents in the Concordia frame before and after mapping when one switch is opened

## AlexNet for Detection and classification

AlexNet is a convolutional neural network (CNN) that was introduced in 2012 by Alex Krizhevsky 'et al.in 2012 . The architecture of AlexNet comprises 8 layers, including 5 convolutional layers and 3 fully connected layers. The layers used for feature extraction in a pre-trained AlexNet model are typically the first five convolutional layers .The remaining three are fully-connected and used for classification (see Fig 5.5).

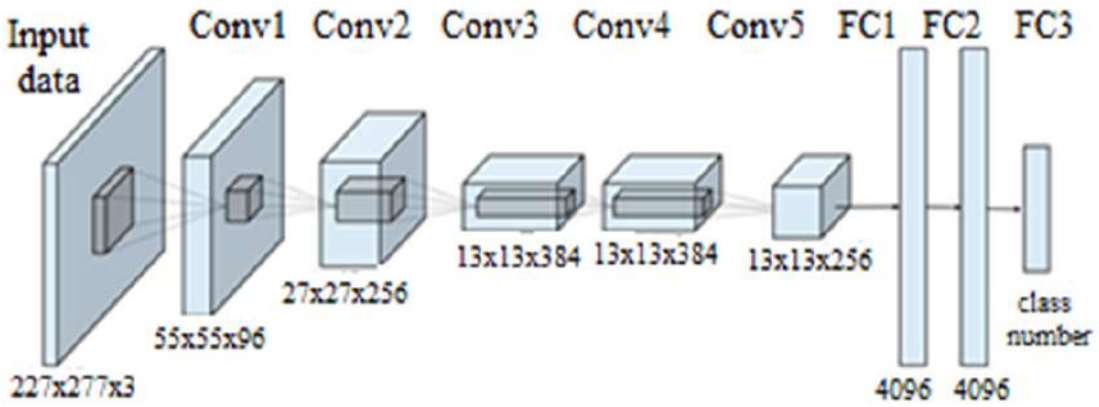


Figure 4.5: AlexNet CNN architecture

## 4.4 Simulation results and discussion

In this study, we addressed a multi-classification problem involving 22 distinct classes, utilizing the AlexNet model for the classification task. The training of the AlexNet model was conducted on a computer equipped with an Intel(R) Core(TM) i9 processor and 32GB of memory, ensuring efficient processing and accurate training results.

### Fault description and labeling

Fault description and labeling are essential components of any fault analysis or diagnostic system. The fault types are labeled and grouped into three distinct groups based on their characteristics which are summarized in Table 5.2: The first group includes the "normal" operating condition without any faults: No fault (healthy): $H$

The second group comprises the six fault types related to single IGBT open-circuit faults, where individual IGBT components within the circuit have an open connection: Single fault in $S_i : S_i, i = 1, ..., 6$

The third group includes the 15 fault types associated with double IGBT open-circuit faults, indicating situations where pairs of IGBT components have open connections: Double faults in $S_i, S_j : S_{ij}, i = 1, ..., 6, j = 1, ..., 6$

Table 4.2: Summary of different labels Fault Types

| ***Fault Type*** | ***Lable*** | ***Fault Type*** | ***Lable*** |
|---|---|---|---|
| No fault (healthy) | $H$ | $T_1$ and $T_6$ Open-circuit | $S_{1,6}$ |
| $T_1$ Open-circuit | $S_1$ | $T_1$ and $T_2$ Open-circuit | $S_{2,3}$ |
| $T_2$ Open-circuit | $S_2$ | $T_2$ and $T_4$ Open-circuit | $S_{2,4}$ |
| $T_3$ Open-circuit | $S_3$ | $T_2$ and $T_5$ Open-circuit | $S_{2,5}$ |
| $T_4$ Open-circuit | $S_4$ | $T_2$ and $T_6$ Open-circuit | $S_{2,6}$ |
| $T_5$ Open-circuit | $S_5$ | $T_3$ and $T_4$ Open-circuit | $S_{3,4}$ |
| $T_6$ Open-circuit | $S_6$ | $T_3$ and $T_5$ Open-circuit | $S_{3,5}$ |
| $T_1$ and $T_2$ Open-circuit | $S_{1,2}$ | $T_3$ and $T_6$ Open-circuit | $S_{3,6}$ |
| $T_1$ and $T_3$ Open-circuit | $S_{1,3}$ | $T_4$ and $T_5$ Open-circuit | $S_{4,5}$ |
| $T_1$ and $T_4$ Open-circuit | $S_{1,4}$ | $T_4$ and $T_6$ Open-circuit | $S_{4,6}$ |
| $T_1$ and $T_5$ Open-circuit | $S_{1,5}$ | $T_5$ and $T_6$ Open-circuit | $S_{5,6}$ |

## Database generation

To construct the dataset, we manually induced open circuits as specified in Table 1 and then simulated the corresponding scenarios. The resulting grayscale images were standardized to a size of 227x227 pixels. These images were generated using the signal-to-image method, employing a sample signal comprising 4500 sampling points. Figure 5.6 illustrates the outcomes of signal conversion under normal and faulty conditions. As can be seen from the conversion results, the converted images under different work conditions look completely different. The dataset comprises 300 images for each pattern input, totaling 6600 images. 300 for a healthy pattern, and 300*21 for various fault occurrences. To analyze this high-dimensional dataset thoroughly, we employed the t-SNE (t-Distributed Stochastic Neighbor Embedding) method, which reduced the dataset's dimensionality to two dimensions .

To analyze this high-dimensional dataset thoroughly, we employed the t-SNE (t-Distributed

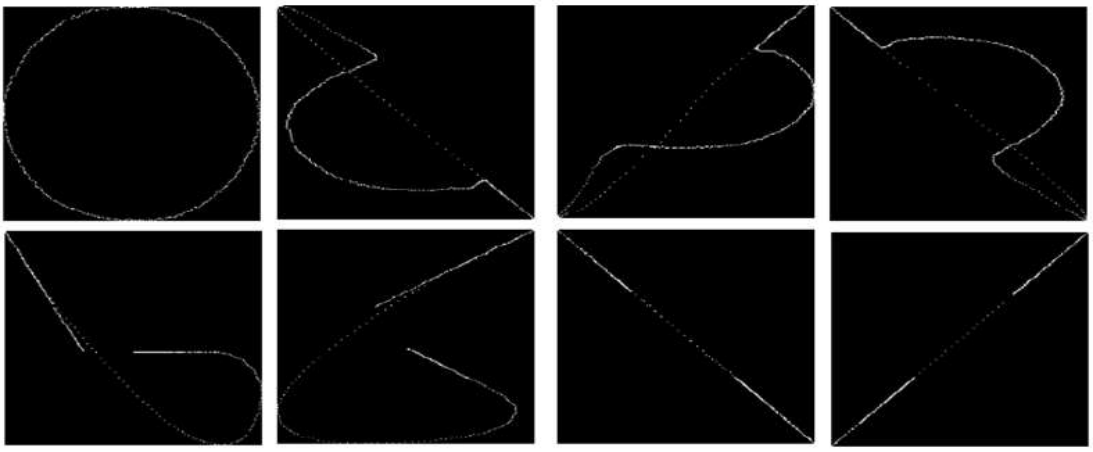

Figure 4.6: Converted images under normal and fault conditions

Stochastic Neighbor Embedding) method, which reduced the dataset's dimensionality to two dimensions to enables the visualization of complex data structures in a more interpretable manner.

In Figure 5.7, the t-SNE visualization was generated using two different distance metrics, Chebyshev and Num PCA Components, resulting in favorable clustering outcomes. The Clarke-Concordia transformation proved to be a successful technique for converting the three current lines into two vectors. Converting these vectors into images through a suitable mapping opens the possibility of utilizing pre-trained Convolutional Neural Networks (CNNs) for fault diagnosis.

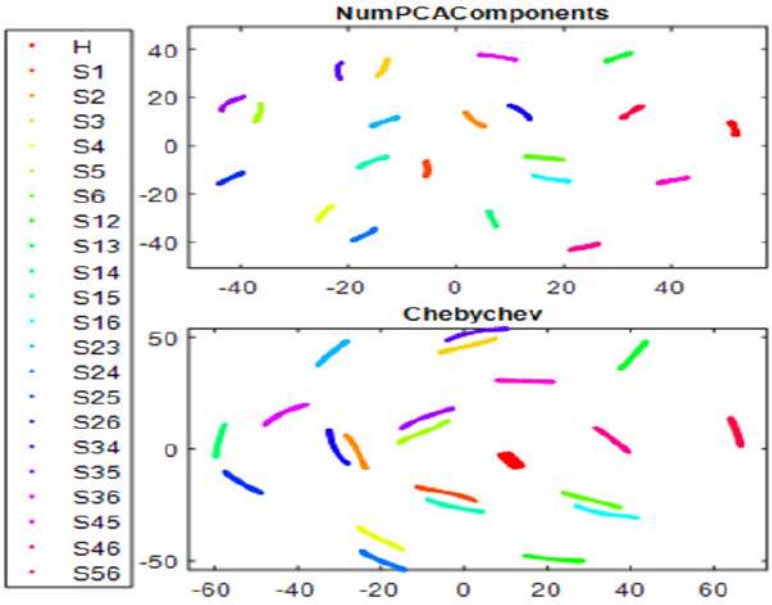


Figure 4.7: t-SNE obtained using two distance metrics

## Performance evaluation

Our proposed method's performance was assessed using five metrics [93]: accuracy (Acc), sensitivity (SN), also known as recall (R), precision (P), specificity (S), and F1-score (F). These metrics were computed using the following formulas outlined in Equations (5.3-5.7).

$$A_{cc} = \frac{TP + TN}{TP + FN} \tag{4.4}$$

$$R = \frac{TP}{TP + FN} \tag{4.5}$$

$$P = \frac{TP}{TP + FP} \tag{4.6}$$

$$S = 2\frac{TN}{TN + FP} \tag{4.7}$$

$$F = 2\frac{P * R}{P + R} \tag{4.8}$$

where:

- TP (True Positive) represents cases where the true value is positive, and the predicted value is also positive.
- FN (False Negative) corresponds to cases where the true value is positive, but the predicted value is negative.
- FP (False Positive) denotes situations where the true value is negative, but the predicted value is positive.
- TN (True Negative) indicates instances where the true value is negative, and the predicted value is also negative.

A confusion matrix is a vital tool in the field of classification. It provides a clear and detailed summary of how well a classification model is performing by displaying the number of true positives, true negatives, false positives, and false negatives ( see table 5.3 ).

Table 5.3 Confusion matrix with various metrics

| | | Actual Class | | |
|---|---|---|---|---|
| | | Positive | Negative | |
| Predicted Class | Positive | TP | FP | Precision : $\frac{T_p}{T_p + F_p}$ |
| | Negative | FN | TN | Negative prediction value : $\frac{T_N}{T_N + F_N}$ |
| | | Sensitivity $\frac{T_p}{T_p + F_N}$ | Specificity $\frac{T_N}{T_N + F_p}$ | Accuracy : $\frac{T_p + T_N}{T_p + T_N + F_p + F_N}$ |

## Results

In the experimentation process, AlexNet was trained to detect various faulty modes using different dataset splits. The data was divided randomly into training and testing sets, with proportions of 80%-20%, 70%-30%, and 60%-40%. The performance analysis results are presented in Table 5.4, showing the evaluation metrics for fault detection.

Upon examination, it is evident that AlexNet achieved its highest performance in the 80%-20%

Table 4.3: Classification results for the three training-testing data split

| **Performance metrics (%)** | **Training-Testing** | | |
|---|---|---|---|
| | ***80%-20%*** ***(240-60) images*** | ***70%-30%*** ***(210-90) images*** | ***60%-40%*** ***(180-120) images*** |
| Accuracy ( Acc ) | 100 | 100 | 99.81 |
| Sensitivity (R ) | 100 | 100 | 100 |
| Precision (P) | 100 | 100 | 99.81 |
| specificity (S) | 100 | 100 | 99.99 |
| F1-score (F) | 100 | 100 | 99.99 |

and 70%-30% split combinations, outperforming the 60%-40% combination. These findings were further supported by the confusion matrix illustrated in Figure 5.8. In this specific scenario, there were only 5 misclassifications out of 2640 patterns, resulting in an impressive accuracy rate of 99.81%. This outcome underscores the effectiveness of the model, particularly when trained on the 80%-20% and 70%-30% data splits, in accurately identifying and classifying faulty modes.

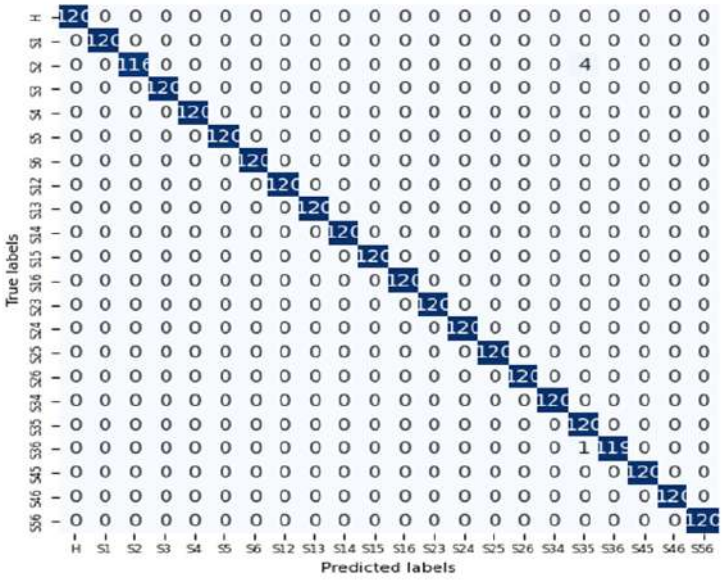


Figure 4.8: Confusion matrix for the 60%-40% combination

Using the described network-training configuration with only 6 epochs, the AlexNet could provide a very high performance of classification. Figure 5.9 illustrates one of the training processes of AlexNet, showcasing a pattern of random fluctuations in accuracy values during the initial epochs. This behavior indicates that the model is continuously learning and adjusting its weights based on the training data. As the training progresses, after the 5th epoch, the accuracy reaches its peak value, achieving 100%. The fact that AlexNet consistently achieved perfect accuracy across various fault cases is highly promising. This success underscores the potential of employing deep learning models for fault diagnosis in source voltage inverters. Ensuring the proper functioning of these systems is crucial, especially in variable speed drive systems and renewable-energy-source-based electric systems. The use of deep learning models with pre-trained CNNs for fault diagnosis in source voltage inverters is an exciting area of research, and has the potential to improve the reliability and efficiency of these systems.


Figure 4.9: Training process of AlexNet for 80%-20% combination

## 4.5 Conclusion

In this paper, transfer learning is applied to detect and classify open-switches faults in IGBTs (Insulated Gate Bipolar Transistor) switch in inverters feeding induction motor. Transfer learning offers the advantage of reducing training time and computational costs since only a few layers of the pre-trained model need to be retrained. The proposed approach utilizes AlexNet, a deep Convolutional Neural Network (CNN), to detect and monitor the open-circuit fault. To facilitate the application of deep CNNs, the $\alpha\beta$ current signals are encoded into 227x227 images using a mapping method based on the analysis of Concordia vectors derived from the line currents. Visualization of the transformed data using t-SNE confirms the separability of the 22 classes. The performance of the proposed method is assessed using five key metrics: accuracy, sensitivity, precision, specificity, and F1-score. Notably, AlexNet exhibits outstanding performance, achieving perfect scores (100%) across all these metrics in the 80%-20% and 70%-30% data split combinations. The proposed method combines data acquisition, pre-processing, and machine learning techniques to detect open switch faults in induction motor inverters. By using deep learning algorithms like AlexNet, the method can achieve high accuracy in fault detection and classification, which can help prevent damage to the motor and improve overall system reliability.

# Chapter 5

# Inverter Reconfiguration for DTC and DTC-SVM

## 5.1 Introduction

It is necessary to diagnose and correct any inverter faults that are found. Fuzzy and neural controls were used in this chapter to simulate the various fault modes for the six switches. The results of this diagnostic exercise will be used to reconfigure the inverter so that the motor drive can continue to operate in a safe manner [43].

## 5.2 Inverter Reconfiguration for DTC and DTC-SVM

To work alongside the inverter's three primary legs, we add three auxiliary legs. The main leg and each auxiliary leg are connected in parallel. When a fault switch occurs, the main leg that carried the fault switch will be switched off by the same reconfiguration signal while the auxiliary leg will be activated. The three-phase inverter that is proposed for reconfiguration is shown structurally in Figure 1. The diagnostic system automatically generates the three reconfiguration signals from inputs C1, C2, and C3, and these signals are predicted to activate or deactivate the inverter arms.

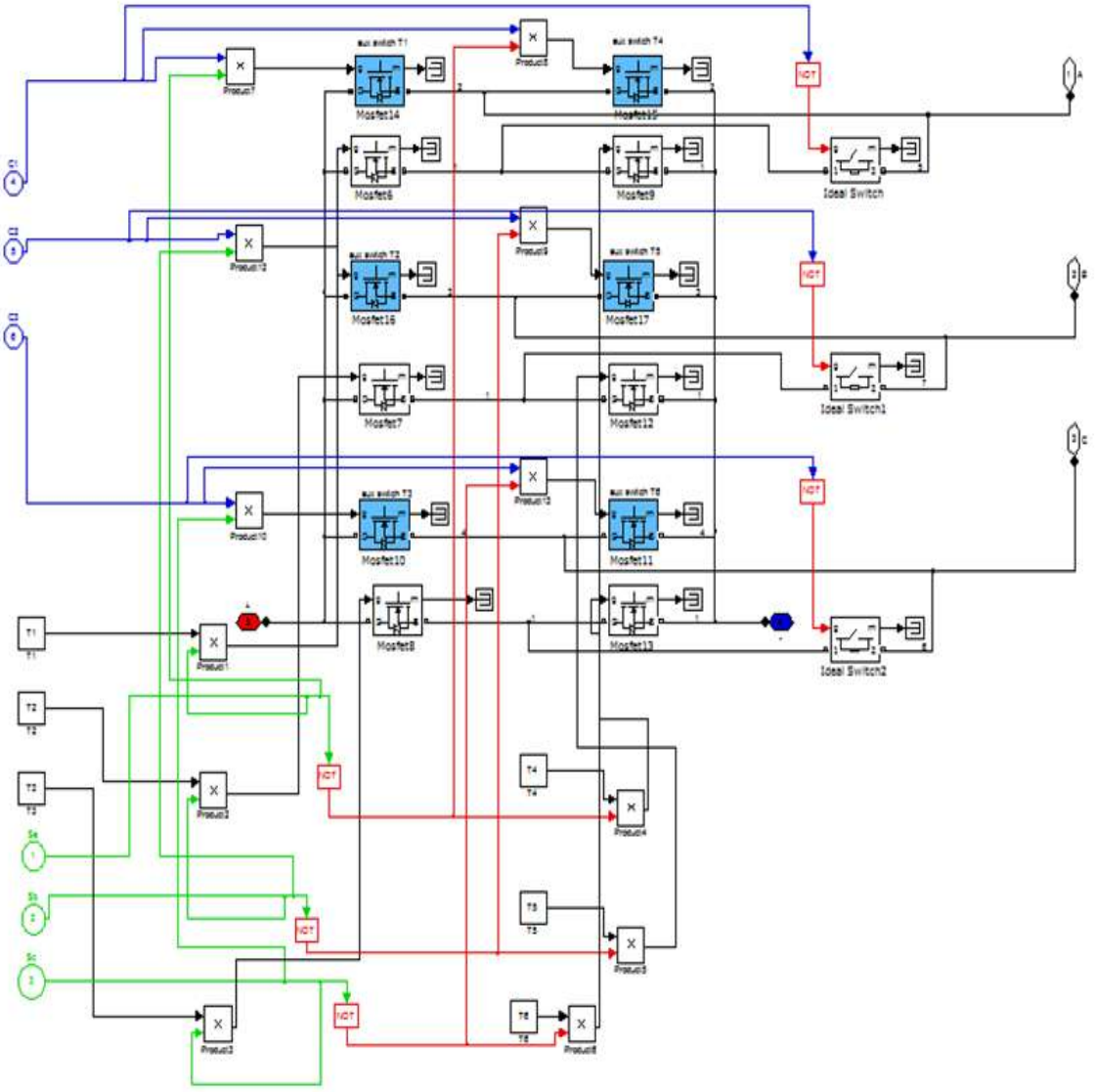

Figure 5.1: SIMULINK Model of PWM Inverter Reconfiguration

## 5.3 Reconfiguration for DTC (with ANN)

A model Simulink for DTC contain a bloc of reconfiguration linked to inverter. A reconfiguration is done using artificial neural network. As a result, when an inverter failure occurs, an order to switch to the auxiliary leg is sent after fault identification and localization.as shown in figure 2

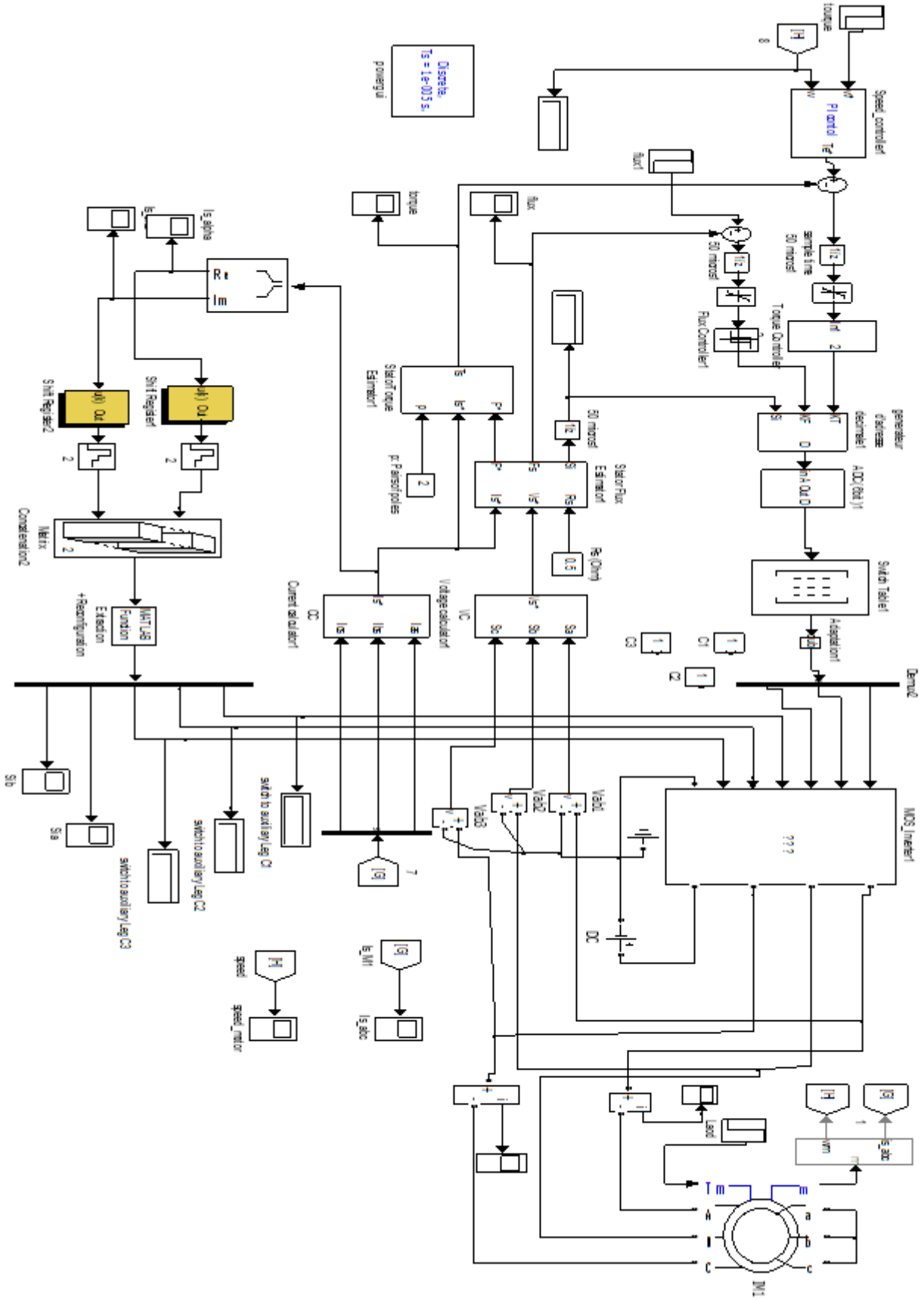

Figure 5.2: Matlab/Simulink block diagram of DTC using ANN for inverter reconfiguration

1. **Input/output Data**

   A network has three hidden layers, tow input ($S_s$,$S_s$) and one output Ti. The notation 9-6-1 indicates the number of neurons for each hidden layers.

2. **Neural Network Training**

   The network will be trained with different faulty modes. The size of the input matrix data is two rows ($S_s$,$S_s$) with 2001 columns for each pattern input. That gives 2001 for a healthy pattern and 2001*6=12006 for fault occurrence. That gives a 14007 data base for neural network training. The output target classification is represented for different speed references.

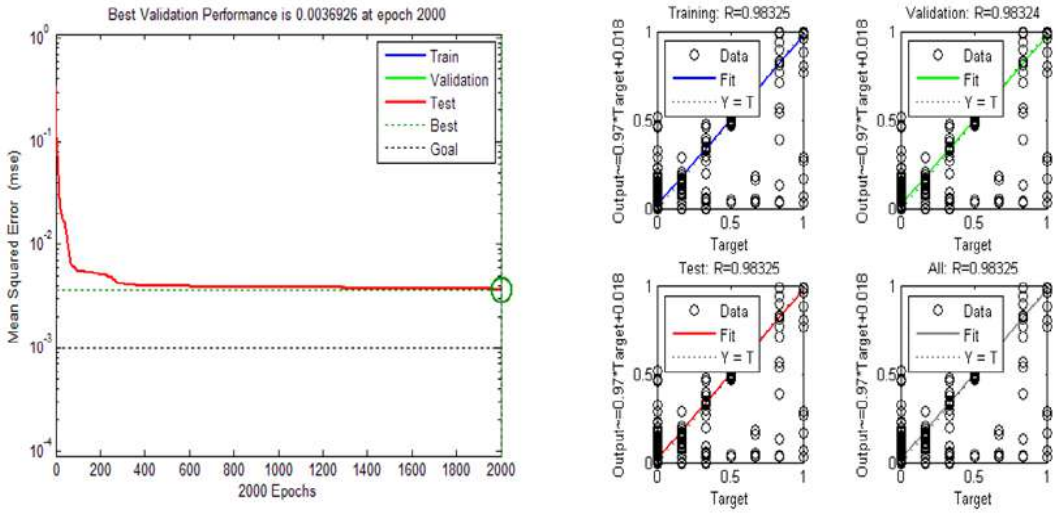


Figure 5.3: Errors in diagnosis training, testing, and validation *(in DTC ANN)*

As shown in is shown in Fig.3, the number of the off-line training to get 0.003 error is 2000 epochs.

- **Simulation results** The diagnosis result is displayed for each phase's three stator currents, motor speed, torque, and flux.

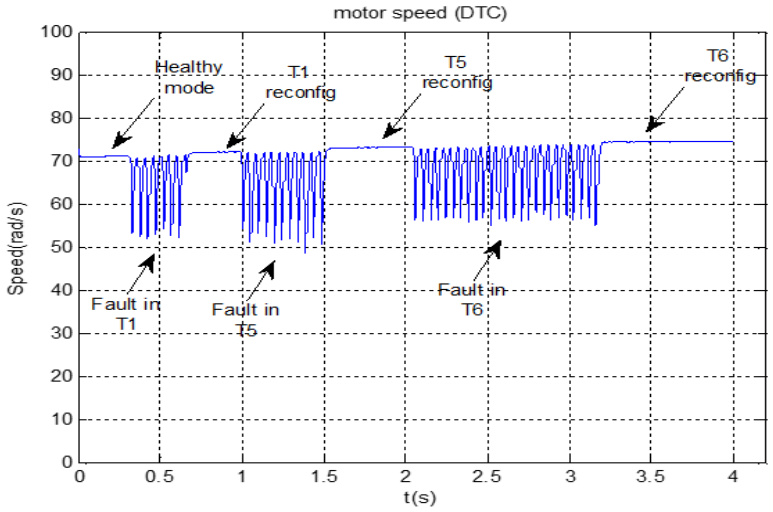


(a) Motor speed

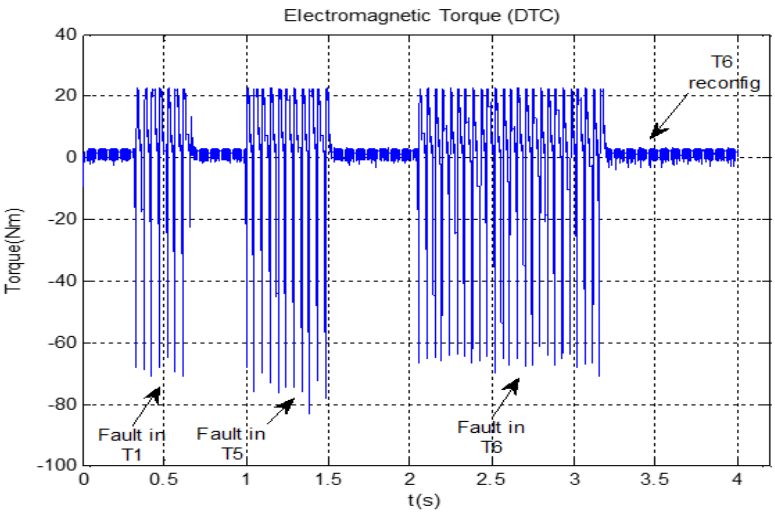


(b) Torque

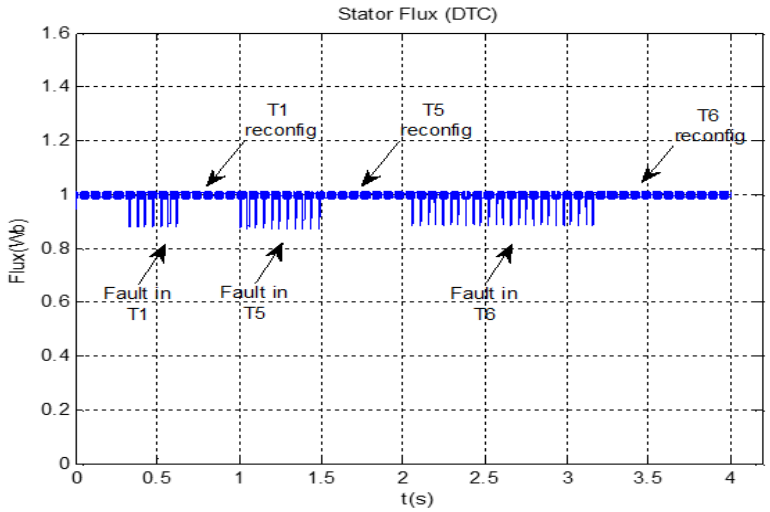


(c) Stator flux

Figure 5.4: Simulation for a sequence of faulty IGBT transistor *(in DTC ANN)*

- **Discussion of Results**

  The simulation is done like the following:

  - Speed reference is 70 (rad/s), stator flux is 1(wb).
  - We made (0.3s) for healthy mode, after we did fault in switch T1. Detection, localization and reconfiguration is done in (0.7s), the same in switch T5, fault in (1s). Detection, localization and reconfiguration is done in (1.6s) also in switch T6, fault in (2s) reconfiguration in (3.25s). Total time for simulation is (4s)

Table 5.1: Summary of reconfiguration Time for DTC ANN

| Open switch fault | T1 | T5 | T6 |
|---|---|---|---|
| Time for reconfiguration | 0.4s | 0.6s | 1.25s |

We select three fault switch for reconfiguration T1, T5 and T6 corresponding three auxiliary leg a maximum time for reconfiguration is (1.25s).

## 5.4 Reconfiguration for DTC-SVM (with fuzzy)

There is a reconfiguration block attached to an inverter in this Simulink model for DTC-SVM as well. The reconfiguration is managed via a fuzzy logic control. Therefore, after fault diagnosis and localization, an instruction to switch to the auxiliary leg is delivered when an inverter failure occurs. The diagnosis result is displayed for each phase's three stator currents, motor speed, torque, and flux.as shown in figure 5

- **Discussion of Results**

  The simulation is illusrated in figure 6 & 7 and done like the following:

  - Speed reference is 75 (rad/s), stator flux is 1(wb).
  - We made (0.55s) for healthy mode, after we did fault in switch T1. Detection, localization and reconfiguration is done in (0.65s), the same in switch T2, fault in (1s). Detection, localization and reconfiguration is done in (1.15s) also in switch T6, fault in (1.55s) reconfiguration in (1.7s). Total time for simulation is (2s)

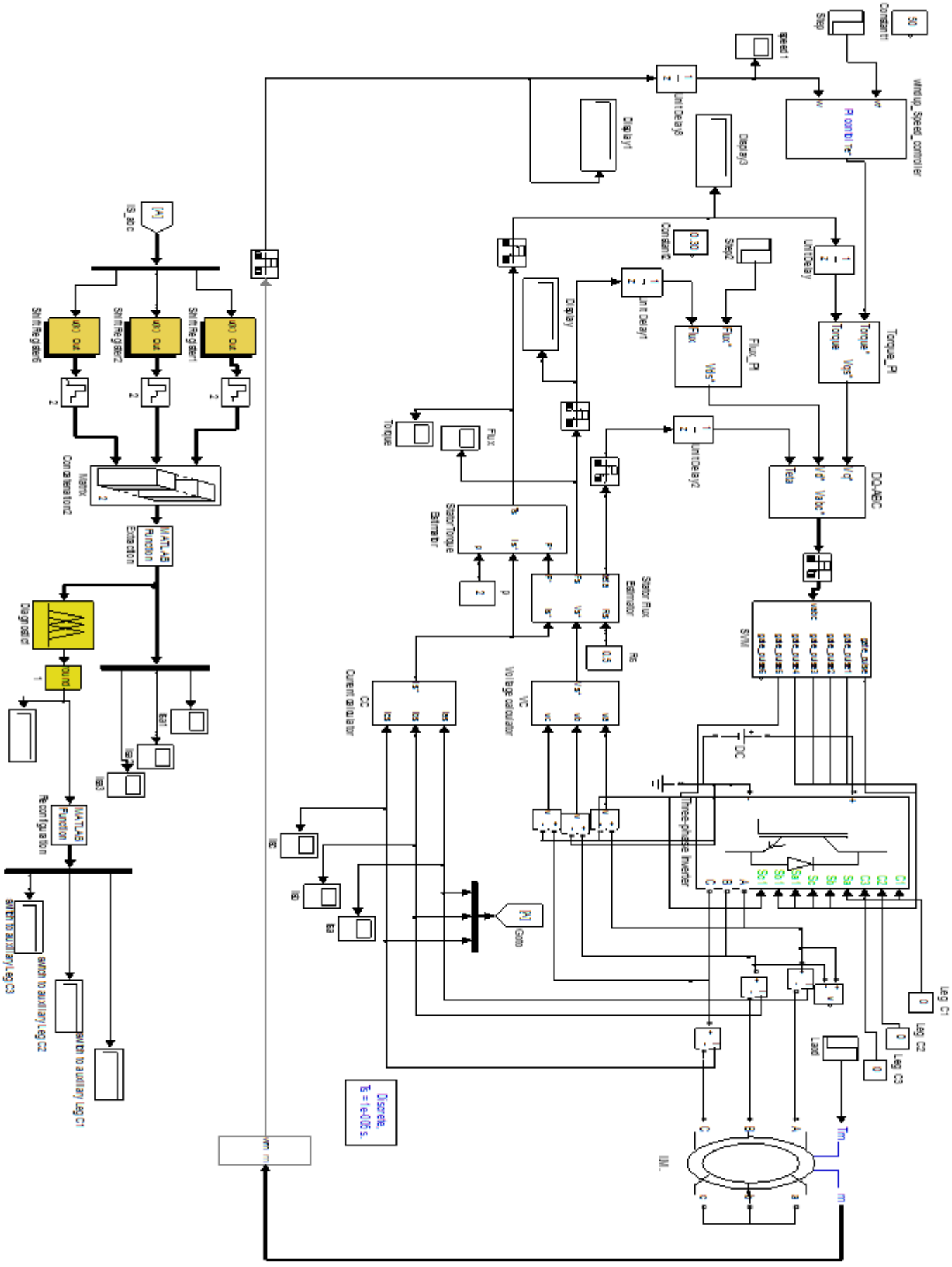


Figure 5.5: Matlab/Simulink block diagram of DTC-SVM using FUZZY for inverter reconfiguration

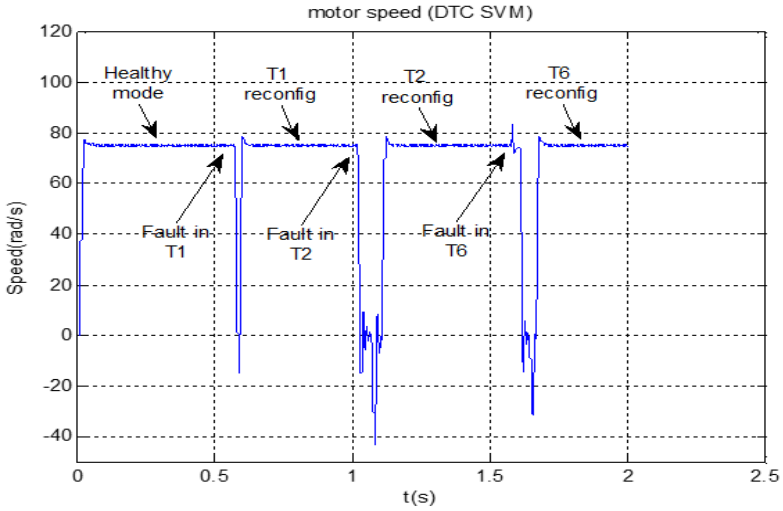


(a) Motor speed

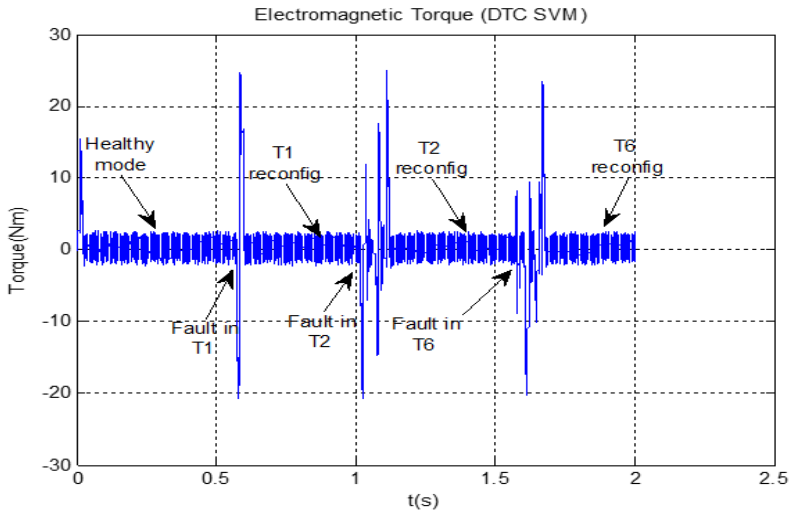


(b) Torque

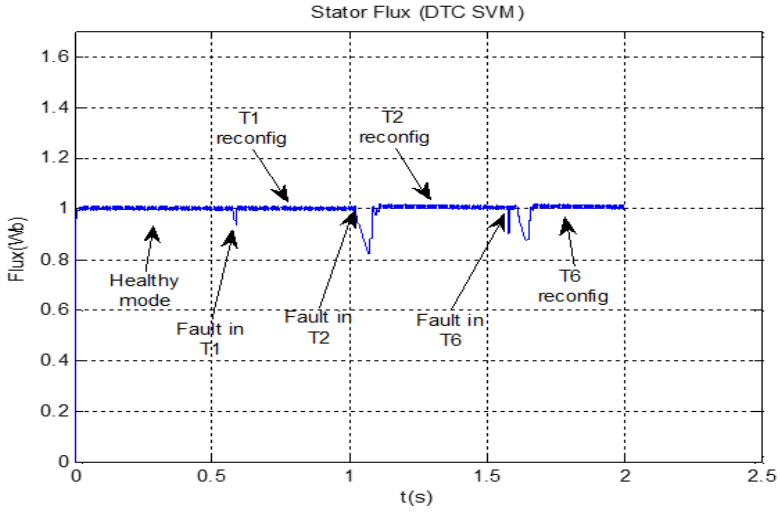


(c) Stator flux

Figure 5.6: Simulation for a sequence of faulty IGBT transistor *(in DTC-SVM FUZZY)*

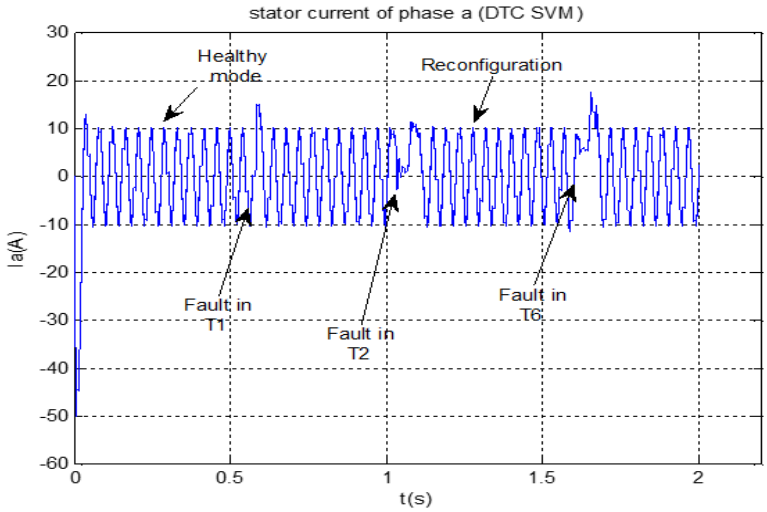


(a) Current phase a

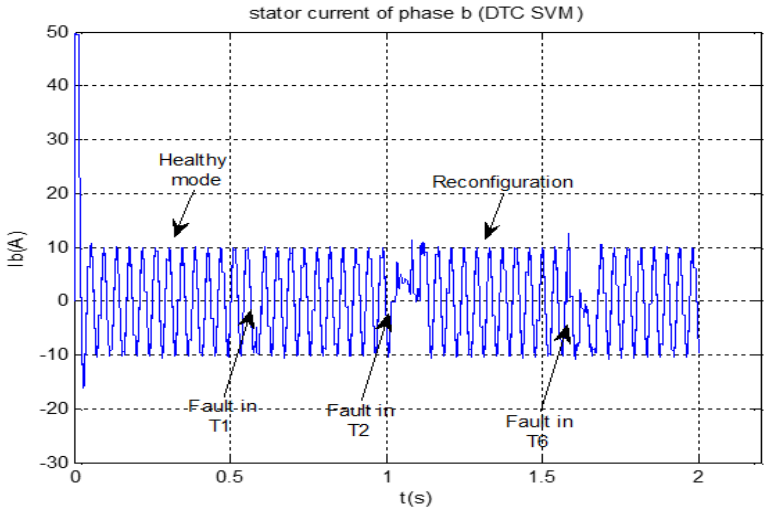


(b) Current phase b

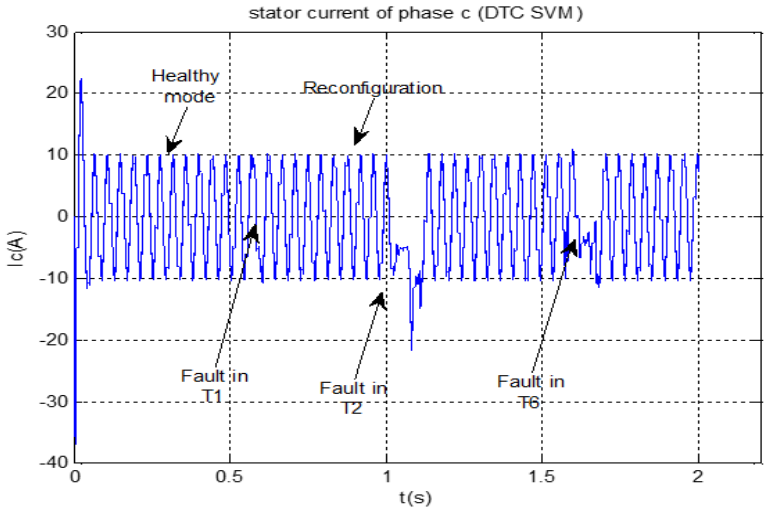


(c) Current phase c

Figure 5.7: Current phase simulation for a sequence of faulty IGBT transistor *(in DTC-SVM FUZZY)*

Table 5.2: Summary of reconfiguration Time for DTC-SVM FUZZY

| Open switch fault | T1 | T2 | T6 |
|---|---|---|---|
| Time for reconfiguration | 0.1s | 0.15s | 0.5s |

We select three fault switch for reconfiguration T1, T2 and T6 corresponding three auxiliary leg a maximum time for reconfiguration is (0.15s).

## 5.5 Reconfiguration for DTC-SVM (with ANN)

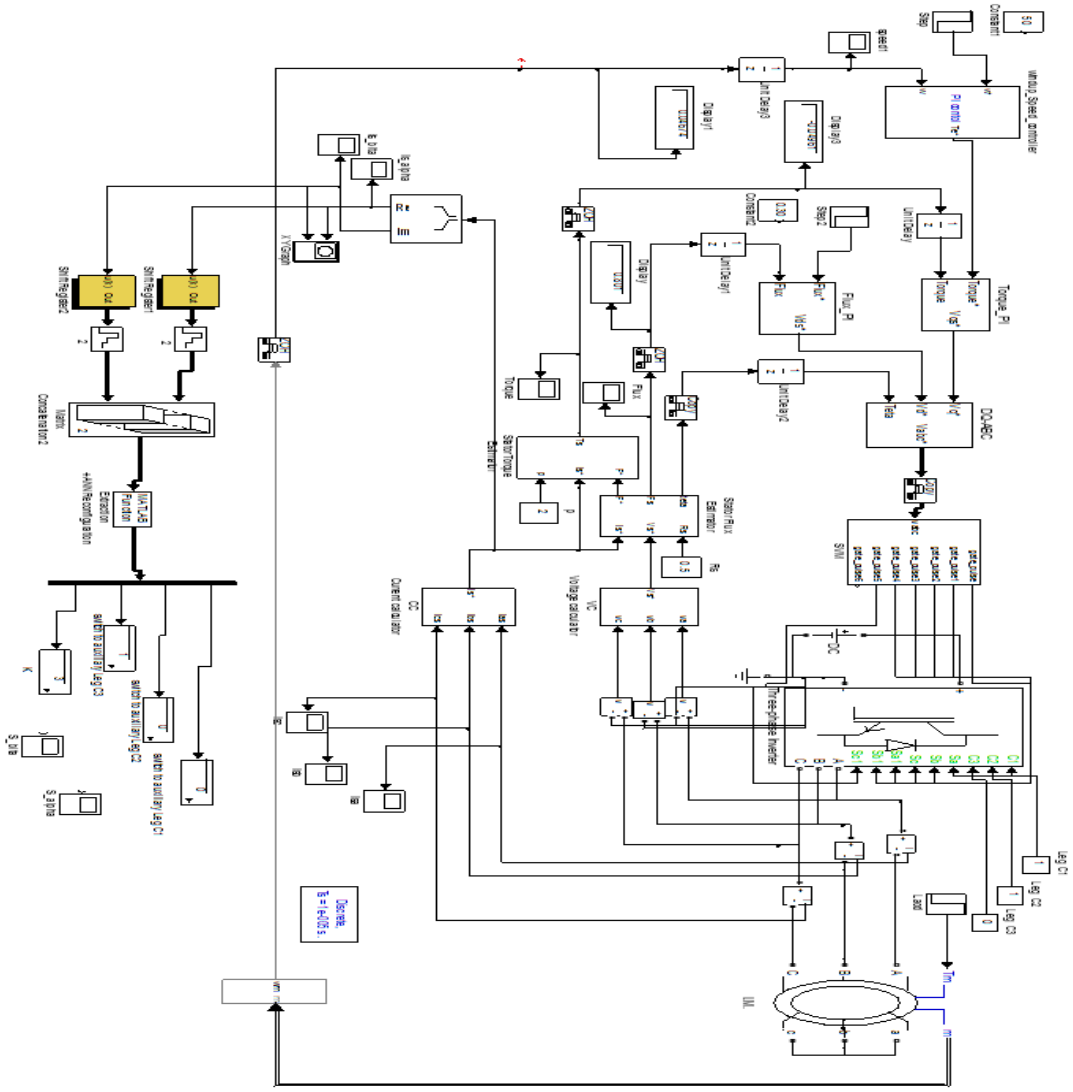

Figure 5.8: Matlab/Simulink block diagram of DTC-SVM using ANN for inverter reconfiguration

The same in this Simulink model DTC-SVM. A reconfiguration block connected to an inverter. The artificial neural network is used for reconfiguration. Therefore, fault detection

and localization had made the order to switch in the auxiliary leg to have been sent when an inverter problem occurred.

1. **Input/output Data**

   A network has three hidden layers, tow input ($S_s$,$S_s$) and one output Ti. The notation 9-6-1 indicates the number of neurons for each hidden layers.

2. **Neural Network Training**

   The network will be trained with different faulty modes. The size of the input matrix data is two rows ($S_s$,$S_s$) with 3960 columns for each pattern input. That gives 3960 for a healthy pattern and 3960*6=23760 for fault occurrence. That gives a 27720 data base for neural network training. The output target classification is represented for different speed references. As shown in is shown in Fig.16, the number of the off-line training to

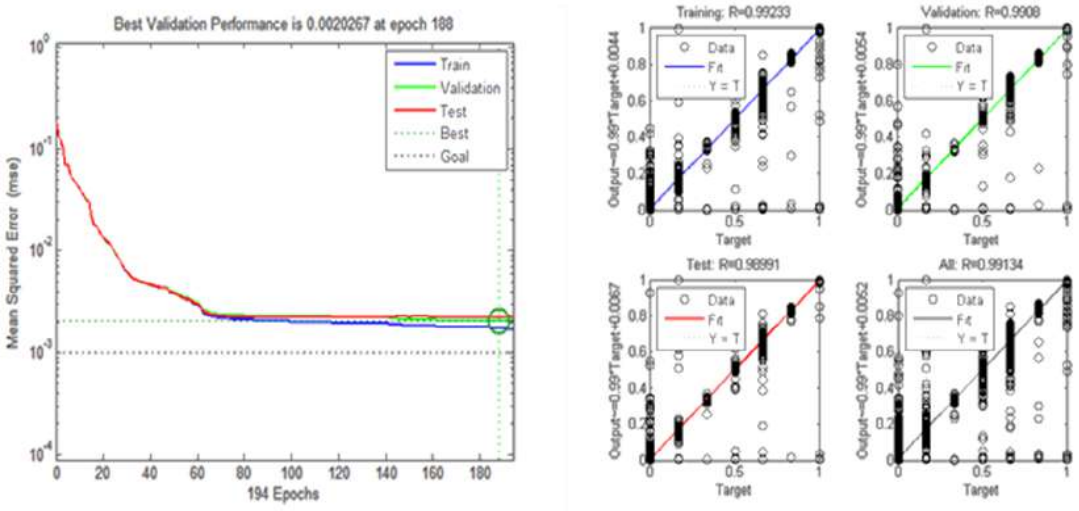


Figure 5.9: Errors in diagnosis training, testing, and validation *(in DTC-SVM ANN)*

get 0.002 error is 194 epochs.

- **Simulation results**

  The diagnosis result is displayed for each phase's three stator currents, motor speed, torque, and flux.

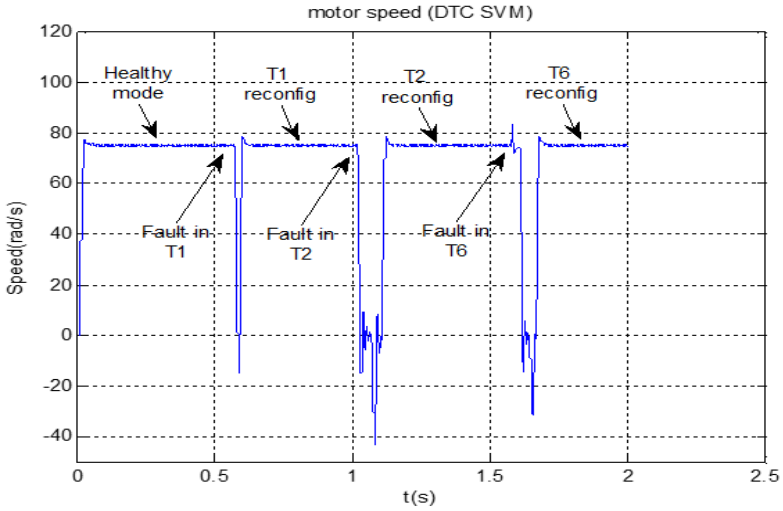


(a) Motor speed

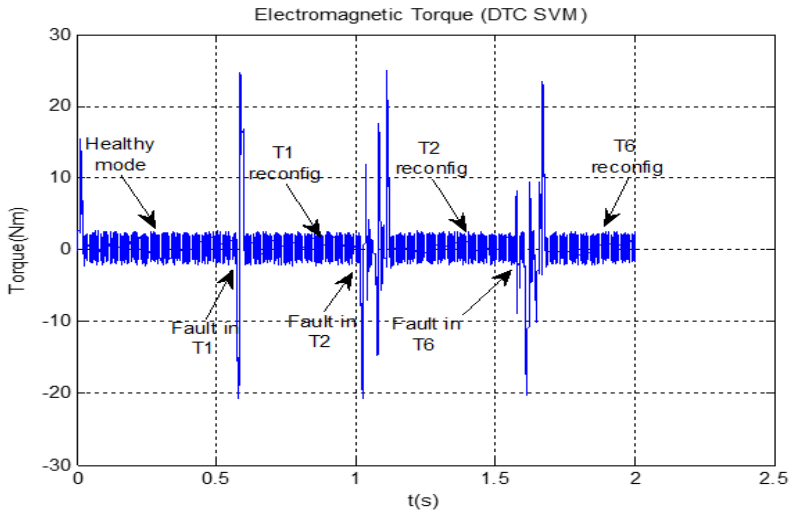


(b) Torque

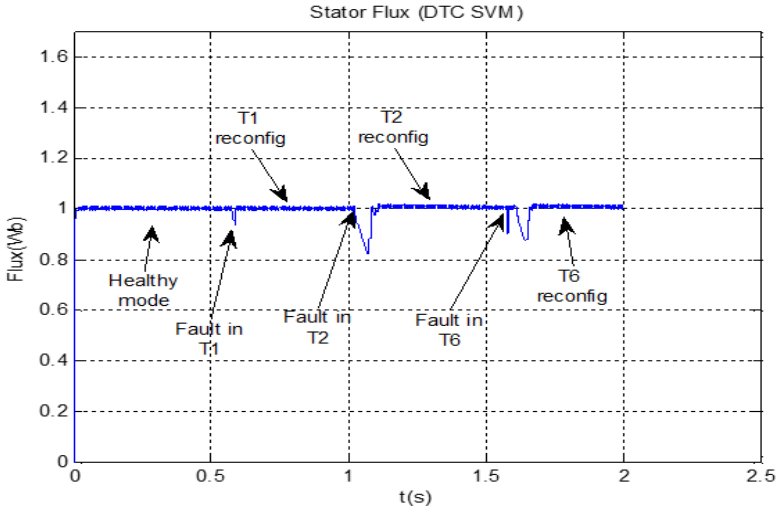


(c) Stator flux

Figure 5.10: Simulation for a sequence of faulty IGBT transistor *(in DTC-SVM FUZZY)*

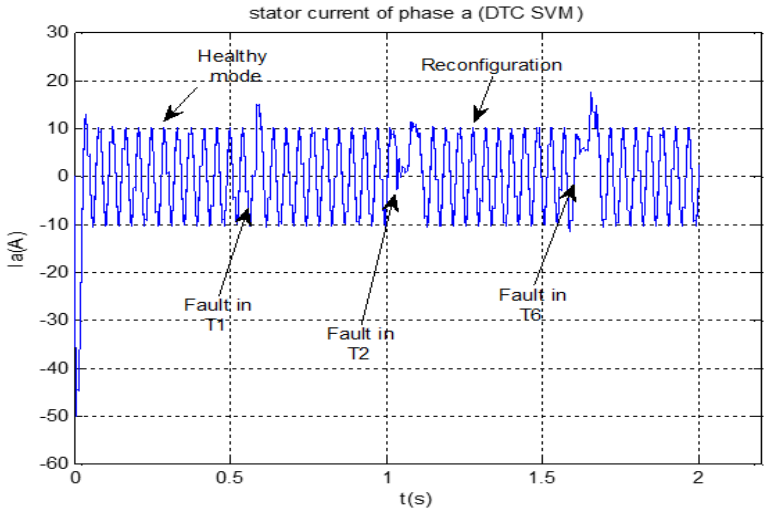


(a) Current phase a

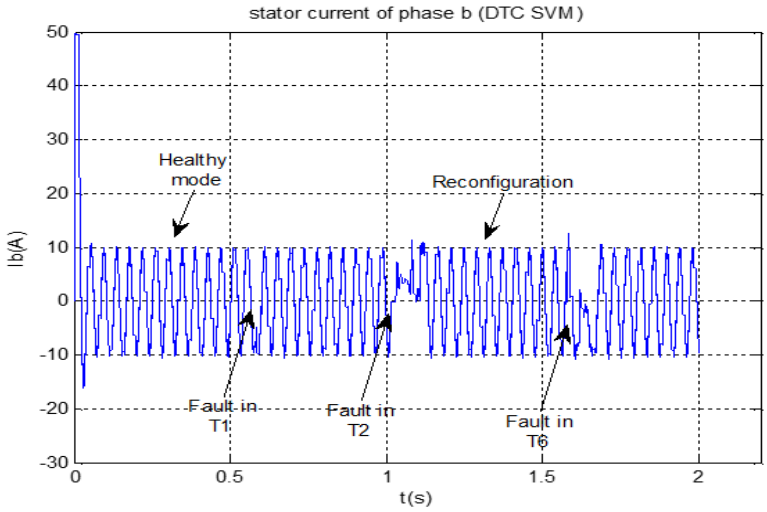


(b) Current phase b

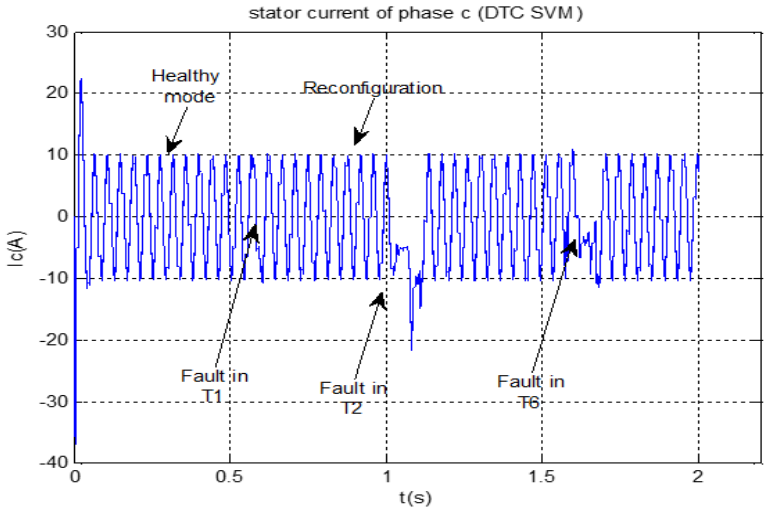


(c) Current phase c

Figure 5.11: Current phase simulation for a sequence of faulty IGBT transistor *(in DTC-SVM FUZZY)*

- **Discussion of Results**

  The simulation is done like the following:

  - Speed reference is 60 (rad/s), stator flux is 0.8(wb).
  - We made (0.54s) for healthy mode, after we did fault in switch T4. Detection, localization and reconfiguration is done in (0.78s), the same in switch T5, fault in (1.2s)reconfiguration is done in (1.3s) also in switch T3, fault in (1.7s) reconfiguration in (1.9s). Total time for simulation is (2.4s)

Table 5.3: Summary of reconfiguration Time for DTC-SVM ANN

| Open switch fault | T4 | T5 | T3 |
|---|---|---|---|
| Time for reconfiguration | 0.24s | 0.1s | 0.2s |

We select three fault switch for reconfiguration T3, T4 and T5 a maximum time for reconfiguration is (0.24s).

## 5.6 Control Strategies Summary

Space vector modulation- direct torque control (DTC-SVM) has fast reconfiguration a cause to their characteristic constant frequency in both ANN and FUZZY. Therefore, direct torque control (DTC) reconfiguration time is more logger.as illustrate in table 4.

| **Model technique** | **DTC ANN** ***(figure 2)*** | **DTC-SVM ANN** ***(figure 8)*** | **DTC-SVM FUZZY** ***(figure 15)*** |
|---|---|---|---|
| Time for reconfiguration | 1.25 s | 0.18 s | 0.15 s |

## 5.7 Conclusion

This chapter focused on diagnosing faults in inverter systems that use induction motor drives that are managed by fuzzy logic and neural networks for both direct torque control (DTC) and space vector modulation-direct torque control (DTC-SVM). That seems like a straightforward and efficient method of operating an induction motor drive. It offers a potential fix for issues with robustness. We looked at how to reconfigure the inverter to detect and diagnose open inverter switching faults in DTC and DTC-SVM. To do this, we used artificial intelligence to simulate the various defect modes for each of the six switches. Based on the results of

our diagnostics, we redesigned the inverter to prevent faults from arising by utilizing neural networks and fuzzy logic in direct torque control and space vector modulation- direct torque control systems able to operate with any stability guarantee.

# GENERAL CONCLUSION

The aim of this thesis was to detect faults, diagnose and reconfigure a three-phase inverter that feeds an induction motor drive, which is controlled through different artificial intelligence techniques like fuzzy logic control (FL), artificial neural network (ANN), and convolution neural network (CNN). We selected two types of control strategies: direct torque control (DTC), and direct torque control with space vector modulation (DTC-SVM).

We presented models of diagnosis, namely DTC_ANN, DTC_FUZZY, DTC-SVM_ANN, and DTC-SVM_FUZZY of induction motor drives feeding a PWM three-phase inverter. This control technique is simple and effective in controlling an induction motor drive, which makes it a promising solution to robustness problems.

The MATLAB SIMULINK program was utilized in the development of the suggested model system. The results of the simulation show how well the anti-windup regulator works to restrict current peaks during changes or inversions in rotational speed and to solve the saturation issue.

Our research has focused on the identification and treatment of short and open inverter switching faults. We employed an artificial intelligence technique to mimic the various forms of defects for each of the six switches. The inverter is reconfigured using the diagnostic information to stop errors from happening. This guarantees the stability of the control system's operation.

As an additional approach to this work, we suggest utilizing other intelligent techniques to enhance the recognition rate and improve diagnostic accuracy for the occurrence of three faults. It is recommended that other control strategies such as Field Oriented Control (FOC) and direct self-control (DSC) be explored.

# Personale Contributions

## Publication

1. Tamissa, Y., Charif, F., Kadri, F., Benchabane, A., 2022. Pattern recognition and diagnosis of short and open circuit faults inverter in induction motor drive using neural networks, Engineering Review, vol.42(3). https://doi.org/10.30765/er.1949.

## Conference

1. Tamissa, Y., Kadri, F., Charif, F., Benchabane, A., 2020. Neural Fault Diagnosis Method for Voltage Source Inverter with a Neural Direct Torque Control of Induction Motor, The First IEEE International Conference on Communications, Control Systems and Signal Processing ( CCSSP 2020), El-Oued, Algeria pp 480-486
   https://doi.org/10.1109/CCSSP49278.2020.9151552

2. F. Kadri, Y. Tamissa, M.A. Hamida, F. Charif, and A. Benchabane, "Fuzzy Fault Diagnosis for Voltage Source Inverter in a Direct Torque Control Induction Motor Drive", 1st International Conference on Sustainable Energy and Advanced Materials IC-SEAM'21, April 21-22, 2021, Ouargla, ALGERIA.

3. Tamissa, Y., Kadri, F., Charif, F., Benchabane, A., 2022. Multiple Fuzzy Diagnosis for Voltage Source Inverter Open Circuit Fault in Torque Direct Control Induction Motor Drive, Forum of Artificial Intelligence and It's Applications (AIAP'2022). University of El-Oued, Algeria.

4. Y. Tamissa, F. Charif, A. Benchabane, and F. Kadri "Pattern Recognition and Diagnosis of Multiple Open Circuit Faults in the Inverter Feed of an Induction Motor Drive Using Neural Networks" October 2022;1st International Conference on Renewable Materials and Energies ICRME22 October 26-27, 2022, Ouargla, ALGERIA

5. A. Benchabane, Y. Tamissa, F. Charif and F. Kadri “AlexNet for Open-Switch Faults Detection in Induction Motor Inverter” May 2023 Fourth International Conference on Technological Advances in Electrical Engineering (ICTAEE’23.), May 23-24 2023; Skikda, Algeria

# Bibliography


[1] I. Takahashi, T. Noguchi, "A new quick-response and high efficiency control strategy of an induction machine", *IEEE Trans. on Industrial Application*, Vol. IA-22, no.5, Sept./Oct. 1986,pp.820-827.

[2] U. Baader, M. Depenbrock, G. Gierse, "Direct Self Control (DSC) of Inverter-Fed-Inducktion Machine - A Basis for Speed Control Without Speed Measurement", *IEEE Trans. of Industry Applications*, Vol. 28, No. 3 May/June 1992, pp.581-588.

[3] F.Mekhalfia1*, D.E. Khodja2, S. Chakroune,"FaultTolerant Control Using Artificial Neural Network for Induction Machine", *Advances in Modelling and Analysis C* Vol. 74, No. 24, December, 2019, pp. 47-55 Journal homepage: http://iieta.org/journals/ama_c https://doi.org/10.18280/ama_c.742-402

[4] Iffouzar Koussaila*, Khaldi Lyes, Djerioui Ali, Houari Azeddine, Ghedamsi Kaci, Benkhoris Mohamed Fouad,"New Analysis Model of Stator Open Phase Faults in a Five-Phase Induction Motor", *Journal Européen des SystèmesAutomatisés* Vol. 53, No. 2, April, 2020, pp. 213-218Journal homepage: http://iieta.org/journals/jesa https://doi.org/10.18280/jesa.530207

[5] F. W. Fuchs, "Some diagnosis methods for voltage source inverters in variable speed drives with induction machines. A survey", *in Proc. IEEE IECON,* Roanoke, VA, Vol. 2, pp. 1378–1385, 2003. DOI: 10.1109/IECON.2003.1280259

[6] Subodh Kanta Barik, Kiran Kumar Jaladi,"Five-Phase Induction Motor DTC-SVM scheme with PI Controller and ANN controller",*Global Colloquium in Recent Advancement and Effectual Researches in Engineering, Science and Technology (RAEREST 2016)*,doi: 10.1016/j.protcy.2016.08.184

[7] B. El Badsi, B. Bouzidi and A. Masmoudi, "DTC Scheme for a Four-Switch Inverter-Fed Induction Motor Emulating the Six-Switch Inverter Operation", *IEEE Transactions on Power Electronics*, Vol. 28, No. 7,July 2013. DOI: 10.1109/TPEL.2012.2225449

[8] V.M.V. Rao, and A. Anand Kumar, "Artificial Neural Network and Adaptive Neuro Fuzzy Control of Direct Torque Control of Induction Motor for Speed and Torque Ripple Control", *2nd International Conference on Trends in Electronics and Informatics (ICOEI)*, 2018pp. 1416-1422 Tirunelveli

[9] Yesma Bendaha;Mazari Benyounes ''Fuzzy direct torque control of induction motor with sensorless speed control using parameters machine estimation" *3rd International Conference on Control, Engineering & Information Technology (CEIT)*, Tlemcen, Algeria,2015

[10] Gong, W., Chen, H., Zhang, Z., Zhang, M., Gao, H.,2020. A Data-Driven-Based Fault Diagnosis Approach for Electrical Power DC-DC Inverter by Using Modified Convolutional Neural Network With Global Average Pooling and 2-D Feature Image, *in IEEE Access*, vol. 8, pp. 73677-73697.

[11] Vas P, Sensorless vector and direct torque control. Oxford Univ. Press; 1998.

[12] Chan TF, Shi K, Applied intelligent control of induction motor drives. John Wiley & Sons; 2011 Jan 19.

[13] Habbi HM, Ajeel HJ, Ali II, Speed control of induction motor using PI and V/F scalar vector controllers, *International Journal of Computer Applications*. 2016 Oct;151(7):36-43.

[14] Usama M, Kim J, "Vector Control Algorithm Based on Different Current Control Switching Techniques for Ac Motor Drives", *InE3S Web of Conferences* 2020 (Vol. 152, p. 03009). EDP Sciences.

[15] Diab AA, Al-Sayed AH, Mohammed HH, Mohammed YS, "Development and Stabilization of Adaptive State Observers for Induction Machines", In Development of Adaptive Speed Observers for Induction Machine System Stabilization 2020 (pp. 19-31). Springer, Singapore.

[16] IDIR Abdelhakim, KIDOUCHE Madjid, ZELMAT Mimoune and AHRICHE Aimad '' A Comparative Study between DTC, SVM-DTC and SVM-DTC with PI Controller of Induction Motor"Département de la maintenance industrielle, Faculté des sciences de l'ingénieur,Université M'Hamed Bougara de Boumerdès, Avenue de l'Indépendance, 35000, Boumerdès, Algeria, (pp. 94-97).

[17] Hingmire P K, Kumar S and Me R 2016 "Development of a V / f Control scheme for controlling the Induction motor- both Open Loop and Closed Loop using MATLAB" . Int. J. Sci. Eng. Appl. Sci. 403–7

[18] Marcin Żelechowski. '' Space Vector Modulated – Direct Torque Controlled (DTC – SVM) Inverter – Fed Induction Motor Drive" Warsaw University of Technology Faculty of Electrical Engineering Institute of Control and Industrial Electronics.Warsaw – Poland, 2005. p. 1–175

[19] Fathy Abouzeid, A.; Guerrero, J.M.; Endemaño, A.; Muniategui, I.; Ortega, D.; Larrazabal, I.; Briz, F. "Control Strategies for Induction Motors in Railway Traction Applications". Energies 2020, 13, 700. https://doi.org/10.3390/en13030700

[20] Najib El Ouanjli et al. "Modern improvement techniques of direct torque control for induction motor drives". a review. Protection and Control of Modern Power Systems. Springer Open; 2019. p. 1–12. https://doi.org/10.1186/s41601-019-0125-5.

[21] Hartono, H., Sudjoko, R. I., & Iswahyudi, P. (2019, November). "Speed control of three phase induction motor using universal bridge and PID controller". *In Journal of Physics: Conference Series* (Vol. 1381, No. 1, p. 012053). IOP Publishing. doi:10.1088/1742-6596/1381/1/012053

[22] Carbone, L.; Cosso, S.; Kumar, K.; Marchesoni, M.; Passalacqua, M.; Vaccaro, L. Stability Analysis of Open-Loop V/Hz Controlled Asynchronous Machines and Two Novel Mitigation Strategies for Oscillations Suppression. Energies 2022, 15, 1404. https://doi.org/10.3390/en15041404

[23] Annuar, K. A. M., Sapiee, M. R., Nor, R. M., Azali, M. S. M., Shah, M. B. N., & Rozali, S. M. (2019). Squirrel cage induction motor scalar control constant V/F analysis. *TELKOMNIKA (Telecommunication Computing Electronics and Control)*, 17(1), 417-424. DOI: 10.12928/TELKOMNIKA.v17i1.8818

[24] S. Mishra, A. B. Palazzolo, X. Han, Y. Li and C. Kulhanek, "Torsional Vibrations in Open Loop Volts Hertz Variable Frequency Drive Induction Motor Driven Mechanical Systems," 2020 *IEEE Texas Power and Energy Conference (TPEC)*, College Station, TX, USA, 2020, pp. 1-6, doi: 10.1109/TPEC48276.2020.9042586.

[25] Kohlrusz, G., & Fodor, D. (2011). "Comparison of scalar and vector control strategies of induction motors". *Hungarian Journal of Industry and Chemistry*, 265-270.

[26] Zeb K, Haider A, Uddin W, Qureshi MB, Mehmood CA, Jazlan A, Sreeram V, Indirect Vector Control of Induction Motor using Adaptive Sliding Mode Controller, *In2016 Australian Control Conference (AuCC)* 2016 Nov 3 (pp. 358-363). IEEE.

[27] Tsuji M, Iwamoto K, Hamasaki SI, Del Pizzo A," A simplified speed-sensorless vector control for induction motor", *In2016 International Symposium on Power Electronics, Electrical Drives*, Automation and Motion (SPEEDAM) 2016 Jun 22 (pp. 522-527). IEEE.

[28] Abu-Rub H, Schmirgel H, Holtz J, "Maximum torque production in rotor field oriented control of an induction motor at field weakening", In2007 *IEEE International Symposium on Industrial Electronics* 2007 Jun 4 (pp. 1159-1164). IEEE.

[29] Meera Shareef Sheik and K Balaji 'Comparison of Artificial Controller Based MRAS Speed Observer for Field Oriented Control of Induction Motor'2020 IOP *Conf. Ser.: Mater. Sci. Eng.* Vol 925 (01)2019 DOI 10.1088/1757-899X/925/1/012019

[30] Yan, H. et al. (2023) 'Open-circuit fault diagnosis in voltage source inverter for motor drive by using Deep Neural Network', Engineering Applications of Artificial Intelligence, 120, p. 105866. doi:10.1016/j.engappai.2023.105866.

[31] Asghar, F., Talha, M. and Kim, S.H. (2017) 'Comparative study of three fault diagnostic methods for three phase inverter with induction motor', INTERNATIONAL JOURNAL of FUZZY LOGIC and INTELLIGENT SYSTEMS, 17(4), pp. 245–256. doi:10.5391/ijfis.2017.17.4.245.

[32] Xu, L., Cao, M., Song, B., Zhang, J., Liu, Y., Alsaadi, F.E., 2018. Open-Circuit Fault Diagnosis of Power Rectifier using Sparse Autoencoder based Deep Neural Network, Neurocomputing .

[33] Wang, B., Feng, X., & Wang, R. (2023). Open-circuit fault diagnosis for permanent magnet synchronous motor drives based on voltage residual analysis. Energies, 16(15), 5722. doi:https://doi.org/10.3390/en16155722

[34] Hailin Hu, Fu Feng, Tao Wang,"Open-circuit fault diagnosis of NPC inverter IGBT based on independent component analysis and neural network", Energy Reports, Volume6,Supplement9,2020,Pages134143,https://doi.org/10.1016/j.egyr.2020.11.273

[35] Pyasi, K., & N, P. K. (2020). Finite element analysis on multiple IGBT switch open-circuit fault in PWM inverter fed induction motor. *IOP Conference Series.Materials Science and Engineering,* 872(1) doi:https://doi.org/10.1088/1757-899X/872/1/012047

[36] Siddhant Gudhe, B.B. Pimple" Improved Torque Response of induction Motor Drive using Direct Torque Control Technique Applying Fuzzy Logic Control" *1st IEEE International Conference on Power Electronics. Intelligent Control and Energy Systems* (ICPEICES-2016) DOI: 10.1109/ICPEICES.2016.7853611

[37] Farid Kadri, Younes Tamissa, Mohamed Assaad Hamida, Fella Charif, and Abderrazak Benchabane '' Fuzzy Fault Diagnosis for Voltage Source Inverter in a Direct Torque Control Induction Motor Drive '' *1st International Conference on Sustainable Energy and Advanced Materials* IC-SEAM'21 April 21-22, 2021, Ouargla, ALGERIA

[38] Hassen Reghioui, Saad Belhamdi, Ammar Abdelkarim, Hellali Lallouani ,'' Enhancement of Space Vector Modulation Based-Direct Torque Control Using Fuzzy PI Controller for Doubly Star Induction Motor" *Advances in Modelling and Analysis C* Vol. 74, No. 2-4, December, 2019, pp. 63-70 Journal homepage: http://iieta.org/journals/ama_c https://doi.org/10.18280/ama_c.742-404

[39] Tamissa Younes & Kadri Farid & Charif Fella & Benchabane Abderrazak, and M.A. Hamida, "Multiple Fuzzy Diagnosis for Voltage Source Inverter Open Circuit Fault in Torque Direct Control Induction Motor Drive", *Forum of Artificial*

*Intelligence and Its Applications. Faculty of Exat science.* University of Eloued, 2022.

[40] Y. Laxmi Narasimha Rao and G. Ravindranath,"Fuzzy Controller for DTC-SVM of Induction Motor Using Sample Reference Phase Voltages",Springer Nature Singapore Pte Ltd. 2020 V. K. Giri et al. (eds.), Computing Algorithms with Applications in Engineering, Algorithms for Intelligent Systems, https://doi.org/10.1007/978-981-15-2369-4_25,pp 295-303

[41] Jagan Mohana Rao Malla, Dr. Manoj Kumar Sahu and Prof. P K Subudhi,"DTC-SVM of Induction Motor by Applying Two Fuzzy Logic Controllers", *International Conference on Electrical, Electronics, and Optimization Techniques* (ICEEOT) 2016 IEEE DOI: 10.1109/ICEEOT.2016.7755662

[42] L. Bin and S.K. Sharma, "A Literature Review of IGBT Fault Diagnostic and Protection Methods for Power Inverters", *Transactions on Industry Applications*, Vol 45, No 5, pp. 1770-1777, Sept-Oct. 2009 IEEE. DOI: 10.1109/TIA.2009.2027535

[43] Tamissa Younes & Kadri Farid & Charif Fella & Benchabane Abderrazak "Neural Fault Diagnosis Method for Voltage Source Inverter with a Neural Direct Torque Control of Induction Motor"2020 *IEEE The First IEEE International Conference on Communications, Control Systems and Signal Processing* ( CCSSP 2020)16-17 March 2020 El-Oued, Algeria pp 480-486. DOI: 10.1109/CCSSP49278.2020.9151552

[44] M. Sivakumar and R. M. S. Parvathi , "PSO Technique in Fault Diagnosis of Multilevel Inverter Drive System", *Europ Jour of Scient Res*, Vol. 61 No.1, pp. 29-41, juin 2011.

[45] F. Kadri, S. Drid, F. Djeffal, and L. Chrifi-Alaoui, "Neural Classification Method in Fault Detection and Diagnosis for Voltage Source Inverter in Variable Speed Drive with Induction Motor", EVER'13, 27-30 Monte Carlo, Monaco,March 2013.

[46] Lochan Babani, Sadhana Jadhav, and Bhalchandra Chaudhari,"Scaled Conjugate Gradient Based Adaptive ANN Control for SVM-DTC Induction Motor

Drive",*IFIP International Federation for Information Processing 2016 Published by Springer International Publishing* Switzerland 2016. All Rights Reserved

[47] Fuchs, F.W. (2003). "Some diagnosis methods for voltage source inverters in variable speed drives with induction machines-a survey". In IECON'03. *29th Annual Conference of the IEEE Industrial Electronics Society*, pp. 1378-1385. https://doi.org/10.1109/IECON.2003.1280259

[48] Kadri, F., Hamida, M.A. (2020). "Simple threshold method in fault diagnosis for voltage source inverter in a direct torque control induction motor drive". *Recent Patents on Engineering*, 14(4): 598-609. https://doi.org/10.2174/1872212113666191002121902

[49] Kadri, F., Drid, S., Djarah, D., Djeffal, F. (2010). "Direct torque control of induction motor fed by three phase PWM inverter using fuzzy logic and neural network". *In Sixth International Conference on Electrical Engineering*, pp. 12-16.

[50] A. Achalhi, N. Belbounaguia and M. Bezza, "A novel modified DTC scheme with speed fuzzy-PI controller," 2018 *4th International Conference on Optimization and Applications (ICOA), Mohammedia*, Morocco, 2018, pp. 1-5, doi: 10.1109/ICOA.2018.8370507.

[51] F. Kadri, S. Bensalem, and K. Houfar, "PI Speed Control for Fuzzy Direct Torque Control of induction motor using Fuzzy switching pattern" ,*First International Conference on Electrical Engineering*, CIGET09. 25-26 Octobre/2009, Tebessa, Algeria.

[52] Mandarapu, Srikanth, Sree Rama Lolla and Suresh Kumar. "Digital PI Controller Using Anti-Wind-Up Mechanism for A Speed Controlled Electric Drive System." (2013).

[53] S. Jnayah and A. Khedher, "Fuzzy-Self-Tuning PI Speed Regulator for DTC of Three-Level Inverter fed IM," 2020 *17th International Multi-Conference on Systems, Signals & Devices* (SSD), Monastir, Tunisia, 2020, pp. 709-714, doi: 10.1109/SSD49366.2020.9364128.

[54] Costa, Bruno Leandro, et al."Metaheuristics optimization applied to PI controllers tuning of a DTC-SVM drive for three-phase induction motors". *Applied Soft Computing*, vol. 62, 2018, pp. 776–788, https://doi.org/10.1016/j.asoc.2017.09.007.

[55] C. Bohn and D. P. Atherton, "An analysis package comparing PID anti-windup strategies," *in IEEE Control Systems Magazine*, vol. 15, no. 2, pp. 34-40, April 1995, doi: 10.1109/37.375281.

[56] Costa, Bruno Leandro, Clayton Luiz Graciola, Bruno Augusto Angélico, Alessandro Goedtel, Marcelo Favoretto Castoldi, et al. "A practical framework for tuning DTC-SVM drive of three-phase induction motors",*Control Engineering Practice*, vol. 88, 2019, pp. 119–127, https://doi.org/10.1016/j.conengprac.2019.05.003.

[57] Y.J. Ko and K.B. Lee, "Fault diagnosis of a voltage-fed PWM inverter for a three-parallel power conversion system in a wind turbine", Jour of Pow Elect, Vol. 10, No. 6, November 2010.

[58] Vu, HG. Yahoui, H. "IGBT open-circuit fault detection for voltage source inverters using DC bus magnetic field signal". Electr Eng Vol.103, pp. 1691–1700, 2021. https://doi.org/10.1007/s00202-020-01161-w

[59] AM. Khelif, A. Bendiabdellah, and BDE. Cherif, "Short-circuit fault diagnosis of the DC-Link capacitor and its impact on an electrical drive system", *International Journal of Electrical and Computer Engineering* (IJECE), vol. 10, no. 3, pp. 2807-2814, June 2020, DOI: 10.11591/ijece.v10i3.pp2807-2814.

[60] T. Amanuel, A. Ghirmay, H. Ghebremeskel, and RG. Bahlibi, " Comparative Analysis of Signal Processing Techniques for Fault Detection in Three Phase Induction Motor". *Journal of Electronics and Informatics*, 3(1), 61-76, 2021. doi:10.36548/jei.2021.1.006

[61] R. B. Dhumale , S. D. Lokhande,"Comparative Study of Fault Diagnostic Methods in Voltage Source Inverter Fed Three Phase Induction Motor Drive", *IOP Conference Series: Materials Science and Engineering*, 197,2017.

[62] Ko, Y.J., Lee, K.B. (2010). "Fault diagnosis of a voltage-fed PWM inverter for a three-parallel power conversion system in a wind turbine". *Journal of Power Electronic*s, 10(6): 686-693.

[63] Bawankule, P.P., Gokhale, S.S."Direct torque control of induction motors based on space vector modulation". 2016 *International Conference on Energy Efficient Technologies for Sustainability* (ICEETS), Nagercoil, India. http://dx.doi.org/10.1109/ICEETS.2016.7583817

[64] Manap, M., Nikolovski, S., Skamyin, A., Karim, R., Sutikno, T., Jopri, M.H. (2021)." An analysis of voltage source inverter switches fault classification using short time Fourier transform". arXiv preprint arXiv:2111.06566. https://doi.org/10.11591/ijpeds.v12.i4.pp2209-2220

[65] Sun, X., Song, C., Zhang, Y., Sha, X., & Diao, N. (2023). "An Open-Circuit Fault Diagnosis Algorithm Based on Signal Normalization Preprocessing for Motor Drive Inverter". *IEEE Transactions on Instrumentation and Measurement*, 72, 1-12

[66] [127]. Cherif, B.D.E., Bendjebbar, M., Benouzza, N., Boudinar, H., Bendiabdellah, A."A comparative study between two open-circuit fault detection and localization techniques in a threephase inverter fed induction motor". In 2016 *8th International Conference on Modelling, Identification and Control* (ICMIC), Algiers, Algeria, pp. 1-7. https://doi.org/10.1109/ICMIC.2016.7857513

[67] Cherif, B.D.E., Bendiabdellah, A., Bendjebbar, M., Telli, A. (2018). "A comparative study between methods of detection and localisation of open-circuit faults in a three phase voltage inverter fed induction motor". *International Journal of Modelling, Identification and Control*, 29(4): 327-340. https://doi.org/10.1504/IJMIC.2018.092111

[68] B. Cherif, A. Bendiabdellah, M. Bendjebbar, A. Tamer, "Neural Network Based Fault Diagnosis of Three Phase Inverter Fed Vector Control Induction Motor", *Periodica Polytechnica Electrical Engineering and Computer Science*, 63(4), pp. 295–305, 2019

[69] Kadri, F., Hamida, M.A. (2020). "Neural direct torque control for induction motor under voltage source inverter open switch fault". *Re-*

*cent Advances in Electrical & Electronic Engineering (Formerly Recent Patents on Electrical & Electronic Engineering)*, 13(4): 571-579. https://doi.org/10.2174/1874476105666190830103616

[70] Tamissa, Y., Charif, F., Kadri, F. Benchabane, A. (2022). "Pattern recognition and diagnosis of short and open circuit faults inverter in induction motor drive using neural networks". *Engineering Review*, 42 (3), 138-148. https://doi.org/10.30765/er.1949

[71] Abdelkader, R., Cherif, B.D., Bendiabdellah, A., & Kaddour, A. (2022). "An Open-Circuit Faults Diagnosis Approach for Three-Phase Inverters Based on an Improved Variational Mode Decomposition, Correlation Coefficients, and Statistical Indicators". *IEEE Transactions on Instrumentation and Measurement*, 71, 1-9.

[72] Hinton .G.E. ,nd Roweis .S.T.(2002). "Stochastic Neighbor Embedding. In Advances in Neural Information Processing Systems", volume 15, pages 833–840, Cambridge, MA, USA, 2002. The MIT Press.

[73] Xia, Y., Gou, B. & Xu, Y. "A new ensemble-based classifier for IGBT open-circuit fault diagnosis in three-phase PWM converter". *Prot Control Mod Power Syst* 3, 33 (2018). https://doi.org/10.1186/s41601-018-0109-x

[74] Qiu, G.; Wu, F.; Chen, K.; Wang, L. "A Robust Accuracy Weighted Random Forests Algorithm for IGBTs Fault Diagnosis in PWM Converters without Additional Sensors". Appl. Sci. 2022, 12, 2121. https://doi.org/10.3390/app12042121

[75] Bae, C., Lee,D., Nguyen, T. H., 2019. "Detection and identification of multiple IGBT open-circuit faults in PWM inverters for AC machine drives", *IET Power Electron.*, vol. 12(4), pp. 923–931.

[76] Yong, C., Zhang, J., Chen, Z., 2020. "Current observer-based online open-switch fault diagnosis for voltage-source inverter", *ISA Transactions*, vol. 99, pp. 445-453, Doi:10.1016/j.isatra.2019.09.019.

[77] Cheng, S., Zhao, J., Chen, C., Li, K., Wu, X., Yu, T., Yu, Y., 2020. "An open-circuit fault-diagnosis method for inverters based on phase current, Transportation Safety and Environment", vol. 2(2), pp. 148–160, https://doi.org/10.1093/tse/tdaa008

[78] Zhang, J., Zhang, Z., Yu, L., Bian, Z., 2019. "Fault-tolerant control of DSBLDC motor drive under open-circuit faults", *IET Electric Power Applications*, vol.13, pp. 494-502. https://doi.org/10.1049/iet-epa.2018.5240

[79] Laidani, I., Bourouba, N., 2022."Analog Circuit Fault Classification and Data Reduction Using PCA-ANFIS Technique Aided by K-means Clustering Approach ,*Advances in Electrical and Computer Engineering*", 22(4).DOI:10.4316/AECE.2022.04009

[80] Hailin, H., Fu, F., Tao, W., 2020. "Open-circuit fault diagnosis of NPC inverter IGBT based on independent component analysis and neural network", Energy Reports, vol. 6(9), pp. 134-143, https://doi.org/10.1016/j.egyr.2020.11.273.

[81] Cherif, B., Bendiabdellah, A., 2018. "Detection of Two-Level Inverter Open-Circuit Fault Using a Combined DWT-NN Approach", *Journal of Control Science and Engineering.*

[82] Hu, H., Feng, F., Wang, T., 2020. "Open-circuit fault diagnosis of NPC inverter IGBT based on independent component analysis and neural network", Energy Reports,Vol. 6(9), pp. 134-143.

[83] Chouhan, A., Gangsar, P., Porwal, R., Mechefske, C.K., 2020. "Artificial neural network based fault diagnostics for three phase induction motors under similar operating conditions",Vibro engineering Procedia, vol. 30.

[84] Asghar, F., Talha, M., Kim, SH., 2016. "Neural Network Based Fault Detection and Diagnosis System for Three-Phase Inverter in Variable Speed Drive with Induction Motor", *Journal of Control Science and Engineering* .

[85] [146]. Reyes-Malanche, J.A., Villalobos-Pina, F.J., Cabal-Yepez, E., Alvarez-Salas, R., Rodriguez-Donate, C., 2021. "Open-Circuit Fault Diagnosis in Power Inverters Through Currents Analysis in Time Domain", *in IEEE Transactions on Instrumentation and Measurement*, vol. 70, pp. 1-12.

[86] Shu, C., Ya-Ting, C., Tian-Jian, Y., Xun, W., 2016. "A novel diagnostic technique for open-circuited faults of inverters based on output Line-to-Line voltage model", *IEEE Trans. Ind. Electron.*, vol. 63(7), pp. 4412-4421.

[87] Krizhevsky, A., Sutskever, I., Hinton, G., 2012. "ImageNet Classification with Deep Convolutional Neural Networks", Advances in Neural Information Processing Systems 25 .

[88] Sabour, M., Bachir, G., Henini, N.,2020. "Deep Learning Approach for open switch Fault Diagnosis in Matrix Frequency Converter", *Electrotechnical Review* , vol. 96(11), 155-160.

[89] Van Der Maaten, L., Hinton, G., 2008. "Visualizing Data using t-SNE, *Journal of Machine Learning Research*", vol.9, pp. 2579-2605.